ATMOSPHERIC DYNAMICS

ATS 601/602

Department of Atmospheric Science
Colorado State University
Fort Collins, Colorado 80523

Fall 2008

1 Introduction

This course is concerned with the dynamics of the earth's atmosphere. Atmospheric dynamics is a branch of geophysical fluid dynamics, which also includes the dynamics of the oceans, commonly referred to as physical oceanography. Although we shall concentrate on atmospheric dynamics, much of our analysis will apply with little modification to physical oceanography.

The state of the "dry" atmosphere is often considered to be described by seven fields—the three components of velocity u, v, w, the density ρ, the specific entropy s, temperature T and the pressure p, all of which are functions of position and time. We can write a complete system of seven equations (five prognostic equations and two diagnostic equations) for these seven variables. These equations come from the three components of the vector form of Newton's law of motion, the mass conservation principle, the entropy conservation principle, the diagnostic equation relating entropy, temperature and density, and, finally, the ideal gas law. This set of seven equations constitutes "dry dynamics." To make the theory come alive with the real weather, we must add other variables and equations. For example, we could add equations for the water vapor content, the liquid and ice contents (or even their size spectra since different sizes have different fall speeds) and the ozone content. While these additional variables are necessary to answer questions such as the role of clouds in global climate change and the role of human activity in the depletion of ozone, models with all these variables can become quite overwhelming in their complexity. In most of this course we shall concentrate on dry dynamics. Even this idealization will keep us quite busy. At the end of the course we shall discuss moist, nonhydrostatic models. To begin, let's review the ideal gas law, the concept of material derivative, mass conservation for a compressible fluid, thermodynamics, and noninertial reference frames. At the end of this chapter we review the complete system of equations for a dry atmosphere.

1.1 Ideal gas law

The gaseous composition of the earth's atmosphere is given in Table 1.1. Approximately 78.08% of the molecules in our atmosphere are nitrogen, and approximately 20.95% are oxygen. The inert gases Argon, Neon, Helium, and Krypton also occur in small percentages. Ozone, an extremely important constituent of the stratosphere, and carbon dioxide also occur in small percentages that are variable on seasonal and longer time scales. Water vapor is a highly variable constituent. Near the surface over the warm tropical oceans, nearly 4% of the atmosphere's molecules may be water vapor. In contrast, in the cold air at the tropopause a typical value is 0.0004%. The fact that atmospheric water substance changes phase between vapor, liquid, and ice is an important part of many phenomena, e.g., the ITCZ, the Hadley circulation, and hurricanes. Because the theory and modeling of the moist atmosphere is difficult, we postpone this topic to later chapters.

Constituent		Molecular Weight	Content (fraction of total molecules)	
Nitrogen	(N_2)	28.016	0.7808	(75.51% by mass)
Oxygen	(O_2)	32.00	0.2095	(23.14% by mass)
Argon	(A)	39.94	0.0093	(1.28% by mass)
Water Vapor	(H_2O)	18.02	0–0.04	
Carbon Dioxide	(CO_2)	44.01	325	parts per million
Neon	(Ne)	20.18	18	parts per million
Helium	(He)	4.00	5	parts per million
Krypton	(Kr)	83.70	1	parts per million
Hydrogen	(H_2)	2.02	0.5	parts per million
Ozone	(O_3)	48.00	0–12	parts per million

Table 1.1: The gaseous composition of the Earth's atmosphere.

For now we ignore water vapor and consider only the other gases listed in Table 1.1. To a good approximation each of these gaseous constituents can be assumed to satisfy its own ideal gas law. However, for dry models of the atmosphere it is convenient to have one gas law for all the dry constituents (i.e., all constituents excluding water vapor).

Thus, consider a mixture of N gases, the n^{th} of which satisfies the ideal gas law

$$p_n = \rho_n \frac{R^*}{m_n} T, \tag{1.1}$$

where $R^* = 8314.3$ J K^{-1} kmole^{-1} is the universal gas constant, p_n is the partial pressure, ρ_n the density, and m_n the molecular weight (kg kmole^{-1}) of the n^{th} gas. Summing (1.1) over all N gases, we obtain

$$p = \rho \frac{R^*}{\bar{m}} T, \tag{1.2}$$

where $\rho = \sum_{n=1}^{N} \rho_n$ is the total density, and where the total pressure $p = \sum_{n=1}^{N} p_n$ is the sum of the partial pressures p_n (Dalton's Law), and where the mean molecular weight $\bar{m}$ is defined by

$$\frac{1}{\bar{m}} = \sum_{n=1}^{N} \frac{1}{m_n} \frac{\rho_n}{\rho}. \tag{1.3}$$

Let the subscript 1 denote nitrogen, the subscript 2 denote oxygen, the subscript 3 denote Argon, etc. Then, $m_1 =$ 28.016 kg kmole^{-1}, $m_2 =$ 32.00 kg kmole^{-1}, $m_3 =$ 39.94 kg kmole^{-1}, $\rho_1/\rho = 0.7551$, $\rho_2/\rho = 0.2314$, $\rho_3/\rho = 0.0128$, etc., so that (1.3) yields $\bar{m} =$ 28.966 kg kmole^{-1} for the mean molecular weight of dry air. Defining $R = R^*/\bar{m} =$ 287.0 J kg^{-1} K^{-1} as the gas constant of dry air, (1.2) becomes

$$p = \rho R T, \tag{1.4}$$

which we shall use as the gas law for dry air.

1.2 Material derivative

Although dry air is composed of widely separated, small, individual molecules, we shall model it as a continuous distribution of matter, i.e., we shall use the continuum hypothesis. There are two primary descriptions of continuum fluids—the Lagrangian description and the Eulerian description. In the Lagrangian description of fluid flow the independent variables are parcel labels (e.g., the initial position of each fluid parcel), and the dependent variables include the actual positions of each parcel as a function of time. Thus, the trajectory of each parcel is a natural output in the Lagrangian description. In the Eulerian description of fluid flow the independent variables are the spatial coordinates and time, and the dependent variables are the velocity, density, and entropy. In the Eulerian description we are concerned more with the fluid velocity at each spatial point rather than where the parcel crossing that point originated. Here we shall use the Eulerian description. For further discussion of the Lagrangian description and a derivation of the mass conservation principle under the Lagrangian description, see Chapter 1 of Salmon's book.

Consider an infinitesimally small fluid element which has position $\mathbf{x} = (x, y, z)$ at time t. As this "material element" moves, its trajectory is given by the function $\mathbf{x}(t)$. Now consider some property of the material element, temperature T say, which varies as the element moves so that $T = T(x(t), y(t), z(t), t)$. The time derivative of temperature following the material element is

$$\frac{DT}{Dt} = \frac{\partial T}{\partial t} + \frac{dx}{dt}\frac{\partial T}{\partial x} + \frac{dy}{dt}\frac{\partial T}{\partial y} + \frac{dz}{dt}\frac{\partial T}{\partial z}. \tag{1.5}$$

Note that we have used the symbol D/Dt rather than d/dt for the material derivative. To avoid confusion, we reserve the symbol d/dt for the time derivative of a quantity which is a function of time only. Since

$$\mathbf{u} = (u, v, w) = \left(\frac{dx}{dt}, \frac{dy}{dt}, \frac{dz}{dt} \right), \tag{1.6}$$

(1.5) can also be written

$$\frac{DT}{Dt} = \frac{\partial T}{\partial t} + u\frac{\partial T}{\partial x} + v\frac{\partial T}{\partial y} + w\frac{\partial T}{\partial z} = \frac{\partial T}{\partial t} + \mathbf{u} \cdot \nabla T. \tag{1.7}$$

1.3 Mass conservation

Let ρ denote the fluid density. Then $\rho\mathbf{u} = (\rho u, \rho v, \rho w)$ denotes the vector mass flux. The divergence of the vector mass flux is $\nabla \cdot (\rho\mathbf{u}) = \partial(\rho u)/\partial x + \partial(\rho v)/\partial y + \partial(\rho w)/\partial z$. If mass is conserved, but at a local point there is divergence of the vector mass flux, then the density must decrease at that point, i.e.,

$$\frac{\partial \rho}{\partial t} + \nabla \cdot (\rho\mathbf{u}) = 0. \tag{1.8}$$

Since $\nabla \cdot (\rho\mathbf{u}) = \mathbf{u} \cdot \nabla\rho + \rho\nabla \cdot \mathbf{u}$ and since $D\rho/Dt = \partial\rho/\partial t + \mathbf{u} \cdot \nabla\rho$ by (1.7), we can write (1.8) as

$$\frac{D\rho}{Dt} + \rho\nabla \cdot \mathbf{u} = 0. \tag{1.9}$$

Equations (1.8) and (1.9) are equivalent statements of the mass conservation principle, with (1.8) usually being referred to as the flux form and (1.9) as the advective form.

1.4 Thermodynamic equation

Recall that we are considering air to be an ideal gas, so that it obeys the ideal gas law $p = \rho RT$ or $p\alpha = RT$, where $\alpha = \rho^{-1}$ is the specific volume and R is the gas constant for dry air. Then the first law of thermodynamics can be written

$$c_v\frac{DT}{Dt} + p\frac{D\alpha}{Dt} = Q, \tag{1.10}$$

where c_v is the specific heat of dry air at constant volume and Q is the diabatic heat source, which, in the earth's atmosphere, is primarily due to radiative effects and the change of phase of water. Using the ideal gas law, (1.10) can be written in the form

$$c_p\frac{DT}{Dt} - \alpha\frac{Dp}{Dt} = Q, \tag{1.11}$$

where $c_p = c_v + R$ is the specific heat of dry air at constant pressure.

The experimental values of the specific heats for dry air are $c_p = 1004\,\mathrm{J\,kg^{-1}\,K^{-1}}$ and $c_v = 717\,\mathrm{J\,kg^{-1}\,K^{-1}}$. Note that $c_p \approx \frac{7}{2}R$ and $c_v \approx \frac{5}{2}R$. Why should this be so? Dry air is predominantly made up of N_2 and O_2, two diatomic gases. Each diatomic molecule can be considered as two rigidly connected point masses. Each such molecule has five degrees of freedom, i.e., it can move in three independent directions and can rotate about two independent axes (rotations about the line connecting the two atoms of the diatomic molecule do not count since the atoms are point masses). The specific internal energy of the dry air is c_vT. According to the equipartition theorem, each degree of freedom has a specific energy of $\frac{1}{2}RT$, so that $c_vT = \frac{5}{2}RT$, i.e., $c_v = \frac{5}{2}R$, and since $c_p = c_v + R$, $c_p = \frac{7}{2}R$. It is true that a diatomic molecule is not rigid but can vibrate as the atoms move back and forth along the line connecting them. However, these additional degrees of freedom are not important at atmospheric temperatures. They do become important at much higher temperatures. Note that, for a monatomic gas, rotations are not relevant and the relations are $c_v = \frac{3}{2}R$ and $c_p = \frac{5}{2}R$. It should also be noted that a complete theory of specific heats involves statistical mechanics and quantum theory.

A more compact form of the thermodynamic equation can be found as follows. Dividing by T and using the ideal gas law, we can write (1.11) as

$$c_p\frac{D}{Dt}\left\{\ln\left[T\left(\frac{p_0}{p}\right)^{\kappa}\right]\right\} = \frac{Q}{T}, \tag{1.12}$$

where $\kappa = R/c_p \approx 2/7$ and p_0 is a constant reference pressure. Defining the potential temperature θ as

$$\theta = T\left(\frac{p_0}{p}\right)^{\kappa}, \tag{1.13}$$

we can write (1.12) as

$$c_p\frac{D\ln\theta}{Dt} = \frac{Q}{T}. \tag{1.14}$$

When $Q = 0$, the flow is termed adiabatic, and (1.14) reduces to $D\theta/Dt = 0$. Thus, the potential temperature is materially conserved for adiabatic flow. The physical interpretation of θ is the temperature a material element would have if it were adiabatically expanded (for $p > p_0$) or compressed (for $p < p_0$) to the reference pressure p_0. Usually p_0 is chosen to be 100 kPa, so that $\theta > T$ for most material elements.

Another way to express the thermodynamic equation is in terms of the specific entropy, which is defined by

$$\begin{aligned} s = c_p \ln\left(\frac{\theta}{T_0}\right) &= c_v \ln\left(\frac{T}{T_0}\right) - R\ln\left(\frac{\rho}{\rho_0}\right) \\ &= c_p \ln\left(\frac{T}{T_0}\right) - R\ln\left(\frac{p}{p_0}\right), \end{aligned} \tag{1.15}$$

where T_0 is a constant reference temperature and ρ_0 a constant reference density, with ρ_0, T_0, p_0 related by $p_0 = \rho_0 R T_0$. Written in terms of specific entropy, (1.14) becomes

$$\frac{Ds}{Dt} = \frac{Q}{T}. \tag{1.16}$$

For adiabatic flow, (1.16) reduces to $Ds/Dt = 0$. Since the potential temperature θ and the entropy s are related by

$$\theta = T_0 e^{s/c_p}, \tag{1.17}$$

θ is sometimes referred to as "meteorologist's entropy."

The term "adiabatic," meaning "a"–"diabatic" or "without heating," is usually used to refer to a flow process. For example, air can descend adiabatically on the lee slopes of the Rockies. According to (1.13), p and T of a descending parcel are increasing in such a way that θ is invariant for the parcel. As a second example, the sound waves we use to talk to each other represent an adiabatic flow. They are waves of compression and rarefaction with accompanying variations of p and T that leave θ unchanged, i.e., sound waves are "visible" in the pressure and temperature fields but are "invisible" in the potential temperature (or entropy) field.

The term "homentropic," meaning "homogeneous"–"entropy," is usually used to refer to the state of the atmosphere at a particular time. Thus, a homentropic atmosphere is one in which s (or θ) is the same everywhere. This is an overly idealized view of the actual atmosphere. As shown in problem 1, s and θ generally increase with height, so that the atmosphere is statically stable. The consequences of rotation and static stability lie at the heart of geophysical fluid dynamics.

1.5 Noninertial reference frames

Consider the following experiment, which you can perform with two friends. Get a baseball and go to the merry-go-round at the city park playground. Have your two friends get on exactly opposite sides of the merry-go-round and get it rotating counterclockwise at constant angular velocity, while you get up in a nearby tree to observe from above. Now have the one of your two friends who is holding the baseball and rotating around, throw it at your other friend on the opposite side while you watch from above. When you get together to talk about what happened, you will have differing views. Having viewed the event from above, you will say the baseball simply traveled in a straight line, but that the catcher rotated away while the ball was in the air. Both people on the merry-go-round will say the ball did not travel in a straight line but curved to the right of its original direction of motion. If they possess wild imaginations, they may even claim some mysterious force deflected it to the right.

The reason for the differing interpretations lies in the fact that you observed the event in an inertial reference frame[1] while your friends observed it in a noninertial frame. For example, think of your coordinate system as having its origin at the center of the merry-go-round but having its axes fixed to the earth. Think of your friends' coordinate system as also having its origin at the center of the merry-go-round but having its axes fixed to the merry-go-round. Obviously, the noninertial frame is rotating at constant angular velocity with respect to the inertial frame.

In a sense we live on a spherical merry-go-round. Imagine two coordinate systems whose origins are at the center of the earth. Let the third axis of each coincide with the earth's axis of rotation, so the other axes lie in the equatorial plane. Let one coordinate system be inertial in the sense that its axes do not rotate with the earth but rather always point to the same stars. Let the other coordinate system be noninertial in the sense that its axes are frozen to the rotating earth. The point is that Newton's laws of motion strictly apply only in the inertial frame. But we observe the atmosphere and

[1] Actually, since you were sitting in a tree with roots going into the rotating earth, you also observed the event in a noninertial frame. However, since the merry-go-round was rotating thousands of times faster than the earth, we can neglect the effects of the earth's rotation.

ocean by measuring velocities with respect to the rotating earth, i.e., in the noninertial frame. If the law of motion is going to predict the velocity with respect to the rotating earth, this law must include apparent (or fictitious) forces, one of which is the Coriolis force. Now let's see if we can make these intuitive arguments mathematically precise.

Let the subscript "a" refer to measurements relative to the absolute or fixed (relative to the stars) frame. This is the inertial frame. For an inertial frame whose origin is at the center of the earth, the unit vectors always point to the same distant stars, i.e., the inertial frame does not rotate with the earth. Velocities and accelerations are measured with respect to the "fixed stars." Newton's second law of motion states that the rate of change of momentum of a material element is equal to the net force acting on the element. We shall consider the net force to be the sum of three forces—the pressure gradient force, the gravitational force and the frictional force. Newton's second law of motion then becomes

$$\frac{D_a \mathbf{u}_a}{Dt} = -\alpha \nabla p - \nabla \Phi + \mathbf{F}, \tag{1.18}$$

where $-\alpha\nabla p$ is the pressure gradient force per unit mass, $-\nabla\Phi$ is the gravitational force per unit mass, and $\mathbf{F}$ is the frictional force per unit mass.

In geophysical fluid dynamics we measure motions with respect to the rotating earth, i.e., in terms of $\mathbf{u}$ and not $\mathbf{u}_a$. Let $\boldsymbol{\Omega}$ denote the rotation vector of the earth, i.e., a vector along the axis of the earth's rotation with magnitude equal to the angular velocity (with respect to the stars, not the sun), which is 7.292116×10^{-5} rad s^{-1}. The absolute velocity $\mathbf{u}_a$ is then related to the relative velocity $\mathbf{u}$, the rotation vector $\boldsymbol{\Omega}$ and the position vector $\mathbf{r}$ by

$$\mathbf{u}_a = \mathbf{u} + \boldsymbol{\Omega} \times \mathbf{r}, \tag{1.19a}$$

or, equivalently,

$$\frac{D_a \mathbf{r}}{Dt} = \frac{D\mathbf{r}}{Dt} + \boldsymbol{\Omega} \times \mathbf{r}. \tag{1.19b}$$

In fact, for any vector $\mathbf{A}$ we have

$$\frac{D_a \mathbf{A}}{Dt} = \frac{D\mathbf{A}}{Dt} + \boldsymbol{\Omega} \times \mathbf{A}. \tag{1.20}$$

If we apply (1.20) to (1.19a) we obtain

$$\frac{D_a \mathbf{u}_a}{Dt} = \frac{D\mathbf{u}}{Dt} + 2\boldsymbol{\Omega} \times \mathbf{u} + \boldsymbol{\Omega} \times (\boldsymbol{\Omega} \times \mathbf{r}). \tag{1.21}$$

Using this in (1.18) we obtain

$$\frac{D\mathbf{u}}{Dt} = -\alpha \nabla p - 2\boldsymbol{\Omega} \times \mathbf{u} + \mathbf{g} + \mathbf{F}, \tag{1.22}$$

where

$$\mathbf{g} = -\nabla\Phi - \boldsymbol{\Omega} \times (\boldsymbol{\Omega} \times \mathbf{r}) \tag{1.23}$$

is the acceleration of gravity. The forces $2\boldsymbol{\Omega} \times \mathbf{u}$ (Coriolis) and $\boldsymbol{\Omega} \times (\boldsymbol{\Omega} \times \mathbf{r})$ (centrifugal) are not true forces, but rather apparent forces which arise from our use of a noninertial reference frame.

1.6 The Foucault pendulum

The Foucault pendulum was devised in 1851 by the French physicist Jean Leon Foucault (1819–1868). It is basically a very large pendulum, often suspended in a section of a multi-story building (e.g., the Denver Natural History Museum or the Smithsonian in Washington DC) which is open from the basement floor to the roof. The pendulum bob is usually quite massive and is connected to a ceiling ball joint by a thin wire, which we will consider massless. In larger buildings the pendulum length may be on the order of 20 m. The period of an ordinary, simple pendulum is the time it takes for one complete swing and is given by $2\pi\sqrt{\ell/g}$, where ℓ is the pendulum length and g is the acceleration of gravity. For $\ell = 20$ m and $g = 9.8$ ms^{-2}, this period is about 9 seconds.

The most interesting feature of the Foucault pendulum is that it reveals the effect of the Coriolis force. To see this, imagine you are watching such a slowly oscillating pendulum bob swing back and forth, alternately away and then toward you. As the pendulum swings away from you, it should be deflected slightly to your right by the Coriolis force (assuming you are in the northern hemisphere), while as it swings toward you it should be deflected slightly to your left. In other words, it is always being deflected to the right of its motion. Thus, the plane formed by the oscillating pendulum support wire should rotate clockwise when viewed from above. We shall prove that this plane makes a complete clockwise rotation in the time $2\pi/(\Omega\sin\phi)$, which is called a *pendulum day*. Here Ω is the rotation rate of the earth in rad s^{-1} and ϕ is the latitude (note that $2\pi/\Omega = 23.934$ hours is the length of a sidereal day). At 40N a pendulum day is 37.24 hours. Often a downward pointing spike is attached to the bottom of the pendulum bob and a circle of small pegs is set up on the floor near the outer limits of the pendulum swings. As the plane of oscillation turns clockwise the pegs are knocked down by the spike. Since the spike can knock down pegs on both ends of its swing, all the pegs are knocked down in half a pendulum day, which is 18.62 hours at 40N. Museum employees sometimes mark the times at which certain pegs were knocked down, since the human attention span is usually not long enough to observe a significant fraction of a pendulum day.

To describe the motion of the pendulum bob let us select a coordinate system with x pointing eastward, y pointing northward and z upward along the local vertical. We shall limit our analysis to oscillations of small amplitude, so that the horizontal excursions of the pendulum are small compared to the length of the pendulum. Under this condition the pendulum bob stays nearly in the horizontal plane, so that the vertical velocity component $\dot{z}$ can be neglected compared to the horizontal components $\dot{x}$ and $\dot{y}$. The pendulum bob has three forces acting on it—gravity, the tension of the support wire and Coriolis. Newton's law applied to the pendulum bob is

$$\ddot{\mathbf{x}} = \mathbf{g} + \frac{\mathbf{T}}{m} - 2\mathbf{\Omega}\times\dot{\mathbf{x}}, \tag{1.24}$$

where $\mathbf{x}$ is the vector position of the pendulum bob, m the mass of the pendulum bob, $\mathbf{T}/m$ is the acceleration produced by the suspension wire tension force $\mathbf{T} \approx (-Tx/\ell, -Ty/\ell, T)$, $\dot{\mathbf{x}} \approx (\dot{x}, \dot{y}, 0)$ the velocity components, and $\mathbf{g} = (0, 0, -g)$ the acceleration of gravity. Since

$$2\mathbf{\Omega}\times\dot{\mathbf{x}} = \begin{vmatrix} \mathbf{i} & \mathbf{j} & \mathbf{k} \\ 0 & 2\Omega\cos\phi & 2\Omega\sin\phi \\ \dot{x} & \dot{y} & 0 \end{vmatrix} = -\dot{y}2\Omega\sin\phi\,\mathbf{i} + \dot{x}2\Omega\sin\phi\,\mathbf{j} - \dot{x}2\Omega\cos\phi\,\mathbf{k}, \tag{1.25}$$

we can write (1.24) in component form as

$$\ddot{x} - f\dot{y} + \frac{T}{m}\frac{x}{\ell} = 0, \tag{1.26}$$

$$\ddot{y} + f\dot{x} + \frac{T}{m}\frac{y}{\ell} = 0, \tag{1.27}$$

$$\frac{T}{m} = g, \tag{1.28}$$

where $f = 2\Omega\sin\phi$ is the Coriolis parameter and ϕ the latitude. Here we have neglected the Coriolis term in the vertical equation of motion since it is much smaller than g or T/m. Using (1.28) in (1.26) and (1.27), and defining $\nu^2 = g/\ell$, we obtain

$$\ddot{x} - f\dot{y} + \nu^2 x = 0, \tag{1.29}$$

$$\ddot{y} + f\dot{x} + \nu^2 y = 0. \tag{1.30}$$

These two equations are coupled through the Coriolis terms. Instead of solving two equations for the two real variables $x(t), y(t)$, we can solve a single equation for the complex variable $q(t) = x(t) + iy(t)$. Adding (1.29) and i times (1.30), we obtain

$$\ddot{q} + if\dot{q} + \nu^2 q = 0. \tag{1.31}$$

The solution of (1.31) is

$$q(t) = e^{-i\frac{1}{2}ft}\left(Ae^{i\nu t} + Be^{-i\nu t}\right), \tag{1.32}$$

where A and B are complex constants which depend on the initial conditions. In deriving (1.32) we have assumed $f^2 << \nu^2$. For simplicity let us assume that $q = 0$ at $t = 0$, so that $A + B = 0$. Let us also assume $\dot{x} = 0$ at $t = 0$. Using these conditions in (1.32) and separating the result into real and imaginary parts we obtain

$$x(t) = \frac{\dot{y}_0}{\nu}\sin(\tfrac{1}{2}ft)\sin(\nu t), \tag{1.33}$$

$$y(t) = \frac{\dot{y}_0}{\nu}\cos(\tfrac{1}{2}ft)\sin(\nu t), \tag{1.34}$$

where $\dot{y}_0$ is the initial y-component of velocity. Thus, (1.33)–(1.34) are the solutions of (1.29)–(1.30). These solutions, which give the position of the pendulum bob at any instant, show that we start off with the pendulum oscillating in the y-direction, but when $ft = \pi$ it is oscillating in the x-direction. One complete rotation of the plane of oscillation has occurred when $ft = 4\pi$, i.e., one pendulum day is $2\pi/(\Omega \sin\phi)$.

While the Coriolis force may seem quite small (since it takes ten or fifteen thousand swings of the pendulum before the plane of oscillation rotates completely around), it is crucial for large scale motions of the atmosphere and ocean. An important difference between the atmosphere and the Foucault pendulum bob is that atmospheric parcels do not reverse their direction every 5 seconds. In large scale atmospheric motions there tends to be mutual adjustment between the wind field and the pressure field so that there is an approximate balance between the horizontal components of $\alpha\nabla p$ and $2\mathbf{\Omega} \times \mathbf{v}$. This is called geostrophic balance and will be an important theme in later chapters.

1.7 The complete system of equations for a dry atmosphere

To summarize, let us now collect the vector momentum equation (1.22), the mass conservation equation (1.9), the thermodynamic equation (1.16), the definition of specific entropy (1.15), and the gas law (1.4) to obtain

$$\frac{D\mathbf{u}}{Dt} = -\frac{1}{\rho}\nabla p - 2\mathbf{\Omega} \times \mathbf{u} - \nabla\Phi - \mathbf{\Omega} \times (\mathbf{\Omega} \times \mathbf{r}) + \mathbf{F}, \tag{1.35}$$

$$\frac{D\rho}{Dt} + \rho\nabla \cdot \mathbf{u} = 0, \tag{1.36}$$

$$\frac{Ds}{Dt} = \frac{Q}{T}, \tag{1.37}$$

$$s = c_v \ln\left(\frac{T}{T_0}\right) - R\ln\left(\frac{\rho}{\rho_0}\right), \tag{1.38}$$

$$p = \rho R T. \tag{1.39}$$

We can regard (1.35)–(1.39) as a closed system of seven scalar equations for the five scalar predictive variables $\mathbf{u}$, ρ, s and the two diagnostic variables T and p. Knowing ρ and s from the predictions using (1.36) and (1.37), the diagnostic determination of T from (1.38) is facilitated by rewriting (1.38) in the form

$$T = T_0 \left(\frac{\rho}{\rho_0}\right)^{R/c_v} e^{s/c_v}. \tag{1.40}$$

Later, when we discuss the dynamics of a moist atmosphere, we shall generalize the system (1.35)–(1.39) by adding two more predictive equations for two new predictive variables—the density of airborne water substance (vapor and cloud particles) and the density of precipitating water substance. In addition, the formula for entropy will become more complicated and we will have two ideal gas laws, one for the partial pressure of dry air and one for the partial pressure of water vapor. The pressure gradient force in the momentum equation will then involve the total pressure, i.e., the sum of the partial pressures of dry air and water vapor. In the moist case, the formula for entropy does not allow a rearrangement analogous to (1.40), so that temperature must be iteratively determined from a transcendental equation for T.

Required Reading

- Holton, chapter 1.
- Salmon, chapter 1.
- Gill, chapters 1–3.

Problems

1. The table below gives the pressure and temperature for the mean sounding from the Marshall Islands area of the equatorial Pacific. Plot this mean sounding on a tephigram or a skew-T, log p diagram. Fill in two additional columns, one for potential temperature and one for entropy (use $T_0 = 300$ K for the reference temperature).

   - Where is the tropopause for this mean sounding?
   - How much does the potential temperature increase across the troposphere?
   - What happens to the entropy curve if you change the reference temperature T_0 to 273.15 K?

Pressure (mb)	Temperature (C)
50	−60.63
100	−73.42
150	−68.51
200	−55.42
250	−43.37
300	−33.22
350	−24.82
400	−17.66
450	−11.73
500	−6.71
550	−2.25
600	1.68
650	5.40
700	8.78
750	11.75
800	14.41
850	16.90
900	19.69
950	22.75
1000	26.08
1010	26.78

2 Fundamentals

Near the middle of the 19^{th} century, long before the birth of geophysical fluid dynamics, Helmholtz in Germany and Kelvin in Great Britain independently realized the importance of the rotational aspects of fluid flow. Helmholtz' arguments involved the vorticity equation while Kelvin's arguments involved the circulation equation (or circulation theorem). These are two complementary ways of studying the rotational aspects of the flow. They are both derived from the vector momentum equation—the vorticity equation being obtained by taking the curl of the momentum equation, and the circulation theorem being obtained by taking a line integral of the momentum equation. In geophysical fluid dynamics attention is often centered on the rotational aspects of the flow. Then, the concepts of relative vorticity, absolute vorticity, potential vorticity, and circulation come to center stage. In this chapter we review each of these fundamental concepts.

2.1 Vorticity and circulation

Letting $\mathbf{u}$ denote the vector velocity relative to the rotating earth, the relative vorticity $\boldsymbol{\zeta}$ is defined by

$$\boldsymbol{\zeta} = \nabla \times \mathbf{u}. \tag{2.1}$$

Letting $\boldsymbol{\Omega}$ denote the angular velocity vector of the earth's rotation, and $\mathbf{r}$ denote the position vector, the absolute vorticity $\boldsymbol{\zeta}_a$ is defined by

$$\boldsymbol{\zeta}_a = \nabla \times \mathbf{u}_a = \nabla \times (\mathbf{u} + \boldsymbol{\Omega} \times \mathbf{r}) = 2\boldsymbol{\Omega} + \nabla \times \mathbf{u}. \tag{2.2}$$

The definitions (2.1) and (2.2) involve the curl operator and are coordinate independent. Geophysical fluid dynamics problems can be formulated in a variety of coordinate systems, the most common being cartesian, cylindrical (polar), and spherical. The expression of the curl operator in each of these coordinates is discussed in Appendix B. Using cartesian coordinates with x, y, z denoting the eastward, northward, and vertical directions, u, v, w the corresponding velocity components, and $\mathbf{i}, \mathbf{j}, \mathbf{k}$ the corresponding unit vectors, the relative vorticity is expressed as

$$\nabla \times \mathbf{u} = \begin{vmatrix} \mathbf{i} & \mathbf{j} & \mathbf{k} \\ \dfrac{\partial}{\partial x} & \dfrac{\partial}{\partial y} & \dfrac{\partial}{\partial z} \\ u & v & w \end{vmatrix} = \left(\frac{\partial w}{\partial y} - \frac{\partial v}{\partial z}\right)\mathbf{i} + \left(\frac{\partial u}{\partial z} - \frac{\partial w}{\partial x}\right)\mathbf{j} + \left(\frac{\partial v}{\partial x} - \frac{\partial u}{\partial y}\right)\mathbf{k}. \tag{2.3}$$

In the study of atmospheric vortices such as hurricanes and tornadoes it is often convenient to use cylindrical coordinates (r, ϕ, z), where r is the radius, ϕ is the tangential angle, and z is the vertical distance. The vector velocity is $\mathbf{u} = u\mathbf{i} + v\mathbf{j} + w\mathbf{k}$, where u, v, w are now the radial, tangential, and vertical components of velocity, and $\mathbf{i}, \mathbf{j}, \mathbf{k}$ are the respective unit vectors. In cylindrical coordinates the curl of the vector velocity is

$$\nabla \times \mathbf{u} = \frac{1}{r}\begin{vmatrix} \mathbf{i} & r\mathbf{j} & \mathbf{k} \\ \dfrac{\partial}{\partial r} & \dfrac{\partial}{\partial \phi} & \dfrac{\partial}{\partial z} \\ u & rv & w \end{vmatrix} = \left(\frac{\partial w}{r\partial \phi} - \frac{\partial v}{\partial z}\right)\mathbf{i} + \left(\frac{\partial u}{\partial z} - \frac{\partial w}{\partial r}\right)\mathbf{j} + \left(\frac{\partial (rv)}{r\partial r} - \frac{\partial u}{r\partial \phi}\right)\mathbf{k}. \tag{2.4}$$

One useful idealized two-dimensional vortex is called the Rankine vortex, in which $u = 0$, $w = 0$, and the tangential wind v is assumed to depend on r only, with the explicit form for v given by

$$v(r) = v_0 \begin{cases} r/r_0 & \text{if } 0 \le r \le r_0 \\ r_0/r & \text{if } r_0 \le r < \infty, \end{cases} \tag{2.5}$$

where v_0 and r_0 are specified parameters which determine the maximum wind and the radius of maximum wind respectively. The vorticity of this Rankine flow is

$$\nabla \times \mathbf{u} = \frac{\partial (rv)}{r\partial r}\mathbf{k} = \mathbf{k}\frac{2v_0}{r_0} \begin{cases} 1 & \text{if } 0 \le r < r_0 \\ 0 & \text{if } r_0 < r < \infty. \end{cases} \tag{2.6}$$

Note that the vertical component of vorticity can also be written as $\partial v/\partial r + v/r$. For a Rankine vortex $\partial v/\partial r$ and v/r are the same magnitude and same sign inside r_0, but are the same magnitude and opposite sign outside r_0. Thus, a Rankine vortex has constant vorticity inside r_0 and zero vorticity outside r_0.

Now consider the Rankine vortex in the limit as $r_0 \to 0$ and $v_0 \to \infty$ in such a way that the product $r_0 v_0$ remains fixed. This is a point vortex, i.e., all the vorticity is concentrated at a point, and the flow is irrotational (zero vorticity) everywhere except at that point. One could imagine a swarm of hundreds or thousands of point vortices, mutually advecting each other around in a chaotic fashion. Such models have proved useful in the study of two-dimensional turbulence. One fascinating result involves an initial swarm of point vortices, half of which have clockwise spin and half of which have anticlockwise spin, with the two types chaotically mixed up in the initial state. As the flow evolves under mutual advection, the two types segregate, with the result that a large cyclonic flow covers half the domain and a large anticyclonic flow the other half of the domain. Order has emerged out of chaos.

In numerical weather prediction (NWP) models and global climate models (GCM's) it is often convenient to use spherical coordinates (λ, ϕ, r), where λ is the longitude, ϕ is the latitude, and r is the distance from the center of the earth. The vector velocity is $\mathbf{u} = u\mathbf{i} + v\mathbf{j} + w\mathbf{k}$, where u, v, w are the zonal, meridional, and vertical components of velocity, and $\mathbf{i}, \mathbf{j}, \mathbf{k}$ are the respective unit vectors. In spherical coordinates the curl of the vector velocity is

$$\nabla \times \mathbf{u} = \frac{1}{r^2 \cos\phi} \begin{vmatrix} \mathbf{i} r\cos\phi & \mathbf{j} r & \mathbf{k} \\ \dfrac{\partial}{\partial \lambda} & \dfrac{\partial}{\partial \phi} & \dfrac{\partial}{\partial r} \\ ur\cos\phi & vr & w \end{vmatrix}$$

$$= \left(\frac{\partial w}{r\partial \phi} - \frac{\partial (rv)}{r\partial r} \right)\mathbf{i} + \left(\frac{\partial (ru)}{r\partial r} - \frac{\partial w}{r\cos\phi\partial\lambda} \right)\mathbf{j} + \left(\frac{\partial v}{r\cos\phi\partial\lambda} - \frac{\partial (u\cos\phi)}{r\cos\phi\partial\phi} \right)\mathbf{k}. \tag{2.7}$$

In addition, defining the velocity due to the earth's rotation as $\mathbf{u}_e = \mathbf{\Omega} \times \mathbf{r} = \mathbf{i}\Omega r\cos\phi$, we have

$$\nabla \times \mathbf{u}_e = \frac{1}{r^2 \cos\phi} \begin{vmatrix} \mathbf{i} r\cos\phi & \mathbf{j} r & \mathbf{k} \\ \dfrac{\partial}{\partial \lambda} & \dfrac{\partial}{\partial \phi} & \dfrac{\partial}{\partial r} \\ \Omega r^2\cos^2\phi & 0 & 0 \end{vmatrix} = \mathbf{j}2\Omega\cos\phi + \mathbf{k}2\Omega\sin\phi = 2\mathbf{\Omega}, \tag{2.8}$$

confirming the last equality in (2.2).

Now that we have defined the vorticity vector, let us consider the concepts of vortex lines and vortex tubes. A vortex line (also called a vortex filament) is a line in the fluid which is everywhere parallel to the vorticity vector. Now consider all the vortex lines which pass through a closed curve, as shown in Fig. 2.1. The ends of this tube have unit normal vectors denoted by $\mathbf{n}_1$ and $\mathbf{n}_2$, both in the direction of the vorticity vector. Applying Gauss' theorem (see Appendix A), we obtain

$$\iiint \nabla \cdot \boldsymbol{\zeta}\, dV = \iint \boldsymbol{\zeta} \cdot \mathbf{n}\, dA, \tag{2.9}$$

where $\mathbf{n}$ is the unit outward normal to the surface of the vortex tube. Since $\nabla \cdot \boldsymbol{\zeta} = 0$, the left hand side of (2.9) vanishes. Since the vorticity vector is tangent to the sides of the tube, the only contributions to the right hand side of (2.9) come from the ends of the tube. Thus,

$$\iint \boldsymbol{\zeta} \cdot \mathbf{n}\, dA_1 = \iint \boldsymbol{\zeta} \cdot \mathbf{n}\, dA_2, \tag{2.10}$$

which shows that the strength of the vortex tube is the same at every cross section.

Now that we understand the concepts of vorticity, vortex lines, and vortex tubes, let us consider the concept of circulation. The relative circulation is defined by

$$C = \oint \mathbf{u} \cdot d\mathbf{r}, \tag{2.11}$$

and the absolute circulation by

$$C_a = \oint \mathbf{u}_a \cdot d\mathbf{r}, \tag{2.12}$$

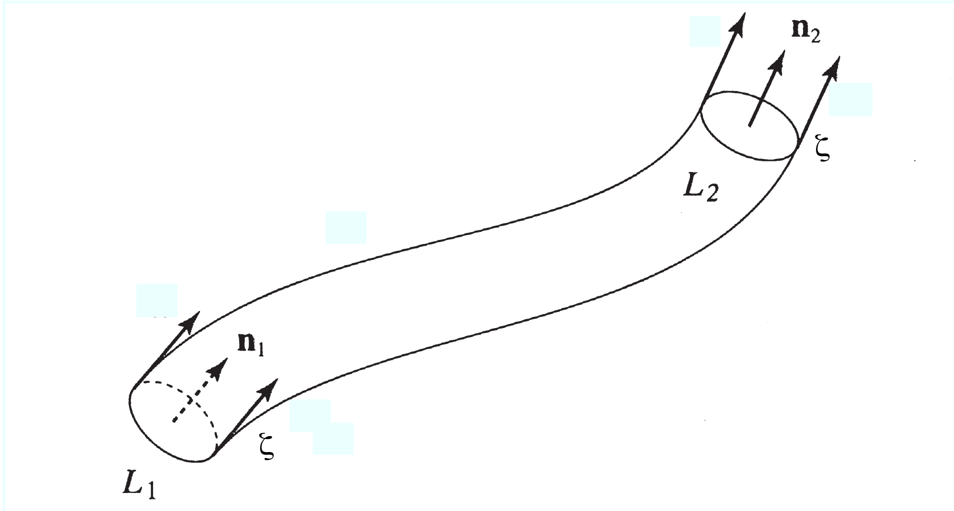

Figure 2.1: A vortex tube, whose sides are composed of vortex lines. Vortex lines are everywhere tangent to the vorticity vector. From Salmon 1998.

where the integral is around an arbitrary closed curve and $d\mathbf{r}$ is the vector element of length along the closed curve. Obviously, while the vector relative vorticity $\boldsymbol{\zeta} = \nabla \times \mathbf{u}$ is a pointwise measure of fluid rotation, the circulation C is a bulk measure of fluid rotation. It is very important to note that the closed curve in (2.11) and (2.12) is arbitrary. In particular, it may be fixed in space, or it may be defined by moving fluid particles.

What is the relationship between the vorticity $\boldsymbol{\zeta}$ and the circulation C? A first reaction to this question might be that there is none since $\boldsymbol{\zeta}$ is a vector and C is a scalar. However, the line integral in the definition of C is along an arbitrary circuit. In particular the circuit could be in the x-y plane, so in this case the circulation might be related to the z component of $\boldsymbol{\zeta}$. Similarly, a circuit in the y-z plane could be be related to the x component of $\boldsymbol{\zeta}$, and a circuit in the x-z plane could be be related to the y component of $\boldsymbol{\zeta}$. The circuit does not have to lie in one of the three cartesian coordinate planes. For example, it could lie in a surface of constant ρ, or a surface of constant p, or a surface of constant θ. This last case will prove very important in the derivation of Kelvin's circulation theorem (section 2.5).

To better understand the relationship of vorticity and circulation let us consider the case when the line integral in C lies in the x-y plane. Assume the circuit is a small rectangle with sides of length δx and δy, as shown in Fig. 2.2. The horizontal velocity at the center of the rectangle is u, v. The velocity components vary in space. For example, the v component on the right edge is approximately $v + \frac{1}{2}(\partial v/\partial x)\delta x$, and the v component on the left edge is approximately $v - \frac{1}{2}(\partial v/\partial x)\delta x$, where $\frac{1}{2}\delta x$ is the distance from the center to the left and right edges. Similarly, the u component on the top edge is approximately $u + \frac{1}{2}(\partial u/\partial y)\delta y$, and the u component on the bottom edge is approximately $u - \frac{1}{2}(\partial u/\partial y)\delta y$. The circulation is computed by taking the line integral of $\mathbf{u} \cdot d\mathbf{r}$, i.e.,

$$
\begin{aligned}
C &= \oint \mathbf{u} \cdot d\mathbf{r} \\
&= \left(u - \tfrac{1}{2}\frac{\partial u}{\partial y}\delta y\right)\delta x + \left(v + \tfrac{1}{2}\frac{\partial v}{\partial x}\delta x\right)\delta y - \left(u + \tfrac{1}{2}\frac{\partial u}{\partial y}\delta y\right)\delta x - \left(v - \tfrac{1}{2}\frac{\partial v}{\partial x}\delta x\right)\delta y \\
&= \left(\frac{\partial v}{\partial x} - \frac{\partial u}{\partial y}\right)\delta x \delta y. \qquad (2.13)
\end{aligned}
$$

This shows that, for a small loop, the circulation is approximately equal to the vorticity inside the loop times the area enclosed by the loop.

The exact and general relationship between circulation and vorticity is provided by Stokes' theorem (see Appendix A). Using Stokes's theorem we can rewrite (2.11) and (2.12) as

$$C = \oint \mathbf{u} \cdot d\mathbf{r} = \iint \boldsymbol{\zeta} \cdot \mathbf{n}\, dA, \qquad (2.14)$$

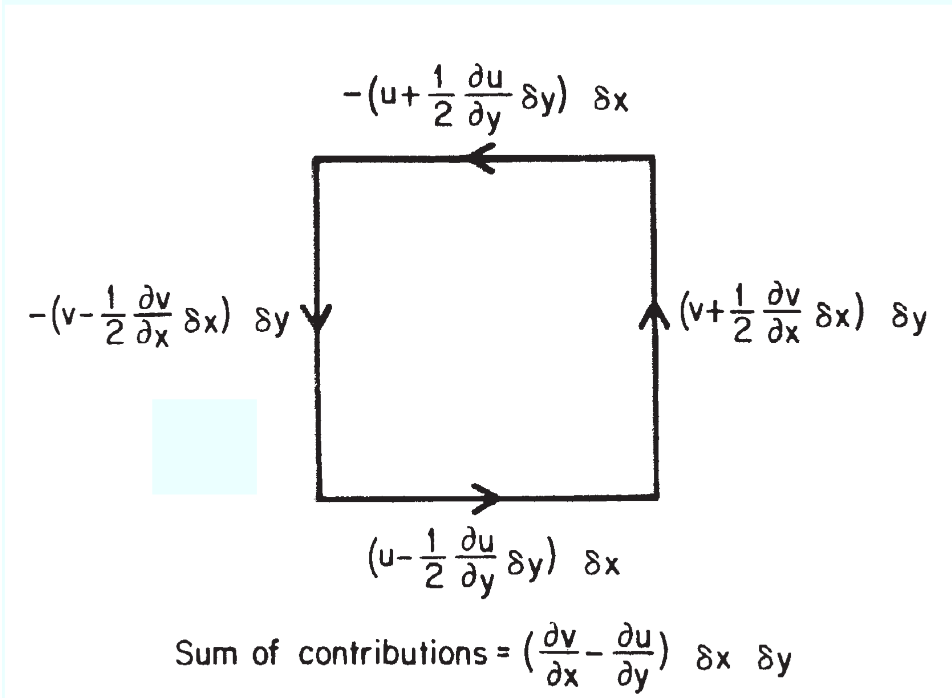

Figure 2.2: A small rectangular circuit with sides δx and δy in the x-y plane. From Gill 1982.

and

$$C_a = \oint \mathbf{u}_a \cdot d\mathbf{r} = \iint (2\boldsymbol{\Omega} + \boldsymbol{\zeta}) \cdot \mathbf{n}\, dA, \tag{2.15}$$

where, in the final equalities, the area integral is over a surface with unit outward normal $\mathbf{n}$ and area element dA. Note that (2.13) is a special case of (2.14).

2.2 Vector vorticity equation

We now derive the vector vorticity equation, i.e., the equation for the time evolution of $\boldsymbol{\zeta}_a$. Defining the absolute vorticity vector $\boldsymbol{\zeta}_a = 2\boldsymbol{\Omega} + \nabla \times \mathbf{u}$, we can write the momentum equation (1.35) as

$$\frac{\partial \mathbf{u}}{\partial t} + \tfrac{1}{2}\nabla(\mathbf{u}\cdot\mathbf{u}) - \mathbf{u}\times\boldsymbol{\zeta}_a = -\nabla\Phi - \boldsymbol{\Omega}\times(\boldsymbol{\Omega}\times\mathbf{r}) - \alpha\nabla p + \mathbf{F}. \tag{2.16}$$

Taking the curl of (2.16), and noting that $\nabla \times [\boldsymbol{\Omega}\times(\boldsymbol{\Omega}\times\mathbf{r})] = 0$ and that (A.8) and (A.4) can be used to show that $-\nabla\times(\alpha\nabla p) = \nabla p \times \nabla\alpha$, we obtain

$$\frac{\partial \boldsymbol{\zeta}_a}{\partial t} - \nabla\times(\mathbf{u}\times\boldsymbol{\zeta}_a) = \nabla p\times\nabla\alpha + \nabla\times\mathbf{F}. \tag{2.17}$$

Using (A.11) we have $\nabla\times(\mathbf{u}\times\boldsymbol{\zeta}_a) = \mathbf{u}(\nabla\cdot\boldsymbol{\zeta}_a) - \boldsymbol{\zeta}_a(\nabla\cdot\mathbf{u}) + (\boldsymbol{\zeta}_a\cdot\nabla)\mathbf{u} - (\mathbf{u}\cdot\nabla)\boldsymbol{\zeta}_a$, and since $\nabla\cdot\boldsymbol{\zeta}_a = 0$, we can write (2.17) as

$$\frac{D\boldsymbol{\zeta}_a}{Dt} + \boldsymbol{\zeta}_a\nabla\cdot\mathbf{u} = (\boldsymbol{\zeta}_a\cdot\nabla)\mathbf{u} + \nabla p\times\nabla\alpha + \nabla\times\mathbf{F}. \tag{2.18}$$

Using the mass continuity equation to eliminate $\nabla\cdot\mathbf{u}$, (2.18) becomes

$$\rho\frac{D}{Dt}\left(\frac{\boldsymbol{\zeta}_a}{\rho}\right) = (\boldsymbol{\zeta}_a\cdot\nabla)\mathbf{u} + \nabla p\times\nabla\alpha + \nabla\times\mathbf{F}. \tag{2.19}$$

The term $(\boldsymbol{\zeta}_a\cdot\nabla)\mathbf{u}$ incorporates the effects of vortex tilting and vortex stretching. To see this we first note that the operator $\boldsymbol{\zeta}_a\cdot\nabla$ is proportional to the derivative along the absolute vorticity vector, and that this operator acts on the vector velocity $\mathbf{u}$, which can have components perpendicular to and parallel to $\boldsymbol{\zeta}_a$. If the component of $\mathbf{u}$ perpendicular to $\boldsymbol{\zeta}_a$ varies in the dirction of $\boldsymbol{\zeta}_a$, then the vortex is tilted. If the component of $\mathbf{u}$ parallel to $\boldsymbol{\zeta}_a$ varies in the direction of $\boldsymbol{\zeta}_a$, then the vortex is stretched or compressed. The remaining two terms on the right hand side of (2.19) are the solenoidal and frictional terms. In the special case of an inviscid, constant density fluid, the last two terms in (2.19) vanish.

2.3 Potential vorticity equation

To derive the potential vorticity (PV) principle, we return to the vector vorticity equation in the form (2.17). Scalar multiplication of (2.17) by $\nabla\theta$ yields

$$\nabla\theta \cdot \frac{\partial \boldsymbol{\zeta}}{\partial t} - \nabla\theta \cdot \nabla \times (\mathbf{u} \times \boldsymbol{\zeta}) = \nabla\theta \cdot (\nabla p \times \nabla\alpha) + (\nabla \times \mathbf{F}) \cdot \nabla\theta. \tag{2.20}$$

The potential temperature θ is a function of p and ρ, so that

$$\nabla\theta = \left(\frac{\partial\theta}{\partial p}\right)_\rho \nabla p + \left(\frac{\partial\theta}{\partial\rho}\right)_p \nabla\rho. \tag{2.21}$$

Since $\nabla p \cdot (\nabla p \times \nabla\rho) = 0$ and $\nabla\rho \cdot (\nabla p \times \nabla\rho) = 0$, (2.21) implies that $\nabla\theta \cdot (\nabla p \times \nabla\rho) = 0$, so the first term on the right hand side of (2.20) vanishes. Now, using (A.10), we obtain $\nabla \cdot [\nabla\theta \times (\mathbf{u} \times \boldsymbol{\zeta}_a)] = -\nabla\theta \cdot \nabla \times (\mathbf{u} \times \boldsymbol{\zeta}_a)$, so that (2.20) becomes

$$\nabla\theta \cdot \frac{\partial \boldsymbol{\zeta}_a}{\partial t} + \nabla \cdot [\nabla\theta \times (\mathbf{u} \times \boldsymbol{\zeta}_a)] = (\nabla \times \mathbf{F}) \cdot \nabla\theta. \tag{2.22}$$

The triple vector product formula (A.2) results in $\nabla\theta \times (\mathbf{u} \times \boldsymbol{\zeta}_a) = \mathbf{u}(\boldsymbol{\zeta}_a \cdot \nabla\theta) - \boldsymbol{\zeta}_a(\mathbf{u} \cdot \nabla\theta)$, which, along with $\mathbf{u} \cdot \nabla\theta = \dot{\theta} - \partial\theta/\partial t$, allows us to write

$$\nabla\theta \times (\mathbf{u} \times \boldsymbol{\zeta}_a) = \mathbf{u}(\boldsymbol{\zeta}_a \cdot \nabla\theta) + \boldsymbol{\zeta}_a \left(\frac{\partial\theta}{\partial t} - \dot{\theta}\right). \tag{2.23}$$

Taking the divergence of (2.23) and using (A.7), we obtain

$$\nabla \cdot [\nabla\theta \times (\mathbf{u} \times \boldsymbol{\zeta}_a)] = \mathbf{u} \cdot \nabla(\boldsymbol{\zeta}_a \cdot \nabla\theta) + (\boldsymbol{\zeta}_a \cdot \nabla\theta)\nabla \cdot \mathbf{u} + \boldsymbol{\zeta}_a \cdot \nabla \left(\frac{\partial\theta}{\partial t} - \dot{\theta}\right), \tag{2.24}$$

since $\nabla \cdot \boldsymbol{\zeta}_a = 0$. Substitution of (2.24) into (2.22) results in

$$\frac{\partial(\boldsymbol{\zeta}_a \cdot \nabla\theta)}{\partial t} + \nabla \cdot [\mathbf{u}(\boldsymbol{\zeta}_a \cdot \nabla\theta)] = \boldsymbol{\zeta}_a \cdot \nabla\dot{\theta} + (\nabla \times \mathbf{F}) \cdot \nabla\theta, \tag{2.25}$$

which can also be written

$$\frac{D}{Dt}(\boldsymbol{\zeta}_a \cdot \nabla\theta) + (\boldsymbol{\zeta}_a \cdot \nabla\theta)\nabla \cdot \mathbf{u} = \boldsymbol{\zeta} \cdot \nabla\dot{\theta} + (\nabla \times \mathbf{F}) \cdot \nabla\theta. \tag{2.26}$$

Multiplication of (2.26) by α and use of the continuity equation (1.36) results in

$$\frac{DP}{Dt} = \frac{1}{\rho}\boldsymbol{\zeta}_a \cdot \nabla\dot{\theta} + \frac{1}{\rho}(\nabla \times \mathbf{F}) \cdot \nabla\theta, \tag{2.27}$$

where

$$P = \frac{1}{\rho}\boldsymbol{\zeta}_a \cdot \nabla\theta = \frac{1}{\rho}(2\boldsymbol{\Omega} + \nabla \times \mathbf{u}) \cdot \nabla\theta \tag{2.28}$$

is the Ertel potential vorticity. In the absence of friction and diabatic heating, the right hand side of (2.27) vanishes and the Ertel potential vorticity is materially conserved. This is one of the most important results in large-scale dynamic meteorology.

Defining $\hat{\mathbf{j}} = \nabla\theta/|\nabla\theta|$ as the unit vector normal to the θ-surface and $\hat{\mathbf{k}} = \boldsymbol{\zeta}_a/|\boldsymbol{\zeta}_a|$ as the unit vector along the absolute vorticity vector, we can rewrite (2.27) as

$$\frac{DP}{Dt} = P\left(\frac{\hat{\mathbf{j}} \cdot (\nabla \times \mathbf{F})}{\hat{\mathbf{j}} \cdot \boldsymbol{\zeta}_a} + \frac{\hat{\mathbf{k}} \cdot \nabla\dot{\theta}}{\hat{\mathbf{k}} \cdot \nabla\theta}\right). \tag{2.29}$$

2.4 Impermeability theorem

To prove the impermeability theorem we return to (2.25). Since $\rho P = \boldsymbol{\zeta}_a \cdot \nabla\theta$, and since (A.5) and (A.7) imply $\boldsymbol{\zeta} \cdot \nabla\dot{\theta} = \nabla \cdot (\boldsymbol{\zeta}\dot{\theta})$, while (A.4) and (A.10) imply $(\nabla \times \mathbf{F}) \cdot \nabla\theta = \nabla \cdot (\mathbf{F} \times \nabla\theta)$, we can rewrite (2.25) as

$$\frac{\partial(\rho P)}{\partial t} + \nabla \cdot \mathbf{J} = 0, \tag{2.30}$$

where

$$\mathbf{J} = \mathbf{u}\rho P - \boldsymbol{\zeta}_a\dot{\theta} - \mathbf{F} \times \nabla\theta \tag{2.31}$$

is the total flux of PV, consisting of the advective flux $\mathbf{u}\rho P$ and the nonadvective flux $-\boldsymbol{\zeta}_a\dot{\theta} - \mathbf{F} \times \nabla\theta$.

Now let's manipulate $\mathbf{J}$ in a way that yields the impermeability theorem. Let $\mathbf{u}_\parallel$ and $\boldsymbol{\zeta}_{a\parallel}$ denote the components of $\mathbf{u}$ and $\boldsymbol{\zeta}_a$ which are parallel to the θ-surface. These components are defined by simply subtracting from $\mathbf{u}$ and $\boldsymbol{\zeta}_a$ the components that are perpendicular to the θ-surface, i.e.,

$$\mathbf{u}_\parallel = \mathbf{u} - \frac{\mathbf{u} \cdot \nabla\theta}{|\nabla\theta|^2}\nabla\theta, \tag{2.32}$$

$$\boldsymbol{\zeta}_{a\parallel} = \boldsymbol{\zeta}_a - \frac{\boldsymbol{\zeta}_a \cdot \nabla\theta}{|\nabla\theta|^2}\nabla\theta. \tag{2.33}$$

Using (2.32) and (2.33) we can rewrite (2.31) as

$$\mathbf{J} = \left(\mathbf{u}_\parallel + \frac{\mathbf{u} \cdot \nabla\theta}{|\nabla\theta|^2}\nabla\theta\right)\rho P - \left(\boldsymbol{\zeta}_{a\parallel} + \frac{\boldsymbol{\zeta}_a \cdot \nabla\theta}{|\nabla\theta|^2}\nabla\theta\right)\dot{\theta} - \mathbf{F} \times \nabla\theta. \tag{2.34}$$

Now notice that the second term in the second large parentheses involves $\boldsymbol{\zeta}_a \cdot \nabla\theta$, which can be written as ρP. This allows the second term in the first large parentheses and the second term in the second large parentheses to be combined, so that (2.31) becomes

$$\mathbf{J} = \mathbf{u}_{\theta\perp}\rho P + \mathbf{u}_\parallel\rho P - \boldsymbol{\zeta}_{a\parallel}\dot{\theta} - \mathbf{F} \times \nabla\theta, \tag{2.35}$$

where

$$\mathbf{u}_{\theta\perp} = -\frac{\partial\theta/\partial t}{|\nabla\theta|^2}\nabla\theta. \tag{2.36}$$

It is important to note that the dot product of $\nabla\theta$ with (2.36) yields $\partial\theta/\partial t + \mathbf{u}_{\theta\perp} \cdot \nabla\theta = 0$, so that if you move with velocity $\mathbf{u}_{\theta\perp}$ (not the velocity of a mass element, which is $\mathbf{u}$), the potential temperature does not change. In other words, $\mathbf{u}_{\theta\perp}$ is the velocity of the isentropic surface normal to itself. Note what has happened: part of the advective flux has combined with part of the diabatic flux to yield $\mathbf{u}_{\theta\perp}\rho P$. The impermeability theorem, as stated by McIntyre, is as follows. *Since the last three terms in (2.35) all represent vectors lying parallel to the local isentropic surface, while the first is just ρP times the normal velocity $\mathbf{u}_{\theta\perp}$ of that surface, it follows that a point moving with velocity $\mathbf{J}/\rho P$ always remains on exactly the same isentropic surface, whether or not the air is moving across that surface as occurs when the diabatic heating $\dot{\theta} \neq 0$. The velocity $\mathbf{J}/\rho P$ can be pictured as the velocity with which PVS molecules or particles would move, discounting notional thermal motions.*

2.5 Circulation theorem

We now derive the circulation equation, i.e., the equation for the time evolution of C_a. Taking the time derivative of (2.15), and assuming the flow to be inviscid, we obtain

$$\begin{aligned}\frac{dC_a}{dt} &= \oint \frac{D}{Dt}\left(\mathbf{u}_a \cdot d\mathbf{r}\right) \\ &= \oint \left[\left(\frac{D\mathbf{u}}{Dt} + \boldsymbol{\Omega}\times\mathbf{u}\right)\cdot d\mathbf{r} + (\mathbf{u}+\boldsymbol{\Omega}\times\mathbf{r})\cdot d\mathbf{u}\right] \\ &= \oint \left(\frac{D\mathbf{u}}{Dt} + 2\boldsymbol{\Omega}\times\mathbf{u}\right)\cdot d\mathbf{r} \\ &= -\oint \left(\frac{1}{\rho}\nabla p + \nabla\Phi\right)\cdot d\mathbf{r} \\ &= -\oint \frac{1}{\rho}\nabla p \cdot d\mathbf{r} \\ &= -\oint \frac{dp}{\rho}. \end{aligned} \tag{2.37}$$

In going from the second to the third line we have used $(\mathbf{u}+\boldsymbol{\Omega}\times\mathbf{r})\cdot d\mathbf{u} = d[\frac{1}{2}\mathbf{u}_a\cdot\mathbf{u}_a] - d[\frac{1}{2}(\boldsymbol{\Omega}\times\mathbf{r})^2] - \mathbf{u}\cdot(\boldsymbol{\Omega}\times d\mathbf{r})$, which, upon integration, yields $\oint(\mathbf{u}+\boldsymbol{\Omega}\times\mathbf{r})\cdot d\mathbf{u} = \oint(\boldsymbol{\Omega}\times\mathbf{u})\cdot d\mathbf{r}$. In going from the third to the fourth line we have used the inviscid form of the momentum equation, and in going from the fourth to the fifth line, we have used $\oint \nabla\Phi\cdot d\mathbf{r} = \oint d\Phi = 0$. Returning to the fifth line in (2.37), and using Stokes' theorem (see Appendix A), we obtain

$$\begin{aligned}\frac{dC_a}{dt} &= -\oint \frac{1}{\rho}\nabla p\cdot d\mathbf{r} \\ &= -\iint \nabla\times\left(\frac{1}{\rho}\nabla p\right)\cdot\mathbf{n}\,dA \\ &= \iint \frac{1}{\rho^2}\left(\nabla\rho\times\nabla p\right)\cdot\mathbf{n}\,dA. \end{aligned} \tag{2.38}$$

If the flow is adiabatic, and if the chain of fluid particles constituting the line integral is initially on a θ-surface, the chain will remain on this same θ-surface. Thus, the surface involved in the area integral in the third line of (2.38) is a θ-surface, and $\mathbf{n}$ must be the unit normal to this θ-surface. This means that $(\nabla\rho\times\nabla p)\cdot\mathbf{n}$ must be proportional to $(\nabla\rho\times\nabla p)\cdot\nabla\theta$. But we argued in section 2.3 that $(\nabla\rho\times\nabla p)\cdot\nabla\theta = 0$, so that $(\nabla\rho\times\nabla p)\cdot\mathbf{n}$ must also vanish, and therefore

$$\frac{d}{dt}\oint \mathbf{u}_a\cdot d\mathbf{r} = 0. \tag{2.39}$$

This is the circulation theorem. It states that, for inviscid adiabatic flow, the circulation around any chain of particles on an isentropic surface, is invariant in time. Note the close connection with the PV equation.

2.6 Helicity

The helicity is defined by

$$H(t) = \iiint \mathbf{u}\cdot\boldsymbol{\zeta}\,dV. \tag{2.40}$$

In the special case when the fluid is homentropic, the equation for the time change of helicity is

$$\begin{aligned}\frac{DH}{Dt} &= \iiint \frac{D}{Dt}\left[\mathbf{u}\cdot(\boldsymbol{\zeta}/\rho)\right]\rho\,dV \\ &= \iiint \left[\frac{D\mathbf{u}}{Dt}\cdot(\boldsymbol{\zeta}/\rho) + \mathbf{u}\cdot\frac{D(\boldsymbol{\zeta}/\rho)}{Dt}\right]\rho\,dV \\ &= \iiint \left[-\nabla P\cdot\boldsymbol{\zeta} + \mathbf{u}\cdot(\boldsymbol{\zeta}\cdot\nabla)\mathbf{u}\right]dV \\ &= \iiint \left[-\nabla\cdot(P\boldsymbol{\zeta}) + \tfrac{1}{2}\nabla\cdot(\boldsymbol{\zeta}\mathbf{u}\cdot\mathbf{u})\right]dV \\ &= 0. \end{aligned} \tag{2.41}$$

The helicity is a measure of the knottedness of vortex tubes. It is not used much in large-scale geophysical fluid dynamics, but is useful in studies of rotating thunderstorms and tornadoes. A tornado has large upward components of both $\mathbf{u}$ and $\boldsymbol{\zeta}$, and hence can have large helicity. We can define helical turbulence as turbulent flow with a significant non-zero helicity. Kraichnan (1973) found that the inertial cascade of energy to smaller scales is slowed down in helical turbulence. Thus, helicity can stabilize a flow against turbulent decay.

Notes

1. A detailed discussion of impermeability is given by Haynes and McIntyre (1987, 1990).
2. For further discussion of helicity, see Moffatt (1969), Moffatt and Tsinober (1992) and Salmon (1998).

Required Reading

- Gill, sections 7.9, 7.11.
- Salmon, chapter 2.
- Holton, chapter 4.

3 The Exact Primitive Equations

3.1 Exact primitive equations in spherical coordinates

The vector equation of motion (1.35) is a compact statement that can be applied in any noninertial reference frame with rotation $\mathbf{\Omega}$. For applications we need to pick a particular coordinate system (e.g., Cartesian, cylindrical, spherical) and expand (1.35) into its components. For numerical weather prediction and general circulation modeling the spherical coordinates (λ, ϕ, r) are commonly used. Here λ is the longitude, ϕ the latitude and r the distance from the center of the earth.

Substituting $\mathbf{a} = \mathbf{b} = \mathbf{u}$ in the vector formula (A.9) of Appendix A, we obtain $(\mathbf{u}\cdot\nabla)\mathbf{u} = (\nabla\times\mathbf{u})\times\mathbf{u}+\frac{1}{2}\nabla(\mathbf{u}\cdot\mathbf{u})$. Thus,

$$\frac{D\mathbf{u}}{Dt} = \frac{\partial \mathbf{u}}{\partial t} + (\nabla\times\mathbf{u})\times\mathbf{u} + \tfrac{1}{2}\nabla(\mathbf{u}\cdot\mathbf{u}), \tag{3.1}$$

and we can write the equation of motion (1.35) as

$$\frac{\partial \mathbf{u}}{\partial t} + (\nabla\times\mathbf{u})\times\mathbf{u} + \tfrac{1}{2}\nabla(\mathbf{u}\cdot\mathbf{u}) + 2\mathbf{\Omega}\times\mathbf{u} = -\frac{1}{\rho}\nabla p + \mathbf{g} + \mathbf{F}. \tag{3.2}$$

The metric expression in spherical coordinates is

$$(dl)^2 = h_\lambda^2(d\lambda)^2 + h_\phi^2(d\phi)^2 + h_r^2(dr)^2, \tag{3.3}$$

where dl is an element of length and $h_\lambda = r\cos\phi,\ h_\phi = r,\ h_r = 1$. If $\mathbf{i}, \mathbf{j}, \mathbf{k}$ denote unit vectors in the eastward, northward and vertical directions, we have for the gradient, divergence and curl (see Appendix B for further discussion)

$$\nabla p = \mathbf{i}\frac{\partial p}{h_\lambda\partial\lambda} + \mathbf{j}\frac{\partial p}{h_\phi\partial\phi} + \mathbf{k}\frac{\partial p}{h_r\partial r}, \tag{3.4}$$

$$\nabla\cdot\mathbf{u} = \frac{1}{h_\lambda h_\phi h_r}\left[\frac{\partial(h_\phi h_r u)}{\partial\lambda} + \frac{\partial(h_\lambda h_r v)}{\partial\phi} + \frac{\partial(h_\lambda h_\phi w)}{\partial r}\right], \tag{3.5}$$

$$\nabla\times\mathbf{u} = \frac{\mathbf{i}}{h_\phi h_r}\left[\frac{\partial(h_r w)}{\partial\phi} - \frac{\partial(h_\phi v)}{\partial r}\right] + \frac{\mathbf{j}}{h_\lambda h_r}\left[\frac{\partial(h_\lambda u)}{\partial r} - \frac{\partial(h_r w)}{\partial\lambda}\right] + \frac{\mathbf{k}}{h_\lambda h_\phi}\left[\frac{\partial(h_\phi v)}{\partial\lambda} - \frac{\partial(h_\lambda u)}{\partial\phi}\right]. \tag{3.6}$$

Let $\mathbf{u}_e$ be a vector of magnitude $\Omega r\cos\phi$ directed eastward, i.e., $\mathbf{u}_e = \mathbf{i}\Omega r\cos\phi$. Then

$$\nabla\times\mathbf{u}_e = \frac{1}{r^2\cos\phi}\begin{vmatrix} r\cos\phi\mathbf{i} & r\mathbf{j} & \mathbf{k} \\ \dfrac{\partial}{\partial\lambda} & \dfrac{\partial}{\partial\phi} & \dfrac{\partial}{\partial r} \\ \Omega r^2\cos^2\phi & 0 & 0 \end{vmatrix} = \mathbf{j}2\Omega\cos\phi + \mathbf{k}2\Omega\sin\phi = 2\mathbf{\Omega}. \tag{3.7}$$

Using (3.7) we can write (3.2) as

$$\frac{\partial \mathbf{u}}{\partial t} - \mathbf{u}\times\Big[\nabla\times(\mathbf{u}+\mathbf{u}_e)\Big] + \tfrac{1}{2}\nabla(\mathbf{u}\cdot\mathbf{u}) = -\frac{1}{\rho}\nabla p + \mathbf{g} + \mathbf{F}. \tag{3.8}$$

We can now write

$$\mathbf{u}\times\Big[\nabla\times(\mathbf{u}+\mathbf{u}_e)\Big] =$$

$$\begin{vmatrix} \mathbf{i} & \mathbf{j} & \mathbf{k} \\ u & v & w \\ \dfrac{1}{h_\phi h_r}\left[\dfrac{\partial(h_r w)}{\partial\phi} - \dfrac{\partial(h_\phi v)}{\partial r}\right] & \dfrac{1}{h_\lambda h_r}\left[\dfrac{\partial\left(h_\lambda(u+u_e)\right)}{\partial r} - \dfrac{\partial(h_r w)}{\partial\lambda}\right] & \dfrac{1}{h_\lambda h_\phi}\left[\dfrac{\partial(h_\phi v)}{\partial\lambda} - \dfrac{\partial\left(h_\lambda(u+u_e)\right)}{\partial\phi}\right] \end{vmatrix}$$

or

$$\mathbf{u}\times\Big[\nabla\times(\mathbf{u}+\mathbf{u}_e)\Big]=\mathbf{i}\left\{\frac{v}{h_\lambda h_\phi}\left[\frac{\partial(h_\phi v)}{\partial\lambda}-\frac{\partial\left(h_\lambda(u+u_e)\right)}{\partial\phi}\right]-\frac{w}{h_\lambda h_r}\left[\frac{\partial\left(h_\lambda(u+u_e)\right)}{\partial r}-\frac{\partial(h_r w)}{\partial\lambda}\right]\right\}$$
$$+\mathbf{j}\left\{\frac{w}{h_\phi h_r}\left[\frac{\partial(h_r w)}{\partial\phi}-\frac{\partial(h_\phi v)}{\partial r}\right]-\frac{u}{h_\lambda h_\phi}\left[\frac{\partial(h_\phi v)}{\partial\lambda}-\frac{\partial\left(h_\lambda(u+u_e)\right)}{\partial\phi}\right]\right\} \tag{3.9}$$
$$+\mathbf{k}\left\{\frac{u}{h_\lambda h_r}\left[\frac{\partial\left(h_\lambda(u+u_e)\right)}{\partial r}-\frac{\partial(h_r w)}{\partial\lambda}\right]-\frac{v}{h_\phi h_r}\left[\frac{\partial(h_r w)}{\partial\phi}-\frac{\partial(h_\phi v)}{\partial r}\right]\right\}$$

and

$$\tfrac{1}{2}\nabla(\mathbf{u}\cdot\mathbf{u})=\mathbf{i}\frac{\partial}{h_\lambda\partial\lambda}\left[\tfrac{1}{2}\left(u^2+v^2+w^2\right)\right]+\mathbf{j}\frac{\partial}{h_\phi\partial\phi}\left[\tfrac{1}{2}\left(u^2+v^2+w^2\right)\right]+\mathbf{k}\frac{\partial}{h_r\partial r}\left[\tfrac{1}{2}\left(u^2+v^2+w^2\right)\right]. \tag{3.10}$$

Using (3.9) and (3.10) in (3.8) we can write the component equations as

$$\frac{\partial u}{\partial t}-\frac{v}{h_\lambda h_\phi}\left[\frac{\partial(h_\phi v)}{\partial\lambda}-\frac{\partial\left(h_\lambda(u+u_e)\right)}{\partial\phi}\right]+\frac{w}{h_\lambda h_r}\left[\frac{\partial\left(h_\lambda(u+u_e)\right)}{\partial r}-\frac{\partial(h_r w)}{\partial\lambda}\right]$$
$$+\frac{\partial}{h_\lambda\partial\lambda}\left[\tfrac{1}{2}(u^2+v^2+w^2)\right]+\frac{1}{\rho}\frac{\partial p}{h_\lambda\partial\lambda}=F_\lambda, \tag{3.11}$$

$$\frac{\partial v}{\partial t}-\frac{w}{h_\phi h_r}\left[\frac{\partial(h_r w)}{\partial\phi}-\frac{\partial(h_\phi v)}{\partial r}\right]+\frac{u}{h_\lambda h_\phi}\left[\frac{\partial(h_\phi v)}{\partial\lambda}-\frac{\partial\left(h_\lambda(u+u_e)\right)}{\partial\phi}\right]$$
$$+\frac{\partial}{h_\phi\partial\phi}\left[\tfrac{1}{2}(u^2+v^2+w^2)\right]+\frac{1}{\rho}\frac{\partial p}{h_\phi\partial\phi}=F_\phi, \tag{3.12}$$

$$\frac{\partial w}{\partial t}-\frac{u}{h_\lambda h_r}\left[\frac{\partial\left(h_\lambda(u+u_e)\right)}{\partial r}-\frac{\partial(h_r w)}{\partial\lambda}\right]+\frac{v}{h_\phi h_r}\left[\frac{\partial(h_r w)}{\partial\phi}-\frac{\partial(h_\phi v)}{\partial r}\right]$$
$$+\frac{\partial}{h_r\partial r}\left[\tfrac{1}{2}(u^2+v^2+w^2)\right]+g+\frac{1}{\rho}\frac{\partial p}{h_r\partial r}=F_r. \tag{3.13}$$

Using $h_\lambda=r\cos\phi$, $h_\phi=r$, $h_r=1$ and $u_e=\Omega r\cos\phi$ we can derive from (3.11)–(3.13) the following rotational forms of the component equations:

$$\frac{\partial u}{\partial t}-v\left[\frac{\partial v}{r\cos\phi\partial\lambda}-\frac{\partial\left((u+\Omega r\cos\phi)\cos\phi\right)}{r\cos\phi\partial\phi}\right]+w\left[\frac{\partial\left(r(u+\Omega r\cos\phi)\right)}{r\partial r}-\frac{\partial w}{r\cos\phi\partial\lambda}\right]$$
$$+\frac{\partial}{r\cos\phi\partial\lambda}\left[\tfrac{1}{2}(u^2+v^2+w^2)\right]+\frac{1}{\rho}\frac{\partial p}{r\cos\phi\partial\lambda}=F_\lambda, \tag{3.14}$$

$$\frac{\partial v}{\partial t}-w\left[\frac{\partial w}{r\partial\phi}-\frac{\partial(rv)}{r\partial r}\right]+u\left[\frac{\partial v}{r\cos\phi\partial\lambda}-\frac{\partial\left((u+\Omega r\cos\phi)\cos\phi\right)}{r\cos\phi\partial\phi}\right]$$
$$+\frac{\partial}{r\partial\phi}\left[\tfrac{1}{2}(u^2+v^2+w^2)\right]+\frac{1}{\rho}\frac{\partial p}{r\partial\phi}=F_\phi, \tag{3.15}$$

$$\frac{\partial w}{\partial t}-u\left[\frac{\partial\left(r(u+\Omega r\cos\phi)\right)}{r\partial r}-\frac{\partial w}{r\cos\phi\partial\lambda}\right]+v\left[\frac{\partial w}{r\partial\phi}-\frac{\partial(rv)}{r\partial r}\right]$$
$$+\frac{\partial}{\partial r}\left[\tfrac{1}{2}(u^2+v^2+w^2)\right]+g+\frac{1}{\rho}\frac{\partial p}{\partial r}=F_r. \tag{3.16}$$

The rotational forms (3.14)–(3.16) can easily be converted into the advective forms

$$\frac{Du}{Dt} - \left(2\Omega + \frac{u}{r\cos\phi}\right)\left(v\sin\phi - w\cos\phi\right) + \frac{1}{\rho}\frac{\partial p}{r\cos\phi\partial\lambda} = F_\lambda, \tag{3.17}$$

$$\frac{Dv}{Dt} + \left(2\Omega + \frac{u}{r\cos\phi}\right)u\sin\phi + \frac{vw}{r} + \frac{1}{\rho}\frac{\partial p}{r\partial\phi} = F_\phi, \tag{3.18}$$

$$\frac{Dw}{Dt} - \left(2\Omega + \frac{u}{r\cos\phi}\right)u\cos\phi - \frac{v^2}{r} + \frac{1}{\rho}\frac{\partial p}{\partial r} + g = F_r, \tag{3.19}$$

where

$$\frac{D}{Dt} = \frac{\partial}{\partial t} + u\frac{\partial}{r\cos\phi\partial\lambda} + v\frac{\partial}{r\partial\phi} + w\frac{\partial}{\partial r}. \tag{3.20}$$

Equations (3.14)–(3.16), or their advective forms (3.17)–(3.19), are called the nonhydrostatic primitive equations or the exact primitive equations. They are not widely used at present. For large scale numerical weather prediction and general circulation modeling two approximations are made—the traditional approximation and the quasi-static approximation. The traditional approximation involves an approximation to the metric expression while the quasi-static approximation involves an approximation to the vertical equation (3.19). We shall study these two approximations in Chapters 4 and 5.

3.2 Summary

To summarize, the exact primitive equations in spherical coordinates are a set of five prognostic equations for u, v, w, ρ, s and two diagnostic equations for T and p:

$$\frac{Du}{Dt} - \left(2\Omega + \frac{u}{r\cos\phi}\right)(v\sin\phi - w\cos\phi) + \frac{1}{\rho}\frac{\partial p}{r\cos\phi\partial\lambda} = F_\lambda, \tag{3.21}$$

$$\frac{Dv}{Dt} + \left(2\Omega + \frac{u}{r\cos\phi}\right)u\sin\phi + \frac{vw}{r} + \frac{1}{\rho}\frac{\partial p}{r\partial\phi} = F_\phi, \tag{3.22}$$

$$\frac{Dw}{Dt} - \left(2\Omega + \frac{u}{r\cos\phi}\right)u\cos\phi - \frac{v^2}{r} + g + \frac{1}{\rho}\frac{\partial p}{\partial r} = F_r, \tag{3.23}$$

$$\frac{D\rho}{Dt} + \rho\left(\frac{\partial u}{r\cos\phi\partial\lambda} + \frac{\partial(v\cos\phi)}{r\cos\phi\partial\phi} + \frac{\partial(r^2 w)}{r^2\partial r}\right) = 0, \tag{3.24}$$

$$\frac{Ds}{Dt} = \frac{Q}{T}, \tag{3.25}$$

$$T = T_0\left(\frac{\rho}{\rho_0}\right)^{R/c_v} e^{s/c_v}. \tag{3.26}$$

$$p = \rho RT, \tag{3.27}$$

where

$$\frac{D}{Dt} = \frac{\partial}{\partial t} + u\frac{\partial}{r\cos\phi\partial\lambda} + v\frac{\partial}{r\partial\phi} + w\frac{\partial}{\partial r}. \tag{3.28}$$

Equations (3.21)–(3.27) constitute a closed system of seven equations in the seven unknowns u, v, w, ρ, s, T, p.

Required Reading

- Holton, section 2.3 (Can you find any errors?).
- Gill, section 4.12 (Can you find any errors?).

Problems

1. (a) Prove that (3.21) can be written as the angular momentum principle

$$\frac{D}{Dt}\left[(\Omega r\cos\phi + u)\, r\cos\phi\right] + \frac{1}{\rho}\frac{\partial p}{\partial\lambda} = F_\lambda r\cos\phi.$$

   (b) For zonally symmetric, inviscid flow, compute the zonal wind of a parcel which has risen, at the equator, from the ocean surface to a height of 16 km above sea level. Assume the zonal velocity was zero at sea level.

   (c) Now assume this parcel moves poleward, at 16 km height, to 30 N. What is its zonal velocity at this latitude?

2. Derive the kinetic energy principle from the exact primitive equations (3.21)–(3.23).

4 Primitive Equations for Shallow Atmospheres

4.1 Primitive equations with the traditional approximation

Let us define the constant a as the radius to mean sea-level and the independent variable z as the height above the sphere with radius a, so that $r = a + z$. Now, $a = 6371$ km while z is less than 20 km for tropospheric models. Thus, it seems reasonable to approximate the metric coefficients by $h_\lambda = a\cos\phi$, $h_\phi = a$, $h_r = 1$ and the velocity due to the earth's rotation by $u_e = \Omega a \cos\phi$. If we use these approximate expressions for the metric coefficients and the velocity due to the earth's rotation in (3.11)–(3.13), we obtain the approximate momentum equations

$$\frac{\partial u}{\partial t} - v\left[\frac{\partial v}{a\cos\phi\partial\lambda} - \frac{\partial\left((u+\Omega a\cos\phi)\cos\phi\right)}{a\cos\phi\partial\phi}\right] + w\left[\frac{\partial\left(u+\Omega a\cos\phi\right)}{\partial z} - \frac{\partial w}{a\cos\phi\partial\lambda}\right] + \frac{\partial}{a\cos\phi\partial\lambda}\left[\tfrac{1}{2}(u^2+v^2+w^2)\right] + \frac{1}{\rho}\frac{\partial p}{a\cos\phi\partial\lambda} = F_\lambda, \quad (4.1)$$

$$\frac{\partial v}{\partial t} - w\left[\frac{\partial w}{a\partial\phi} - \frac{\partial v}{\partial z}\right] + u\left[\frac{\partial v}{a\cos\phi\partial\lambda} - \frac{\partial\left((u+\Omega a\cos\phi)\cos\phi\right)}{a\cos\phi\partial\phi}\right] + \frac{\partial}{a\partial\phi}\left[\tfrac{1}{2}(u^2+v^2+w^2)\right] + \frac{1}{\rho}\frac{\partial p}{a\partial\phi} = F_\phi, \quad (4.2)$$

$$\frac{\partial w}{\partial t} - u\left[\frac{\partial\left(u+\Omega a\cos\phi\right)}{\partial z} - \frac{\partial w}{a\cos\phi\partial\lambda}\right] + v\left[\frac{\partial w}{a\partial\phi} - \frac{\partial v}{\partial z}\right] + \frac{\partial}{\partial z}\left[\tfrac{1}{2}(u^2+v^2+w^2)\right] + g + \frac{1}{\rho}\frac{\partial p}{\partial z} = F_z. \quad (4.3)$$

Equations (4.1)–(4.3) are the nonhydrostatic primitive equations with the "traditional" approximation. Note how they differ from the exact nonhydrostatic primitive equations (3.14)–(3.16). The rotational forms (4.1)–(4.3) can be converted to the advective forms (4.4)–(4.6). See problem 1.

4.2 Summary

We have now presented two different levels of dynamics: the exact nonhydrostatic primitive equations (Chapter 3) and the nonhydrostatic primitive equations with the traditional approximation. To summarize the nonhydrostatic primitive equations with the traditional approximation we need the mass conservation principle, the entropy conservation principle, the definition of specific entropy, and the ideal gas law. The complete systems of primitive equations with the traditional approximation can be summarized as follows:

$$\frac{Du}{Dt} - \left(2\Omega\sin\phi + \frac{u\tan\phi}{a}\right)v + \frac{1}{\rho}\frac{\partial p}{a\cos\phi\partial\lambda} = F_\lambda, \quad (4.4)$$

$$\frac{Dv}{Dt} + \left(2\Omega\sin\phi + \frac{u\tan\phi}{a}\right)u + \frac{1}{\rho}\frac{\partial p}{a\partial\phi} = F_\phi, \quad (4.5)$$

$$\frac{Dw}{Dt} + g + \frac{1}{\rho}\frac{\partial p}{\partial z} = F_z, \quad (4.6)$$

$$\frac{D\rho}{Dt} + \rho\left(\frac{\partial u}{a\cos\phi\partial\lambda} + \frac{\partial(v\cos\phi)}{a\cos\phi\partial\phi} + \frac{\partial w}{\partial z}\right) = 0, \quad (4.7)$$

$$\frac{Ds}{Dt} = \frac{Q}{T}, \quad (4.8)$$

$$T = T_0\left(\frac{\rho}{\rho_0}\right)^{R/c_v} e^{s/c_v}, \quad (4.9)$$

$$p = \rho R T, \quad (4.10)$$

where

$$\frac{D}{Dt} = \frac{\partial}{\partial t} + u\frac{\partial}{a\cos\phi\partial\lambda} + v\frac{\partial}{a\partial\phi} + w\frac{\partial}{\partial z}. \quad (4.11)$$

Just as with the exact system (3.21)–(3.28), the approximate system (4.4)–(4.11) constitutes a closed system of seven equations in the seven unknowns u, v, w, ρ, s, T, p. Equations (4.4)–(4.11) involve rather minor approximations to (3.21)–(3.28) and should give accurate results because the earth's atmosphere is so shallow.

The nonhydrostatic primitive equations with the traditional approximation are not used much in atmospheric science, since they are just as hard to solve as the exact nonhydrostatic primitive equations. However, the nonhydrostatic primitive equations with the traditional approximation are an important intermediate step in understanding the quasi-static primitive equations with the traditional approximation, which are the equations commonly used in large-scale numerical weather prediction and climate modeling. The term "quasi-static" means that a further approximation to (4.4)–(4.11) is introduced. This is discussed in the next chapter.

Problems

1. Convert the rotational forms (4.1)–(4.3) to the advective forms (4.4)–(4.6) and discuss the differences between the exact primitive equations (3.21)–(3.28) and the primitive equations with the traditional approximation, (4.4)–(4.11).

2. Prove that (4.4) can be written as the approximate angular momentum principle

$$\frac{D}{Dt}\left[(\Omega a \cos\phi + u)a\cos\phi\right] + \frac{1}{\rho}\frac{\partial p}{\partial \lambda} = F_\lambda a \cos\phi.$$

   Discuss how this is a slightly distorted form of the exact principle, which you derived in problem 1 of Chapter 3. Using the above approximate angular momentum principle, repeat the calculations you did with the exact principle in problem 1 of Chapter 3. Almost all present NWP models and general circulation models use the traditional approximation and thus have the above approximate angular momentum principle. How large are the zonal wind errors in the tropics due to the traditional approximation in such models?

3. Derive the kinetic energy principle from the traditional approximation (4.4)–(4.6). Discuss its differences with the kinetic energy principle you derived from the exact primitive equations.

4. Some researchers have approximated (3.21) by simply replacing r by a (see Holton's book, page 37). Note that this is a different approximation than (4.4). Discuss why this is a bad idea. Hint: Argue from the angular momentum principle.

5 The Quasi-static Primitive Equations

5.1 Scale analysis

The quasi-static approximation consists of the traditional approximation plus ignoring Dw/Dt and F_z in (4.6). To see when the neglect of Dw/Dt is justified, let the pressure and density be divided into a standard atmosphere part and a deviation therefrom. If the standard atmosphere is defined as being in hydrostatic balance, we have $p = p_s(z) + p'$, $\rho = \rho_s(z) + \rho'$ and $\partial p_s/\partial z = -\rho_s g$. Equation (4.6) can then be written

$$\rho_s \left(1 + \frac{\rho'}{\rho_s}\right) \frac{Dw}{Dt} = -\frac{\partial p'}{\partial z} - \rho' g. \tag{5.1}$$

Assuming $|\rho'/\rho_s| << 1$, when is $\rho_s|Dw/Dt|$ sufficiently small compared with $|\partial p'/\partial z|$? It is important to note that requiring $|Dw/Dt|$ to be small compared to $\rho_s^{-1}|\partial p'/\partial z|$ is much stricter than requiring $|Dw/Dt|$ to be small compared to $\rho^{-1}|\partial p/\partial z|$ because $\rho_s^{-1}|\partial p'/\partial z|$ is much smaller than $\rho^{-1}|\partial p/\partial z|$. To answer this question we define

V : characteristic magnitude of u and v;
W : characteristic magnitude of w;
L : characteristic horizontal scale;
D : characteristic vertical scale;
$1/N$: characteristic time scale.

Then we can estimate the order of magnitude of the terms in (4.4)–(4.6) as

$$\frac{Du}{Dt} \sim NV, \qquad \left(2\Omega\sin\phi + \frac{u\tan\phi}{a}\right) v \sim fV, \qquad \frac{1}{\rho}\frac{\partial p}{a\cos\phi\partial\lambda} \sim \frac{p'}{\rho_s L},$$

$$\frac{Dv}{Dt} \sim NV, \qquad \left(2\Omega\sin\phi + \frac{u\tan\phi}{a}\right) u \sim fV, \qquad \frac{1}{\rho}\frac{\partial p}{a\partial\phi} \sim \frac{p'}{\rho_s L},$$

$$\rho\frac{Dw}{Dt} \sim \rho_s NW, \qquad \frac{\partial p'}{\partial z} \sim \frac{p'}{D}.$$

Two cases arise:

Case (i): $N \geq f$.
The balance in the horizontal momentum equations is primarily between the pressure gradient term and the acceleration term. Thus, $p' \sim \rho_s NLV$ and $\rho|Dw/Dt| << |\partial p'/\partial z|$ when $\rho_s NW << \rho_s NLV/D$ or

$$\left(\frac{W/D}{V/L}\right)\left(\frac{D}{L}\right)^2 << 1.$$

Case (ii): $N \leq f$.
The balance in the horizontal momentum equations is primarily between the pressure gradient term and the Coriolis term. Thus, $p' \sim \rho_s fLV$ and $\rho|Dw/Dt| << |\partial p'/\partial z|$ when $\rho_s NW << \rho_s fLV/D$ or

$$\frac{N}{f}\left(\frac{W/D}{V/L}\right)\left(\frac{D}{L}\right)^2 << 1.$$

Usually $\frac{W/D}{V/L} \leq 1$ and $(D/L)^2 << 1$ is sufficient to justify the quasi-static approximation. In a typical extratropical cyclone $D \sim 10$ km and $L \sim 1000$ km so that $(D/L)^2 \sim 10^{-4}$.

5.2 Summary

We have now presented three different levels of dynamics: the exact primitive equations, the primitive equations with the traditional approximation, and the quasi-static primitive equations. To summarize, for the exact primitive equations we have (3.21)–(3.28), for the primitive equations with the traditional approximation we have (4.4)–(4.11), and for the quasi-static primitive equations we have

$$\frac{Du}{Dt} - \left(2\Omega \sin\phi + \frac{u\tan\phi}{a}\right) v + \frac{1}{\rho}\frac{\partial p}{a\cos\phi\partial\lambda} = F_\lambda, \tag{5.2}$$

$$\frac{Dv}{Dt} + \left(2\Omega \sin\phi + \frac{u\tan\phi}{a}\right) u + \frac{1}{\rho}\frac{\partial p}{a\partial\phi} = F_\phi, \tag{5.3}$$

$$\frac{1}{\rho}\frac{\partial p}{\partial z} = -g, \tag{5.4}$$

$$\frac{D\rho}{Dt} + \rho\left(\frac{\partial u}{a\cos\phi\partial\lambda} + \frac{\partial(v\cos\phi)}{a\cos\phi\partial\phi} + \frac{\partial w}{\partial z}\right) = 0, \tag{5.5}$$

$$\frac{Ds}{Dt} = \frac{Q}{T}, \tag{5.6}$$

$$T = T_0\left(\frac{\rho}{\rho_0}\right)^{R/c_v} e^{s/c_v}. \tag{5.7}$$

$$p = \rho R T, \tag{5.8}$$

where

$$\frac{D}{Dt} = \frac{\partial}{\partial t} + u\frac{\partial}{a\cos\phi\partial\lambda} + v\frac{\partial}{a\partial\phi} + w\frac{\partial}{\partial z}. \tag{5.9}$$

Equations (5.2)–(5.9) constitute a closed system of seven equations in the seven unknowns u, v, w, ρ, s, T, p. Note that, while w is no longer a predicted variable, it must be listed as one of the unknowns since it appears in the operator D/Dt and also in the last term of (5.5).

It is sometimes claimed that the quasi-static equations assume $Dw/Dt = 0$. This claim is erroneous. If it were true, a parcel could never reverse directions in the vertical. What the quasi-static equations assume is that $|Dw/Dt|$ is small compared to $\rho_s^{-1}|\partial p'/\partial z|$. In fact, the quasi-static equations produce solutions with nonzero Dw/Dt. For example, the quasi-static equations can accurately simulate the synopic-scale cyclones and anticyclones of midlatitudes. In typical midlatiude synoptic weather systems, air parcels move eastward through troughs and ridges and, in the process, gently ascend and descend. Thus, since w alternately changes sign, Dw/Dt is not zero. A similar argument involving alternate changes in the sign of w can be made for long gravity waves, which the quasi-static equations also accurately simulate. To actually check that the solutions of the quasi-static system are consistent with the assumptions built into the system, we should *a posteriori* test to see if the predicted values of Dw/Dt have magnitude small compared to $\rho_s^{-1}|\partial p'/\partial z|$. If this is indeed true, we can conclude that the solutions produced by the quasi-static equations are very nearly identical to the solutions that would be produced by the exact primitive equations (which include the Dw/Dt term in the vertical equation of motion).

Large-scale numerical weather prediction and general circulation modeling is done almost exclusively with the quasi-static primitive equations, but the z-coordinate is rarely used. Since ρ and g are positive, (5.4) implies that p monotonically decreases with z, i.e., there is a one-to-one correspondence between p and z. Thus, p could be used as the vertical coordinate in the quasi-static primitive equations. There are many variations on this theme, e.g., the log of pressure, pressure raised to the κ power, or pressure normalized by surface pressure. Almost everything we will do in this book involves some kind of further approximation to (5.2)–(5.9).

Problems

1. Derive the kinetic energy principle from the quasi-static primitive equations (5.2)–(5.4). Compare it with the kinetic energy principle derived from the exact primitive equations (problem 2 of Chapter 3) and with the kinetic energy principle derived from the primitive equations with the traditional approximation (problem 3 of Chapter 4).

2. Some researchers have approximated (3.23) by the hydrostatic equation but have left (3.21) and (3.22) unchanged. Discuss why this is a bad idea.

6 Transformation of the Quasi-static Primitive Equation to a Generalized Vertical Coordinate

6.1 The general $\eta(p, p_s, \theta)$ coordinate

Using the longitude λ, the latitude ϕ, and the physical height z as the independent spatial coordinates, the quasi-static primitive equations (with the traditional approximation) for inviscid, adiabatic flow are

$$\frac{Du}{Dt} - \left(2\Omega\sin\phi + \frac{u\tan\phi}{a}\right)v + \frac{1}{\rho}\left(\frac{\partial p}{a\cos\phi\partial\lambda}\right)_z = 0, \tag{6.1}$$

$$\frac{Dv}{Dt} + \left(2\Omega\sin\phi + \frac{u\tan\phi}{a}\right)u + \frac{1}{\rho}\left(\frac{\partial p}{a\partial\phi}\right)_z = 0, \tag{6.2}$$

$$g + \frac{1}{\rho}\frac{\partial p}{\partial z} = 0, \tag{6.3}$$

$$\frac{1}{\rho}\frac{D\rho}{Dt} + \left(\frac{\partial u}{a\cos\phi\partial\lambda}\right)_z + \left(\frac{\partial(v\cos\phi)}{a\cos\phi\partial\phi}\right)_z + \frac{\partial w}{\partial z} = 0, \tag{6.4}$$

$$c_p\frac{DT}{Dt} - \frac{1}{\rho}\frac{Dp}{Dt} = 0, \tag{6.5}$$

$$p = \rho RT, \tag{6.6}$$

where

$$\frac{D}{Dt} = \left(\frac{\partial}{\partial t}\right)_z + u\left(\frac{\partial}{a\cos\phi\partial\lambda}\right)_z + v\left(\frac{\partial}{a\partial\phi}\right)_z + w\frac{\partial}{\partial z} \tag{6.7}$$

is the material derivative. Equations (6.1)–(6.6) constitute a closed system of six equations in the six dependent variables u, v, w, ρ, T, p, each of which is a function of the independent variables (λ, ϕ, z, t). Note that subscripts have been used in order to explicitly show that z is held fixed during the differentiations with respect to t, λ and ϕ.

We shall now transform (6.1)–(6.7) to the new independent variables (λ, ϕ, η, t), where the new vertical coordinate $\eta(p, p_s, \theta)$ is some function of the pressure p, the surface pressure p_s and the potential temperature θ. After we complete the transformation we shall consider several special cases, such as $\eta = p$, $\eta = \ln(p_0/p)$, $\eta = (c_p\theta_0/g)[1 - (p/p_0)^\kappa]$, $\eta = p/p_s$, and $\eta = \theta$.

We begin by transforming the material derivative (6.7). The required transformation formulas are

$$\left(\frac{\partial}{\partial t}\right)_z = \left(\frac{\partial}{\partial t}\right)_\eta + \left(\frac{\partial\eta}{\partial t}\right)_z\frac{\partial}{\partial\eta}, \tag{6.8}$$

$$\left(\frac{\partial}{a\cos\phi\partial\lambda}\right)_z = \left(\frac{\partial}{a\cos\phi\partial\lambda}\right)_\eta + \left(\frac{\partial\eta}{a\cos\phi\partial\lambda}\right)_z\frac{\partial}{\partial\eta}, \tag{6.9}$$

$$\left(\frac{\partial}{a\partial\phi}\right)_z = \left(\frac{\partial}{a\partial\phi}\right)_\eta + \left(\frac{\partial\eta}{a\partial\phi}\right)_z\frac{\partial}{\partial\eta}, \tag{6.10}$$

$$\frac{\partial}{\partial z} = \frac{\partial\eta}{\partial z}\frac{\partial}{\partial\eta}. \tag{6.11}$$

Adding (6.8) to the sum of u times (6.9), v times (6.10), and w times (6.11), and then comparing the result to (6.7), we obtain (6.26) below, where $\dot\eta = D\eta/Dt$ is the rate at which the parcel is crossing the η surfaces.

To transform the continuity equation (6.4), we first apply (6.9) to u and (6.10) to $v\cos\phi$ to obtain

$$\left(\frac{\partial u}{a\cos\phi\partial\lambda}\right)_z = \left(\frac{\partial u}{a\cos\phi\partial\lambda}\right)_\eta + \frac{\partial u}{\partial\eta}\left(\frac{\partial\eta}{a\cos\phi\partial\lambda}\right)_z, \tag{6.12}$$

$$\left(\frac{\partial(v\cos\phi)}{a\cos\phi\partial\phi}\right)_z = \left(\frac{\partial(v\cos\phi)}{a\cos\phi\partial\phi}\right)_\eta + \frac{\partial v}{\partial\eta}\left(\frac{\partial\eta}{a\partial\phi}\right)_z, \tag{6.13}$$

the left hand sides of which are the second and third terms in (6.4). To transform the fourth term in (6.4) we first note that

$$\frac{\partial \dot{\eta}}{\partial \eta} = \frac{\partial}{\partial \eta}\left(\frac{D\eta}{Dt}\right) = \frac{\partial z}{\partial \eta}\frac{\partial}{\partial z}\left[\left(\frac{\partial \eta}{\partial t}\right)_z + u\left(\frac{\partial \eta}{a\cos\phi\partial\lambda}\right)_z + v\left(\frac{\partial \eta}{a\partial\phi}\right)_z + w\frac{\partial \eta}{\partial z}\right].$$

After some rearrangement this can be written as

$$\frac{\partial w}{\partial z} = \frac{\partial \dot{\eta}}{\partial \eta} - \frac{\partial z}{\partial \eta}\frac{D}{Dt}\left(\frac{\partial \eta}{\partial z}\right) - \frac{\partial u}{\partial \eta}\left(\frac{\partial \eta}{a\cos\phi\partial\lambda}\right)_z - \frac{\partial v}{\partial \eta}\left(\frac{\partial \eta}{a\partial\phi}\right)_z. \tag{6.14}$$

Using (6.12)–(6.14) in the continuity equation (6.4), we obtain

$$\frac{D\ln\rho}{Dt} - \frac{\partial z}{\partial \eta}\frac{D}{Dt}\left(\frac{\partial \eta}{\partial z}\right) + \left(\frac{\partial u}{a\cos\phi\partial\lambda}\right)_\eta + \left(\frac{\partial(v\cos\phi)}{a\cos\phi\partial\phi}\right)_\eta + \frac{\partial\dot{\eta}}{\partial\eta} = 0. \tag{6.15}$$

Since $\rho > 0$, the hydrostatic relation (6.3) can be written as

$$\rho = -\frac{1}{g}\frac{\partial p}{\partial z} = -\frac{1}{g}\frac{\partial p}{\partial \eta}\frac{\partial \eta}{\partial z} = m\left|\frac{\partial \eta}{\partial z}\right|, \tag{6.16}$$

where the pseudo-density m is defined by

$$m = \frac{1}{g}\left|\frac{\partial p}{\partial \eta}\right|. \tag{6.17}$$

The material derivative of (6.16) yields

$$\frac{D\ln\rho}{Dt} = \frac{D\ln m}{Dt} + \frac{D\ln|\partial\eta/\partial z|}{Dt}. \tag{6.18}$$

Substitution of (6.18) into (6.15) yields the transformed continuity equation (6.23), given below. One way of understanding why we call $g^{-1}|\partial p/\partial\eta|$ the pseudo-density is to write the hydrostatic relation in the differential form $-g^{-1}dp = \rho dz$, which can also be written as

$$\frac{1}{g}\left|\frac{\partial p}{\partial \eta}\right|\left|a^2\cos\phi\, d\lambda\, d\phi\, d\eta\right| = \rho\left|a^2\cos\phi\, d\lambda\, d\phi\, dz\right|.$$

Since the right hand side is the density ρ times the element of volume $|a^2\cos\phi\, d\lambda\, d\phi\, dz|$, the left hand side can be interpreted as the pseudodensity $g^{-1}|\partial p/\partial\eta|$ times the element of pseudo-volume $|a^2\cos\phi\, d\lambda\, d\phi\, d\eta|$.

The horizontal components of the pressure gradient force can be expressed in several ways. For example, in the zonal momentum equation we have the equivalent forms

$$\frac{1}{\rho}\left(\frac{\partial p}{\partial\lambda}\right)_z = \left(\frac{\partial\Phi}{\partial\lambda}\right)_p = \left(\frac{\partial\Phi}{\partial\lambda}\right)_\eta + \frac{1}{\rho}\left(\frac{\partial p}{\partial\lambda}\right)_\eta = \left(\frac{\partial M}{\partial\lambda}\right)_\eta - \Pi\left(\frac{\partial\theta}{\partial\lambda}\right)_\eta = \left(\frac{\partial M}{\partial\lambda}\right)_\theta, \tag{6.19}$$

where $\Phi = gz$ is the geopotential, $M = c_pT + \Phi$ the Montgomery potential, and $\Pi = c_p(p/p_0)^\kappa$ the Exner function.

In summary, the quasi-static primitive equations in the η coordinate are

$$\frac{Du}{Dt} - \left(2\Omega\sin\phi + \frac{u\tan\phi}{a}\right)v + \frac{1}{\rho}\left(\frac{\partial p}{a\cos\phi\partial\lambda}\right)_\eta + \left(\frac{\partial\Phi}{a\cos\phi\partial\lambda}\right)_\eta = 0, \tag{6.20}$$

$$\frac{Dv}{Dt} + \left(2\Omega\sin\phi + \frac{u\tan\phi}{a}\right)u + \frac{1}{\rho}\left(\frac{\partial p}{a\partial\phi}\right)_\eta + \left(\frac{\partial\Phi}{a\partial\phi}\right)_\eta = 0, \tag{6.21}$$

$$\frac{\partial\Phi}{\partial\eta} = -\alpha\frac{\partial p}{\partial\eta}, \tag{6.22}$$

$$\frac{1}{m}\frac{Dm}{Dt} + \left(\frac{\partial u}{a\cos\phi\partial\lambda}\right)_\eta + \left(\frac{\partial(v\cos\phi)}{a\cos\phi\partial\phi}\right)_\eta + \frac{\partial\dot{\eta}}{\partial\eta} = 0, \tag{6.23}$$

$$c_p \frac{DT}{Dt} - \frac{1}{\rho}\frac{Dp}{Dt} = 0, \tag{6.24}$$

$$p = \rho RT, \tag{6.25}$$

where

$$\frac{D}{Dt} = \left(\frac{\partial}{\partial t}\right)_\eta + u\left(\frac{\partial}{a\cos\phi\partial\lambda}\right)_\eta + v\left(\frac{\partial}{a\partial\phi}\right)_\eta + \dot{\eta}\frac{\partial}{\partial\eta} \tag{6.26}$$

is the material derivative. Equations (6.20)–(6.25) constitute a closed system of six equations in the six dependent variables $u, v, \dot{\eta}, \rho, T, p$, each of which is a function of the independent variables (λ, ϕ, η, t).

6.2 Pressure coordinate

Now consider the special case of pressure coordinates, $\eta = p$. In pressure coordinates the pseudo-density (6.17) becomes $m = 1/g$, so that the material derivative term in (6.23) vanishes. Thus, pressure coordinates yield the simplest form of the mass continuity equation. Defining the vertical p-velocity ω by $\omega = Dp/Dt = \dot{\eta}$, the quasi-static primitive equations in pressure coordinates are

$$\frac{Du}{Dt} - \left(2\Omega\sin\phi + \frac{u\tan\phi}{a}\right)v + \left(\frac{\partial\Phi}{a\cos\phi\partial\lambda}\right)_p = 0, \tag{6.27}$$

$$\frac{Dv}{Dt} + \left(2\Omega\sin\phi + \frac{u\tan\phi}{a}\right)u + \left(\frac{\partial\Phi}{a\partial\phi}\right)_p = 0, \tag{6.28}$$

$$\frac{\partial\Phi}{\partial p} = -\alpha, \tag{6.29}$$

$$\left(\frac{\partial u}{a\cos\phi\partial\lambda}\right)_p + \left(\frac{\partial(v\cos\phi)}{a\cos\phi\partial\phi}\right)_p + \frac{\partial\omega}{\partial p} = 0, \tag{6.30}$$

$$c_p\frac{DT}{Dt} - \alpha\omega = 0, \tag{6.31}$$

where

$$\frac{D}{Dt} = \left(\frac{\partial}{\partial t}\right)_p + u\left(\frac{\partial}{a\cos\phi\partial\lambda}\right)_p + v\left(\frac{\partial}{a\partial\phi}\right)_p + \omega\frac{\partial}{\partial p}. \tag{6.32}$$

When the context of a discussion indicates that p is being used as the vertical coordinate, the subscripts p are omitted and the partial derivatives with respect to λ, ϕ and t are understood to imply that p is held fixed.

Note that (6.30) is not an approximation of (6.23), i.e., (6.30) is "exact" within the context of the quasi-static system of equations. The reason that (6.30) is so simple is that the pseudo-density is a constant in the p-coordinate. Although the p-coordinate results in a simple form for the continuity equation, the treatment of the lower boundary condition can be cumbersome in the p-coordinate.

6.3 Log-pressure coordinate

Now consider the special case of log-pressure coordinates, $\eta = \ln(p_0/p) \equiv z^*$. In log-pressure coordinates the pseudo-density (6.17) becomes $m = p/g = (p_0/g)e^{-z^*}$, so that all but the vertical advective part of the material derivative term in (6.23) vanishes. Defining the vertical $\ln p$-velocity w^* by $w^* = Dz^*/Dt = \dot{\eta}$, and noting that ω and w^* are related by $\omega = -p_0 e^{-z^*} w^*$, the quasi-static primitive equations are

$$\frac{Du}{Dt} - \left(2\Omega\sin\phi + \frac{u\tan\phi}{a}\right)v + \left(\frac{\partial\Phi}{a\cos\phi\partial\lambda}\right)_{z^*} = 0, \tag{6.33}$$

$$\frac{Dv}{Dt} + \left(2\Omega\sin\phi + \frac{u\tan\phi}{a}\right)u + \left(\frac{\partial\Phi}{a\partial\phi}\right)_{z^*} = 0, \tag{6.34}$$

$$\frac{\partial\Phi}{\partial z^*} = RT, \tag{6.35}$$

$$\left(\frac{\partial u}{a\cos\phi\partial\lambda}\right)_{z^*} + \left(\frac{\partial(v\cos\phi)}{a\cos\phi\partial\phi}\right)_{z^*} + \frac{\partial w^*}{\partial z^*} - w^* = 0, \tag{6.36}$$

$$\frac{DT}{Dt} + \kappa T w^* = 0, \tag{6.37}$$

where

$$\frac{D}{Dt} = \left(\frac{\partial}{\partial t}\right)_{z^*} + u\left(\frac{\partial}{a\cos\phi\partial\lambda}\right)_{z^*} + v\left(\frac{\partial}{a\partial\phi}\right)_{z^*} + w^*\frac{\partial}{\partial z^*}. \tag{6.38}$$

When the context of a discussion indicates that z^* is being used as the vertical coordinate, the subscripts z^* are omitted and the partial derivatives with respect to λ, ϕ and t are understood to imply that z^* is held fixed. The log-pressure coordinate is extensively used in middle atmosphere dynamics, for example in the analysis of the vertical propagation of Rossby waves from the troposphere into the stratosphere and mesosphere. We shall use this coordinate in our discussion of vertical normal modes in Chapter 9.

6.4 Pseudo-height coordinate

Now consider the special case of the pseudo-height coordinate, $\eta = (c_p\theta_0/g)[1-(p/p_0)^\kappa] \equiv \hat{z}$. In the pseudo-height coordinate the pseudo-density (6.17) becomes $m = (p_0/R\theta_0)(1-\hat{z}/\hat{z}_a)^{(1-\kappa)/\kappa} \equiv \hat{\rho}(\hat{z})$, where $\hat{z}_a = c_p\theta_0/g$ is the depth of an adiabatic atmosphere. Note that the pseudo-density $\hat{\rho}(\hat{z})$ is a known function of the pseudo-height $\hat{z}$, and is to be sharply distinguished from the physical space density ρ. Again, all but the vertical advective part of the material derivative term in (6.23) vanishes. Defining the vertical $\hat{z}$-velocity $\hat{w}$ by $\hat{w} = D\hat{z}/Dt = \dot{\eta}$, and noting that ω and $\hat{w}$ are related by $\omega = -g\hat{\rho}\hat{w}$, the quasi-static primitive equations in pseudo-height coordinates are

$$\frac{Du}{Dt} - \left(2\Omega\sin\phi + \frac{u\tan\phi}{a}\right)v + \left(\frac{\partial\Phi}{a\cos\phi\partial\lambda}\right)_{\hat{z}} = 0, \tag{6.39}$$

$$\frac{Dv}{Dt} + \left(2\Omega\sin\phi + \frac{u\tan\phi}{a}\right)u + \left(\frac{\partial\Phi}{a\partial\phi}\right)_{\hat{z}} = 0, \tag{6.40}$$

$$\frac{\partial\Phi}{\partial\hat{z}} = \frac{g}{\theta_0}\theta, \tag{6.41}$$

$$\left(\frac{\partial u}{a\cos\phi\partial\lambda}\right)_{\hat{z}} + \left(\frac{\partial(v\cos\phi)}{a\cos\phi\partial\phi}\right)_{\hat{z}} + \frac{\partial(\hat{\rho}\hat{w})}{\hat{\rho}\partial\hat{z}} = 0, \tag{6.42}$$

$$\frac{D\theta}{Dt} = 0, \tag{6.43}$$

where

$$\frac{D}{Dt} = \left(\frac{\partial}{\partial t}\right)_{\hat{z}} + u\left(\frac{\partial}{a\cos\phi\partial\lambda}\right)_{\hat{z}} + v\left(\frac{\partial}{a\partial\phi}\right)_{\hat{z}} + \hat{w}\frac{\partial}{\partial\hat{z}}. \tag{6.44}$$

When the context of a discussion indicates that $\hat{z}$ is being used as the vertical coordinate, the subscripts $\hat{z}$ are omitted and the partial derivatives with respect to λ, ϕ and t are understood to imply that $\hat{z}$ is held fixed. Although the continuity equation (6.42) is not quite as simple as the p-coordinate version (6.30), equations (6.39)–(6.44) are often preferred over (6.27)–(6.32) because the same variable θ appears on the right hand side of (6.41) and in the material conservation relation (6.43), and because the thermal wind equations take a simple form in the pseudo-height coordinate. Thus, the pseudo-height coordinate is extensively used in quasi-geostrophic and semi-geostrophic studies of baroclinic waves and fronts (see Chapters 13 and 14). We shall use this coordinate in the derivation of the quasi-geostrophic and semi-geostrophic **Q**-vectors, where we take advantage of the simple form of the thermal wind equations.

6.5 Sigma coordinate

Now consider the special case of the sigma coordinate, $\eta = p/p_s \equiv \sigma$. In the sigma coordinate the pseudo-density (6.17) becomes $m = p_s/g$. Note that the pseudo-density p_s/g is a function of (λ, ϕ, t). Now, only the vertical advective part of the material derivative term in (6.23) vanishes. Defining the vertical σ-velocity $\dot{\sigma}$ by $\dot{\sigma} = D\sigma/Dt = \dot{\eta}$, and noting that ω and $\dot{\sigma}$ are related by $\omega = p_s\dot{\sigma} + \sigma Dp_s/Dt$, the quasi-static primitive equations are

$$\frac{Du}{Dt} - \left(2\Omega\sin\phi + \frac{u\tan\phi}{a}\right)v + \left(\frac{\partial\Phi}{a\cos\phi\partial\lambda}\right)_\sigma + \sigma\alpha\frac{\partial p_s}{a\cos\phi\partial\lambda} = 0, \tag{6.45}$$

$$\frac{Dv}{Dt} + \left(2\Omega\sin\phi + \frac{u\tan\phi}{a}\right)u + \left(\frac{\partial\Phi}{a\partial\phi}\right)_\sigma + \sigma\alpha\frac{\partial p_s}{a\partial\phi} = 0, \tag{6.46}$$

$$\frac{\partial\Phi}{\partial\sigma} = -p_s\alpha, \tag{6.47}$$

$$\frac{1}{p_s}\frac{Dp_s}{Dt} + \left(\frac{\partial u}{a\cos\phi\partial\lambda}\right)_\sigma + \left(\frac{\partial(v\cos\phi)}{a\cos\phi\partial\phi}\right)_\sigma + \frac{\partial\dot{\sigma}}{\partial\sigma} = 0, \tag{6.48}$$

$$\frac{D\theta}{Dt} = 0, \tag{6.49}$$

where

$$\frac{D}{Dt} = \left(\frac{\partial}{\partial t}\right)_\sigma + u\left(\frac{\partial}{a\cos\phi\partial\lambda}\right)_\sigma + v\left(\frac{\partial}{a\partial\phi}\right)_\sigma + \dot{\sigma}\frac{\partial}{\partial\sigma}. \tag{6.50}$$

When the context of a discussion indicates that σ is being used as the vertical coordinate, the subscripts σ are omitted and the partial derivatives with respect to λ, ϕ and t are understood to imply that σ is held fixed. In sigma coordinates the lower boundary is the coordinate surface $\sigma = 1$. Because this greatly simplifies the lower boundary condition in models with realistic topography, sigma coordinates and their generalizations are widely used in numerical weather prediction and climate modeling. One disadvantage of this coordinate is that the pressure gradient force splits into two terms, and, near steep topography, these two terms tend to have the same large magnitude but opposite sign. This can lead to numerical errors and poor simulation of flow features near steep topography, such as the Andes.

In sigma coordinate models, (6.48) is usually put into a form which incorporates the upper and lower boundary conditions $\dot{\sigma} = 0$ at $\sigma = 0, 1$. Dropping the subscripts on the partial derivatives, the continuity equation (6.48) can be written in flux form as

$$\frac{\partial p_s}{\partial t} + \frac{\partial(p_s u)}{a\cos\phi\partial\lambda} + \frac{\partial(p_s v\cos\phi)}{a\cos\phi\partial\phi} + \frac{\partial(p_s\dot{\sigma})}{\partial\sigma} = 0. \tag{6.51}$$

Integrating (6.51) vertically from $\sigma = 0$ to $\sigma = 1$, using the upper and lower boundary conditions, we obtain

$$\frac{\partial p_s}{\partial t} = -\int_0^1 \left(\frac{\partial(p_s u)}{a\cos\phi\partial\lambda} + \frac{\partial(p_s v\cos\phi)}{a\cos\phi\partial\phi}\right)d\sigma. \tag{6.52}$$

Similarly, integrating (6.51) from the upper boundary to σ, using the upper boundary condition, we obtain

$$p_s\dot{\sigma} = \sigma\int_0^1 \left(\frac{\partial(p_s u)}{a\cos\phi\partial\lambda} + \frac{\partial(p_s v\cos\phi)}{a\cos\phi\partial\phi}\right)d\sigma' - \int_0^\sigma \left(\frac{\partial(p_s u)}{a\cos\phi\partial\lambda} + \frac{\partial(p_s v\cos\phi)}{a\cos\phi\partial\phi}\right)d\sigma'. \tag{6.53}$$

Equations (6.52) and (6.53) replace (6.48), with (6.52) used to predict the surface pressure and (6.53) used to diagnose the "vertical velocity" $\dot{\sigma}$. It might seem that we have obtained two equations from one equation. However, we have incorporated the boundary conditions, and it should be noted that (6.52) contains only vertically integrated information.

6.6 Isentropic coordinate

Now consider the special case of isentropic coordinates, $\eta = \theta$. In isentropic coordinates the pseudo-density (6.17) becomes $m = -g^{-1}\partial p/\partial\theta \equiv \sigma$. Note that the symbol σ is used for two entirely different quantities in isentropic and sigma coordinates. The quasi-static primitive equations in isentropic coordinates are

$$\frac{Du}{Dt} - \left(2\Omega\sin\phi + \frac{u\tan\phi}{a}\right)v + \left(\frac{\partial M}{a\cos\phi\partial\lambda}\right)_\theta = 0, \tag{6.54}$$

$$\frac{Dv}{Dt} + \left(2\Omega\sin\phi + \frac{u\tan\phi}{a}\right)u + \left(\frac{\partial M}{a\partial\phi}\right)_\theta = 0, \tag{6.55}$$

$$\frac{\partial M}{\partial \theta} = \Pi, \tag{6.56}$$

$$\frac{1}{\sigma}\frac{D\sigma}{Dt} + \left(\frac{\partial u}{a\cos\phi\partial\lambda}\right)_\theta + \left(\frac{\partial(v\cos\phi)}{a\cos\phi\partial\phi}\right)_\theta + \frac{\partial\dot{\theta}}{\partial\theta} = 0, \tag{6.57}$$

where $\Pi = c_p(p/p_0)^\kappa$ is the Exner function, and

$$\frac{D}{Dt} = \left(\frac{\partial}{\partial t}\right)_\theta + u\left(\frac{\partial}{a\cos\phi\partial\lambda}\right)_\theta + v\left(\frac{\partial}{a\partial\phi}\right)_\theta + \dot{\theta}\frac{\partial}{\partial\theta}. \tag{6.58}$$

When the context of a discussion clearly indicates that θ is being used as the vertical coordinate, the subscripts θ are omitted and the partial derivatives with respect to λ, ϕ and t are understood to imply that θ is held fixed. The expression for potential vorticity is very simple in isentropic coordinates. Another advantage of isentropic coordinates is that, for adiabatic flow (i.e., $\dot{\theta} = 0$), the last term in the material derivative (6.58) disappears. In the adiabatic case, an isentropic surface is a material surface (i.e., it is always composed of the same parcels).

6.7 The ECMWF hybrid vertical coordinate

Simmons and Burridge (1981) proposed

$$\eta = \frac{p}{p_s} + \left(\frac{p}{p_s} - 1\right)\left(\frac{p}{p_s} - \frac{p}{p_c}\right), \tag{6.59}$$

where p_c is a constant. Note that $\eta = 1$ when $p = p_s$ and $\eta = 0$ when $p = 0$.

6.8 Arakawa-Konor hybrid σ-p vertical coordinate

Arakawa and Konor (1994) proposed the hybrid coordinate

$$\sigma = F(p, p_s) = a(p, p_S)\left(\frac{p - p_T}{p_S - p_T}\right) + [1 - a(p, p_s)]f(p), \tag{6.60}$$

where $a(p, p_S)$ is a function satisfying $0 \le a(p, p_S) \le 1$ for $p_T \le p \le p_S$. When $a(p, p_S) = 1$ and $p_T = 0$, (6.60) reduces to $\sigma = p/p_S$, the original σ-coordinate proposed by Phillips (1957). When $a(p, p_S) = p/p_S$ $p_T = 0$, and $f(p) = p/p_C$, where p_C is a constant, (6.60) reduces to (6.59), the hybrid coordinate proposed by Simmons and Burridge (1981).

6.9 Konor-Arakawa hybrid θ-p-p_S vertical coordinate

Konor and Arakawa (1997) proposed the hybrid coordinate

$$\zeta = f(\sigma) + g(\sigma)\theta, \tag{6.61}$$

where

$$\sigma = \frac{p_s - p}{p_s - p_T}$$

and where $g(\sigma) \approx 1$ everywhere except near the surface. Require $d\zeta/d\sigma > 0$, so that

$$\frac{df}{d\sigma} + \frac{dg}{d\sigma}\theta + g\frac{\partial\theta}{\partial\sigma} > 0. \tag{6.62}$$

Given $g(\sigma)$ find $f(\sigma)$ from

$$\frac{df}{d\sigma} + \frac{dg}{d\sigma}\theta_{\min} + g\left(\frac{\partial\theta}{\partial\sigma}\right)_{\min} = 0. \tag{6.63}$$

For example, if we choose

$$g(\sigma) = \frac{1 - e^{-\alpha\sigma}}{1 - e^{-\alpha}}, \tag{6.64}$$

then

$$f(\sigma) = \theta_{\min}\left[1 - g(\sigma)\right] + \left(\frac{\partial\theta}{\partial\sigma}\right)_{\min} \frac{1}{1 - e^{-\alpha}} \left(1 - \sigma + \frac{1}{\alpha}e^{-\alpha} - \frac{1}{\alpha}e^{-\alpha\sigma}\right), \tag{6.65}$$

which results in the vertical coordinate

$$\zeta(\theta, \sigma) = \frac{1}{1 - e^{-\alpha}} \left\{\theta_{\min}\left(e^{-\alpha\sigma} - e^{-\alpha}\right) + \theta\left(1 - e^{-\alpha\sigma}\right) + \left(\frac{\partial\theta}{\partial\sigma}\right)_{\min} \left[1 - \sigma - \frac{1}{\alpha}\left(e^{-\alpha\sigma} - e^{-\alpha}\right)\right]\right\}. \tag{6.66}$$

There are three parameters: α, $\theta_{\min}$, $(\partial\theta/\partial\sigma)_{\min}$. Typical numerical values are $\alpha = 10$, $\theta_{\min} = 250\text{K}$, and $(\partial\theta/\partial\sigma)_{\min} = -3\text{K}$.

Problems

1. Consider an arbitrary scalar ψ, which is a function of (λ, ϕ, z, t). We want to transform to a new set of independent variables (Λ, Φ, η, T). Thus, consider $\psi\left(\lambda(\Lambda, \Phi, \eta, T), \phi(\Lambda, \Phi, \eta, T), z(\Lambda, \Phi, \eta, T), t(\Lambda, \Phi, \eta, T)\right)$. For the special case $\Lambda = \lambda$, $\Phi = \phi$, and $T = t$, prove that

$$\left(\frac{\partial\psi}{\partial\lambda}\right)_\eta = \left(\frac{\partial\psi}{\partial\lambda}\right)_z + \left(\frac{\partial z}{\partial\lambda}\right)_\eta \frac{\partial\psi}{\partial z}.$$

2. Use the result of problem 1 to derive the following σ-coordinate form of the pressure gradient force:

$$\frac{1}{\rho}\left(\frac{\partial p}{\partial\lambda}\right)_z = \frac{\sigma}{\rho}\left(\frac{\partial p_s}{\partial\lambda}\right)_\sigma + g\left(\frac{\partial z}{\partial\lambda}\right)_\sigma.$$

   Explain why the subscript σ on the first term on the right hand side can be dropped without confusion. Explain how the two terms on the right hand side tend to be large and of opposite sign near steep topography.

3. Use the result of problem 1 to derive the following θ-coordinate form of the pressure gradient force:

$$\frac{1}{\rho}\left(\frac{\partial p}{\partial\lambda}\right)_z = \left(\frac{\partial M}{\partial\lambda}\right)_\theta.$$

7 Divergent Barotropic Primitive Equations (Shallow Water Equations)

7.1 Horizontal momentum and continuity equations

The terms "divergent barotropic primitive equations" and "shallow water primitive equations" are used synonymously. The shallow water equations can be considered a special case of the quasi-static primitive equations (6.1)–(6.4). To obtain the shallow water equations we consider a thin sheet of constant density fluid covering the earth. The fluid is assumed to have a free upper surface, so that its depth h is a function of (λ, ϕ, t). Since ρ is a constant, the hydrostatic equation $\partial p/\partial z = -\rho g$ can be easily integrated from z to $h(\lambda, \phi, t)$, which results in $p(\lambda, \phi, z, t) = \rho g\left[h(\lambda, \phi, t) - z\right]$. This equation states that the pressure at level z is simply the weight of fluid in the column above level z. The pressure gradient force per unit mass in the eastward and northward directions can now be written as

$$\frac{1}{\rho}\frac{\partial p}{a\cos\phi\partial\lambda} = g\frac{\partial h}{a\cos\phi\partial\lambda} \qquad \text{and} \qquad \frac{1}{\rho}\frac{\partial p}{a\partial\phi} = g\frac{\partial h}{a\partial\phi}. \tag{7.1}$$

Although the pressure is a function of z, the pressure gradient is not a function of z. If u and v are initially independent of z, they will be predicted by (6.1) and (6.2) to remain independent of z. Thus, $u(\lambda, \phi, t)$ and $v(\lambda, \phi, t)$ obey (7.4) and (7.5) below, with the material derivative given by (7.7). Note that, even though $w \neq 0$, the vertical advection terms disappear from the material derivative (7.7) because $\partial u/\partial z = \partial v/\partial z = 0$.

Under the assumption of constant density, the continuity equation (6.4) reduces to

$$\frac{\partial u}{a\cos\phi\partial\lambda} + \frac{\partial(v\cos\phi)}{a\cos\phi\partial\phi} + \frac{\partial w}{\partial z} = 0. \tag{7.2}$$

If we integrate (7.2) from $z = 0$ to $z = h$, under the assumption that $w = 0$ at $z = 0$, we obtain

$$h\left(\frac{\partial u}{a\cos\phi\partial\lambda} + \frac{\partial(v\cos\phi)}{a\cos\phi\partial\phi}\right) + w(h) = 0. \tag{7.3}$$

Since $w(h) = Dh/Dt$, (7.3) reduces to (7.6) below.

In summary, the governing equations for an incompressible, inviscid, shallow water fluid on the sphere are

$$\frac{Du}{Dt} - \left(2\Omega\sin\phi + \frac{u\tan\phi}{a}\right)v + g\frac{\partial h}{a\cos\phi\partial\lambda} = 0, \tag{7.4}$$

$$\frac{Dv}{Dt} + \left(2\Omega\sin\phi + \frac{u\tan\phi}{a}\right)u + g\frac{\partial h}{a\partial\phi} = 0, \tag{7.5}$$

$$\frac{Dh}{Dt} + h\left(\frac{\partial u}{a\cos\phi\partial\lambda} + \frac{\partial(v\cos\phi)}{a\cos\phi\partial\phi}\right) = 0, \tag{7.6}$$

where

$$\frac{D}{Dt} = \frac{\partial}{\partial t} + u\frac{\partial}{a\cos\phi\partial\lambda} + v\frac{\partial}{a\partial\phi}. \tag{7.7}$$

Equations (7.4)–(7.6) constitute a closed system of three equations in the three dependent variables u, v, h, all of which are functions of the independent variables (λ, ϕ, t).

Even though they omit vertical structure, the shallow water equations are used extensively in geophysical fluid dynamics. The literature on any problem involving primarily the horizontal aspects of the flow will almost certainly contain applications of shallow water theory. Examples include horizontal wave propagation (e.g., geostrophic adjustment) and barotropic instability problems. The shallow water equations are also a test bed for the horizontal spatial discretization (e.g., finite difference, finite element, spectral) and temporal discretization schemes used in numerical weather prediction models and general circulation models. The golden rule seems to be that, if the discretization scheme won't work on the shallow water equations, then it won't work on the more complicated equations.

7.2 Potential vorticity principle for the shallow water equations

To derive the shallow water potential vorticity equation we first write the momentum equations (7.4)–(7.5) in their rotational form

$$\frac{\partial u}{\partial t} - \zeta v + \frac{\partial}{a\cos\phi\partial\lambda}\left[gh + \tfrac{1}{2}(u^2+v^2)\right] = 0, \tag{7.8}$$

$$\frac{\partial v}{\partial t} + \zeta u + \frac{\partial}{a\partial\phi}\left[gh + \tfrac{1}{2}(u^2+v^2)\right] = 0, \tag{7.9}$$

where

$$\zeta = 2\Omega\sin\phi + \frac{\partial v}{a\cos\phi\partial\lambda} - \frac{\partial(u\cos\phi)}{a\cos\phi\partial\phi} \tag{7.10}$$

is the absolute vorticity. Cross-differentiating (7.8) and (7.9) we obtain

$$\frac{D\zeta}{Dt} + \zeta\left(\frac{\partial u}{a\cos\phi\partial\lambda} + \frac{\partial(v\cos\phi)}{a\cos\phi\partial\phi}\right) = 0. \tag{7.11}$$

Eliminating the divergence between (7.11) and (7.6) we obtain

$$\frac{DP}{Dt} = 0, \tag{7.12}$$

where

$$P = \left(\frac{\bar{h}}{h}\right)\zeta = \frac{\bar{h}}{h}\left(2\Omega\sin\phi + \frac{\partial v}{a\cos\phi\partial\lambda} - \frac{\partial(u\cos\phi)}{a\cos\phi\partial\phi}\right). \tag{7.13}$$

Here we have introduced $\bar{h}$, the constant mean depth of the fluid, so that the potential vorticity P will have the same units as the absolute vorticity ζ. We can now interpret the potential vorticity P as the absolute vorticity a fluid column would acquire if its actual depth h were changed to the reference depth $\bar{h}$. If $h < \bar{h}$, then $P > \zeta$ and the column must be stretched to acquire the reference depth. Conversely, if $h > \bar{h}$, then $P < \zeta$ and the column must be squashed to acquire the reference depth. It is helpful for some to think about an analogy between potential temperature and potential vorticity. Potential temperature is the temperature the fluid would acquire if it moved adiabatically to a reference pressure. Potential vorticity is the vorticity the fluid would acquire if it were vertically stretched or shrunk to a reference depth.

Since D/Dt is the derivative following a fluid column, (7.12) says that the absolute vorticity of the column and the depth of the column must change in such a way that the ratio ζ/h is invariant. The potential vorticity conservation relation (7.12) becomes a powerful tool when the flow is nearly balanced (e.g., geostrophically balanced). Then u and v are geostrophically related to h, so that instead of depending on u, v and h, the potential vorticity depends only on h. In fact, h can be recovered from P, although this invertibility principle is somewhat complicated because it requires solving a second order, elliptic, partial differential equation for h. In Chapter 10 we shall study the simplest, linear, geostrophic adjustment problem. The inversion of PV to find the geostrophically balanced h will turn out to be a central part of geostrophic adjustment theory.

7.3 Some numerical solutions

As an application of the shallow water equations let us now consider the breakdown of a zonally symmetric PV strip. This is an idealization of the lower tropospheric flow associated with the Intertropical Convergence Zone (ITCZ). The initial absolute vorticity field is given by

$$\zeta(\lambda,\phi,0) = \begin{cases} 2\Omega\sin\phi + \xi_s & \text{for} \quad |\phi-\phi_c| \le \phi_w/2, \\ 2\Omega\sin\phi & \text{otherwise,} \end{cases} \tag{7.14}$$

where ϕ_c, ϕ_w and ξ_s are the central latitude, width and magnitude of the vorticity strip, respectively. For the calculations shown here $\phi_c = 15°\text{N}$, $\phi_w = 7°$ and $\xi_s = 3.0 \times 10^{-5}\ \text{s}^{-1}$.

The meridional gradient of absolute vorticity is negative on the northern edge of the PV strip described above and positive everywhere else. Hence, there is a reversal in the poleward gradient of PV and Rayleigh's necessary condition for barotropic instability of a nondivergent flow is satisfied. This means that counterpropagating vorticity waves are possible, with the wave on the poleward edge of the strip propagating eastward relative to the zonal flow and the wave on the equatorward edge of the strip propagating westward relative to the zonal flow. On the poleward (equatorward) edge of the PV strip the easterly (westerly) flow opposes the relative eastward (westward) propagation of the vorticity wave. In fact, these counterpropagating waves can phase lock and amplify, a result closely connected with the Fjørtoft necessary condition for instability of nondivergent, barotropic flow (Drazin and Reid 1981). Of course, the simulations to be presented here use the divergent barotropic model so the above nondivergent Rayleigh and Fjørtoft theorems are not strictly applicable. However, if the more general divergent barotropic stability results of Ripa (1983) are used, the conclusions concerning the possible instability of the above flow are unchanged.

A nondivergent linear normal mode stability analysis (Dritschel and Polvani 1992) of the aforementioned PV strip was calculated. The most unstable mode obtained has zonal wavenumber nine, a westward phase speed of 2.3 ms^{-1} and an e-folding time of 2.1 days. In the begining of the nonlinear shallow water simulation the fluid is provided with a finite amplitude initial perturbation which will grow by extracting energy from the mean flow through the barotropic instability process. A natural choice for this perturbation is the most unstable mode calculated in the linear stability analysis. Hence, in the shallow water simulation the PV strip was initially perturbed with a wavenumber nine disturbance having an amplitude of 10^{-7} s^{-1}.

In the shallow water simulation, the mean initial fluid height, $\bar{h}$, was set to 450 m which implies a gravity wave phase speed of 67.1 ms^{-1} and an equatorial Rossby length $\left[a(g\bar{h})^{1/2}/(2\Omega)\right]^{1/2}$ of 1712 km. Nonlinear balance (Charney 1960) was initially assumed. The initial zonal wind difference across the PV strip was approximately 19 ms^{-1}. The height, wind and PV fields were nearly zonally symmetric. After five days (Fig. 7.1a), the cyclonic PV strip and corresponding mass and wind fields are undulating due to the growth of the initially imposed perturbation through barotropic instability. During breakdown the high PV is pooled into cyclones that are connected by high PV filaments. These cyclones are initially zonally elongated (Fig. 7.1b). As breakdown proceeds, the cyclones tend to axisymmetrize (Fig. 7.1c) while the filaments become thinner and wrap around the cyclones. Axisymmetrization occurs as PV is stripped out of the cyclone core forming the PV filaments. Strain and adverse shear created by the cyclone prevent the PV filaments from breaking down due to barotropic instability. These PV filaments may be related to the outer spiral bands of hurricanes. At 15 days (Fig. 7.1c) the filaments of high PV that linked the cyclones have been detached. This occurs because the model dissipation is stronger in the smaller scales.

The horizontal scale of the resulting instabilities is approximately 3800 km with a westward propagation of about 2.7 ms^{-1}. Breakdown occurs sooner when the amplitude of the initial imposed perturbation is larger. In fact, this suggests that if easterly waves propagate from the Atlantic into the East Pacific they may initiate and/or accelerate the ITCZ breakdown process in the latter region.

In this simulation there was exchange of mass between the two hemispheres with intrusion of negative (positive) PV air from the Southern (Northern) into the Northern (Southern) Hemisphere (Fig. 7.1c). In these regions the necessary condition for occurrence of inertial instability, that is $fP < 0$, is met. However, inertially unstable modes have very slow growth rates for flows with large $\bar{h}$ and therefore are not apparent in any of the simulations shown here.

Additional simulations (not shown) reveal the effect of changing the width and intensity of the PV strip. In agreement with linear normal mode stability analysis, wider (narrower) PV strips broke down into larger (smaller) cyclones and an increase (decrease) in shear resulted in faster (slower) breakdown.

Although time averages of zonal winds in the East Pacific do not have meridional shear as large as the one used in this experiment, it is possible that high shear exists on individual days. Also, as seen in the linear normal mode stability analysis, weaker shear profiles will break down as well, but with slower growth rates.

As a second application of the shallow water equations let us consider the movement of five intense cyclonic vortices (hurricanes) uniformly spaced along 15N at $t = 0$. The atmosphere outside the vortices is assumed to be at rest initially in Fig. 7.2a but to have low latitude easterlies and midlatitude westerlies in Fig. 7.3a. Figures 7.2a–d and Figs. 7.3a–d display the PV contours and the wind vectors at 1,4,7,11 days. Note that the vortices propagate toward the northwest and generate Rossby waves to their east. In Fig. 7.2 the Rossby waves evolve into broadening troughs while in Fig. 7.3 the Rossby waves evolve into thinning troughs which trail off to the southwest. The thinning troughs look very much like the so-called tropical upper tropospheric troughs (TUTTS) observed in nature.

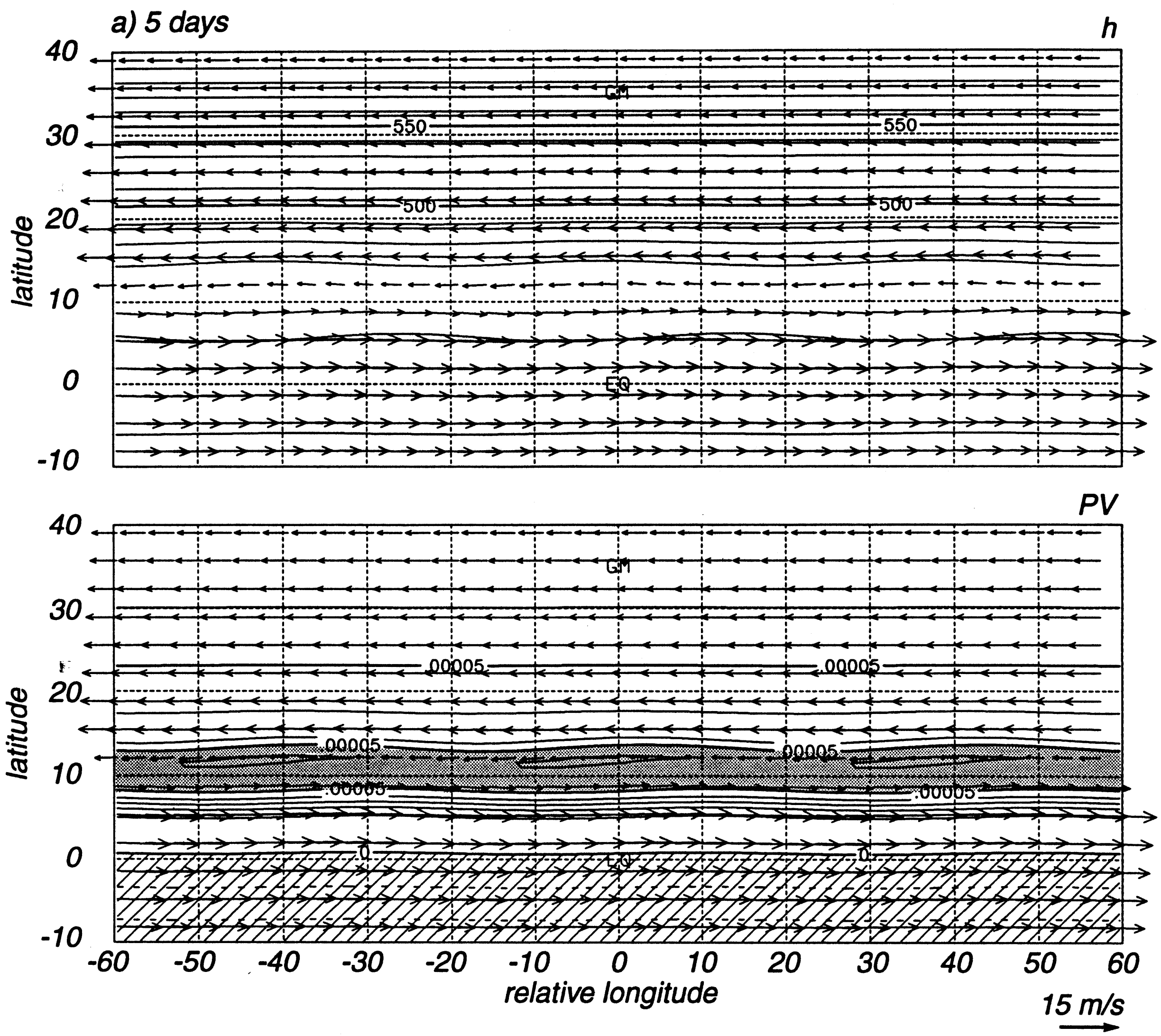

Figure 7.1: Breakdown of a 4.5° wide zonally symmetric vorticity strip centered at 10N with maximum relative vorticity 3.0×10^{-5} s^{-1}. The displayed fields are fluid depth (m), PV (s^{-1}), and winds (m s^{-1}) at (a) 5 days, (b) 10 days, and (c) 15 days. From Nieto Ferreira and Schubert 1997.

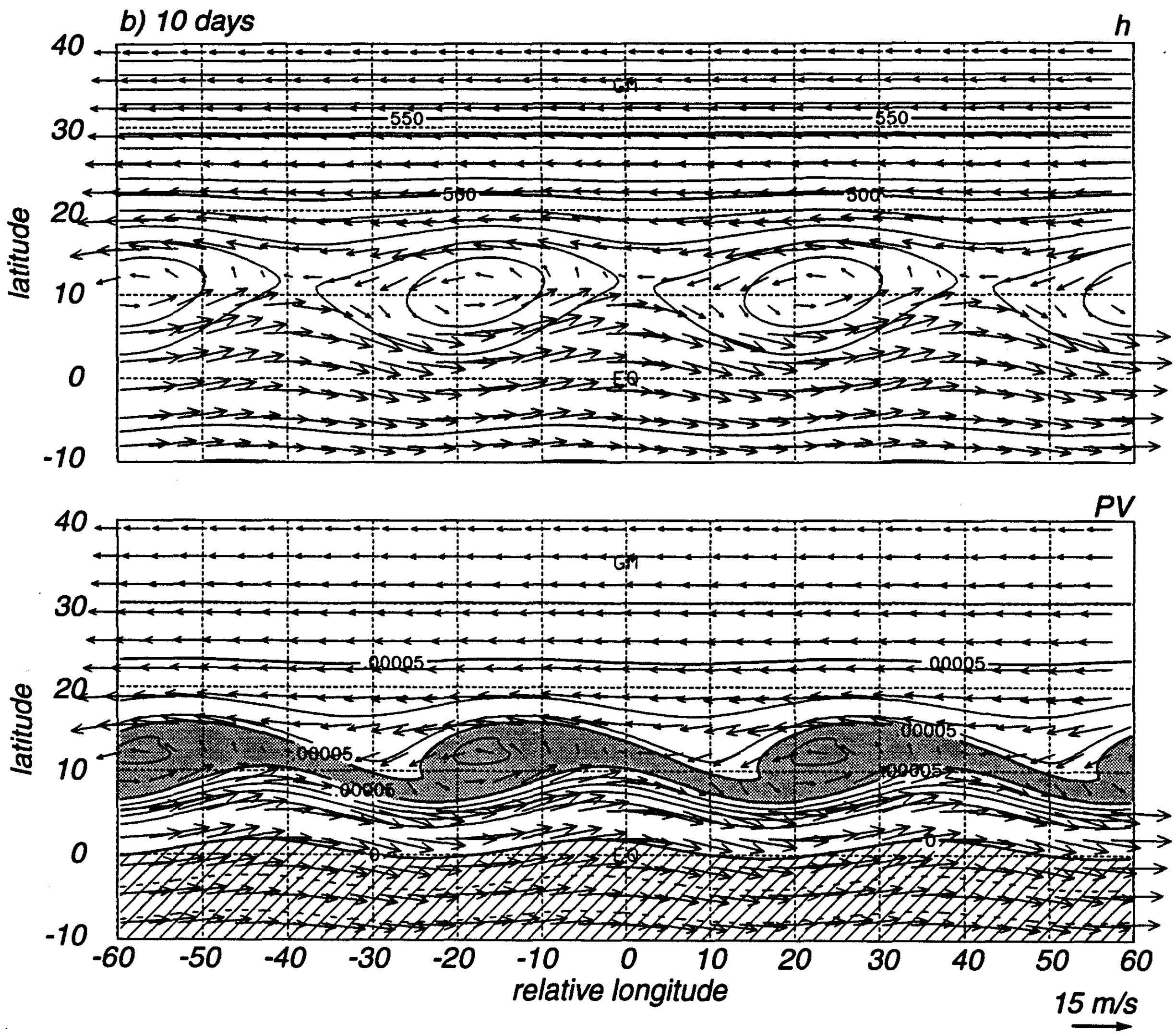

Figure 7.1: (Continued)

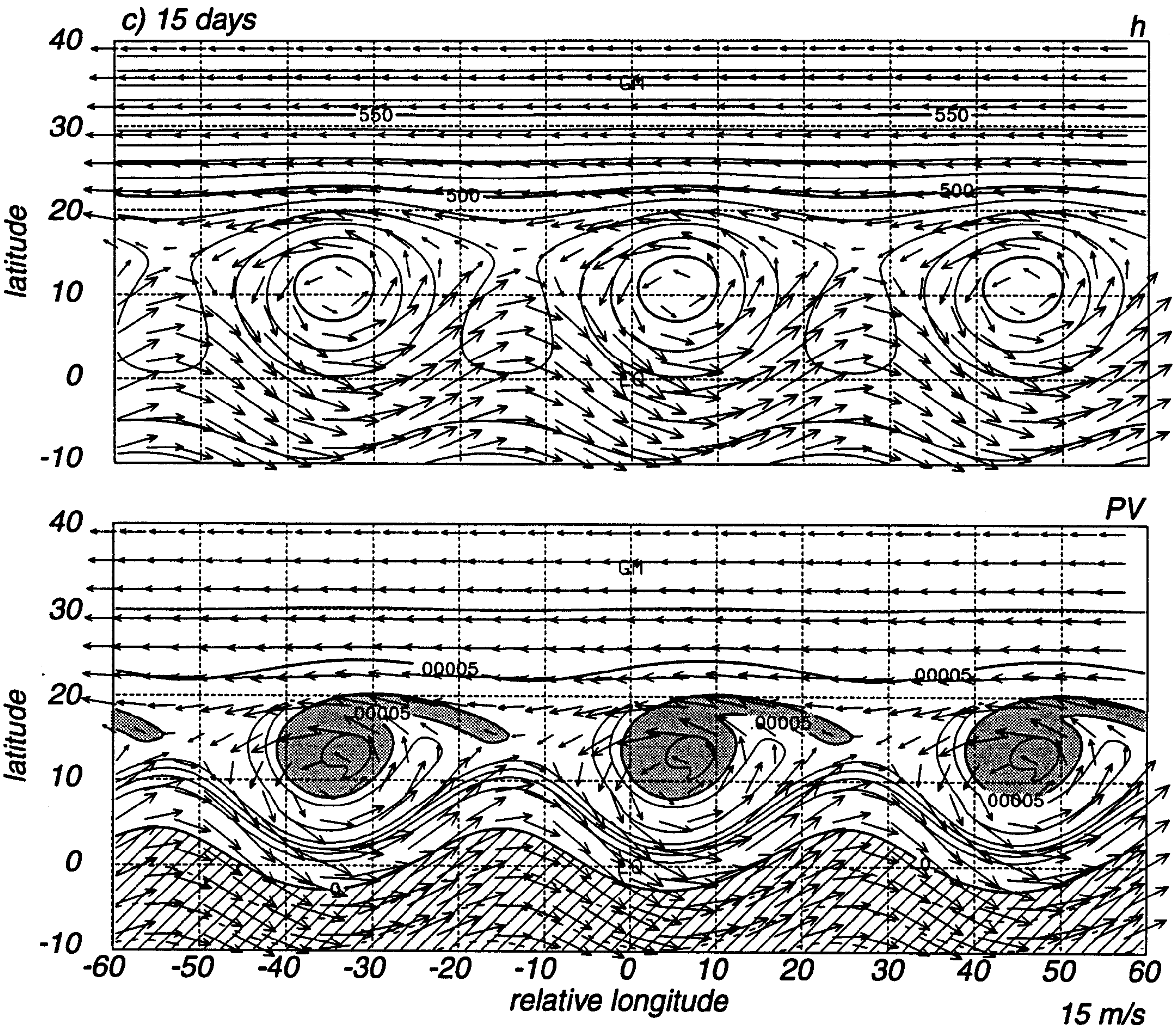

Figure 7.1: (Continued)

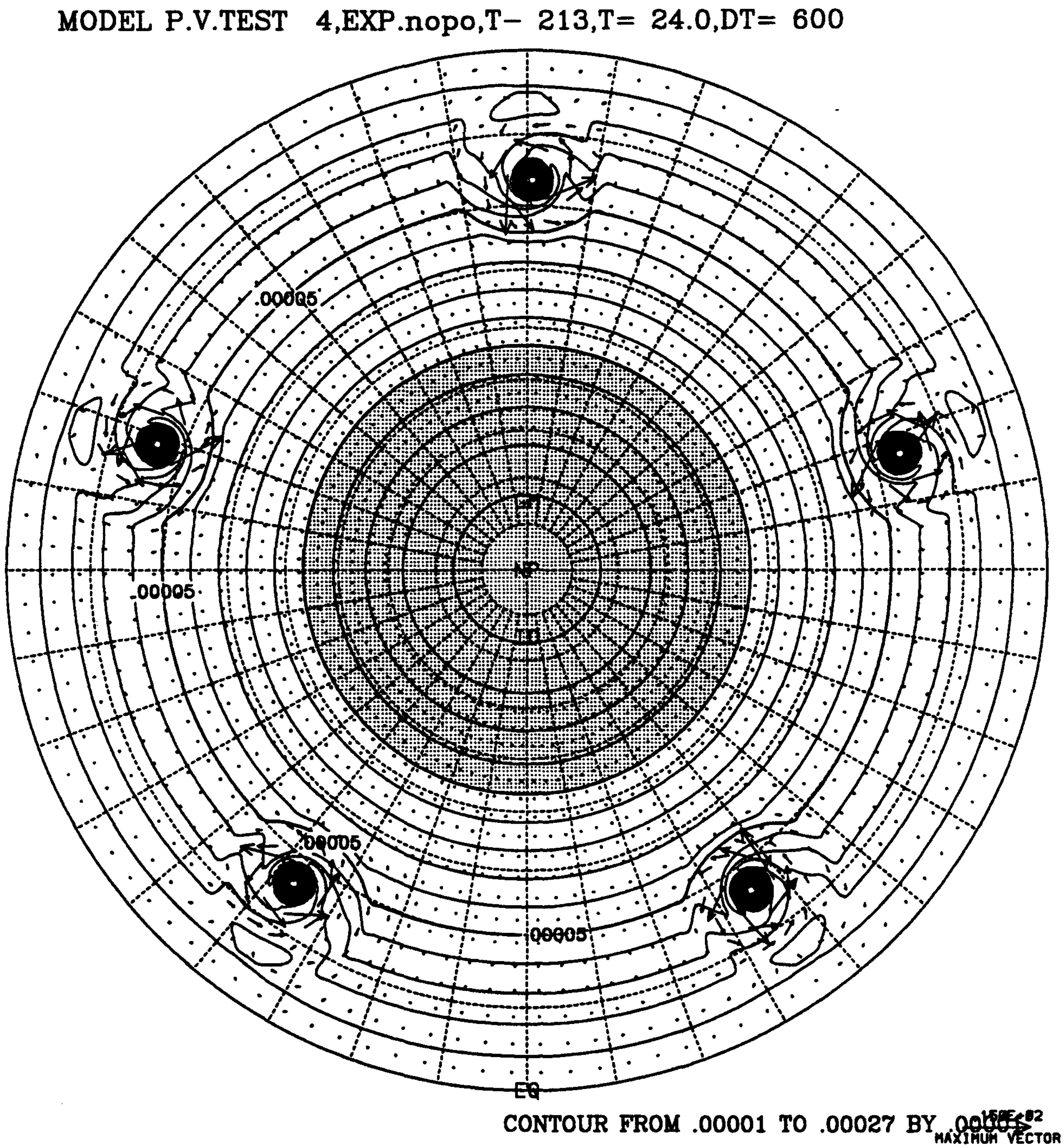

Figure 7.2: The movement of five model tropical cyclones embedded in an environment at rest. The displayed fields are wind (m s^{-1}) and PV (s^{-1}) at (a) 1 day, (b) 4 days, (c) 7 days, and (d) 11 days. From Nieto Ferreira and Schubert 1999.

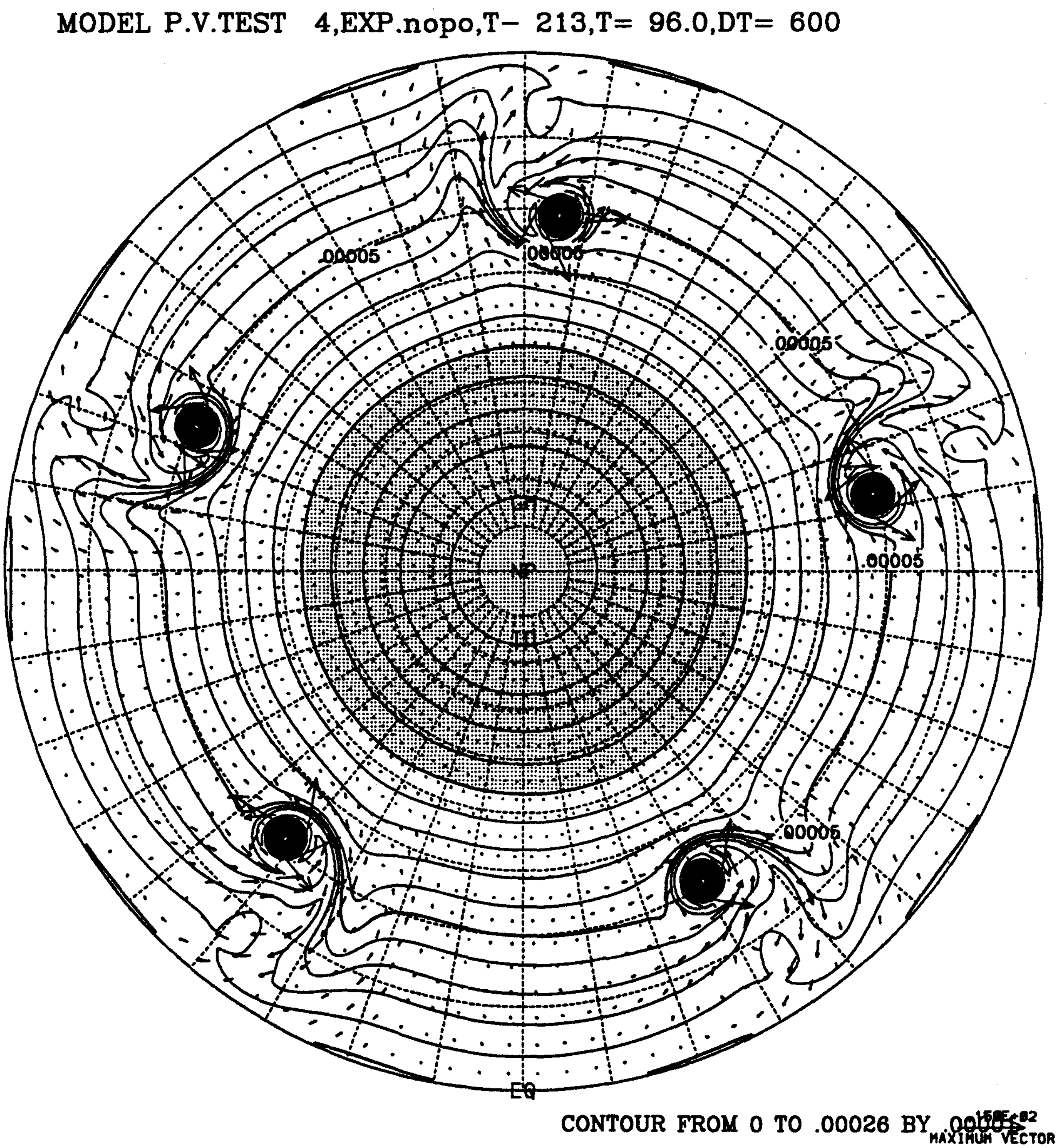

Figure 7.2: (Continued)

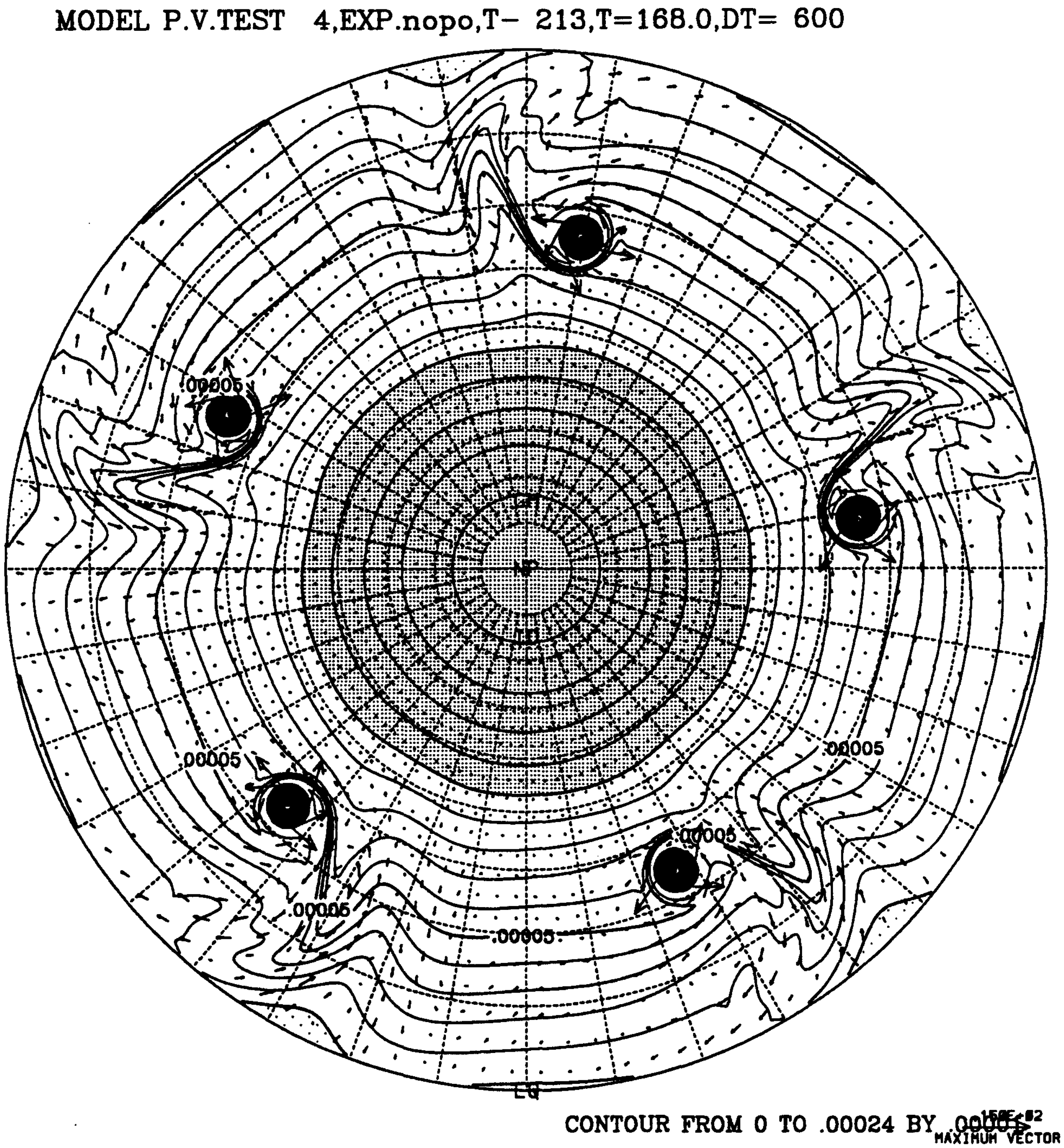

Figure 7.2: (Continued)

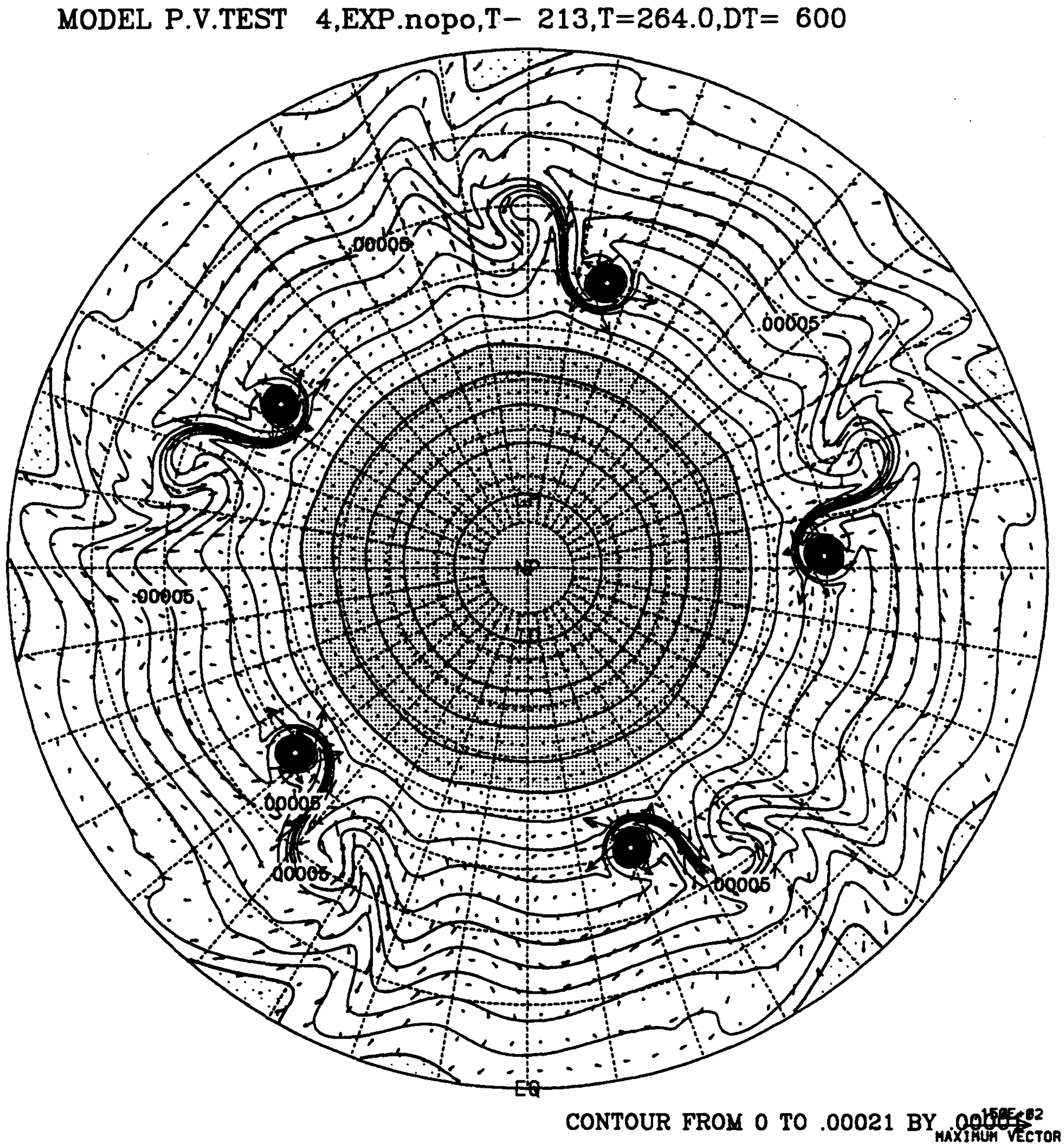

Figure 7.2: (Continued)

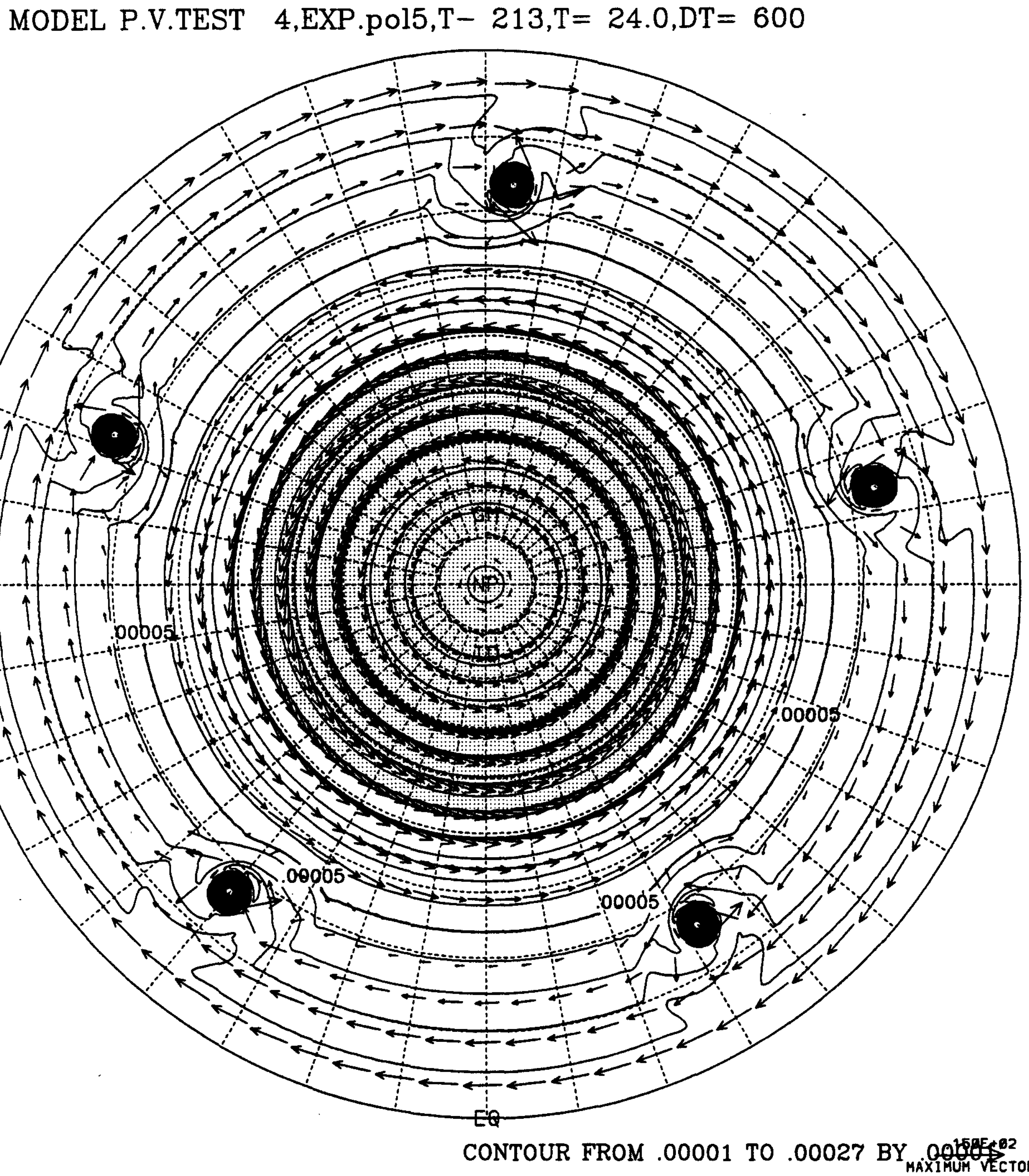

Figure 7.3: The movement of five model tropical cyclones embedded in an environment of low latitude easterlies and midlatitude westerlies. The displayed fields are wind (m s^{-1}) and PV (s^{-1}) at (a) 1 day, (b) 4 days, (c) 7 days, and (d) 11 days. From Nieto Ferreira and Schubert 1999.

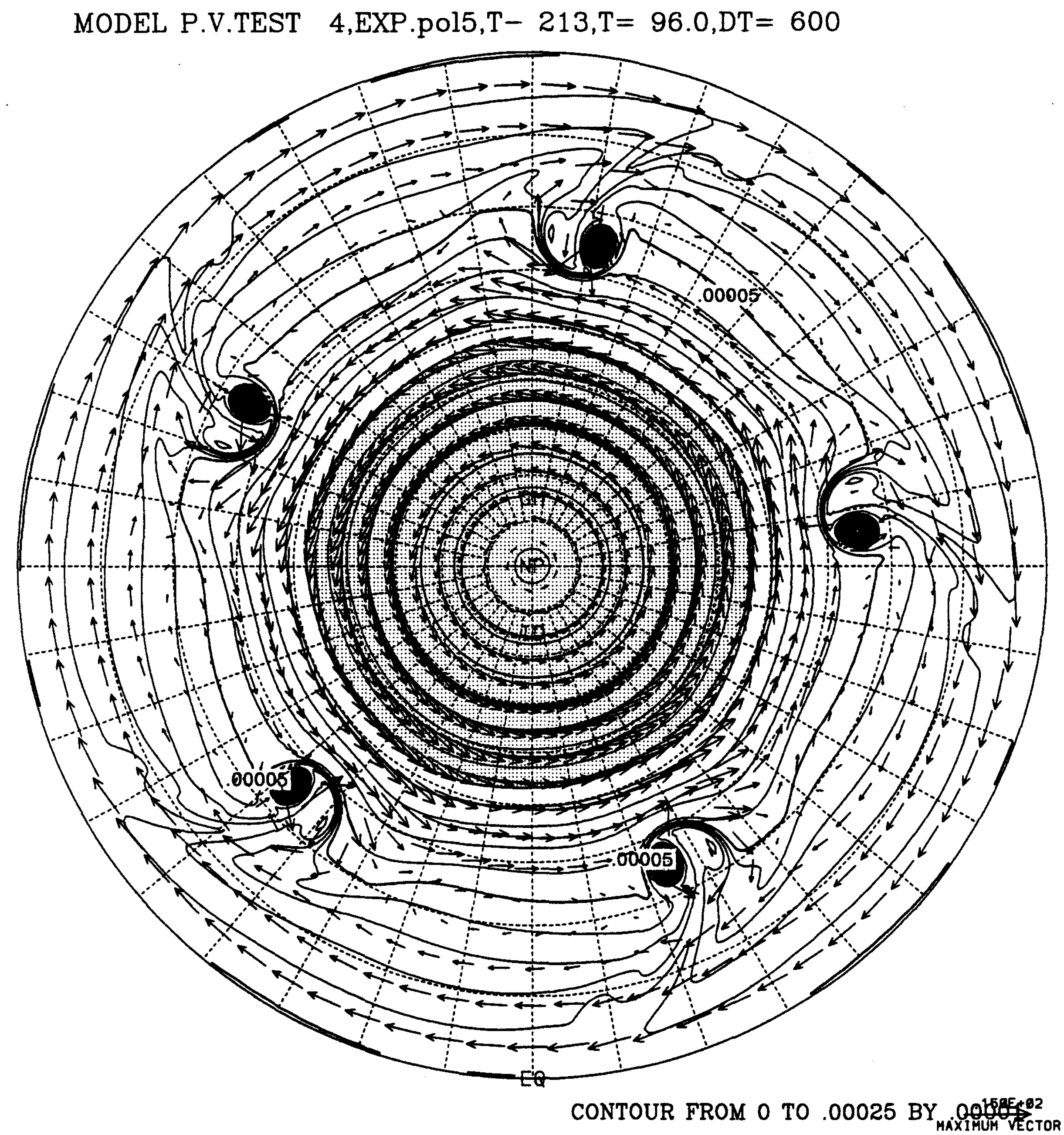

Figure 7.3: (Continued)

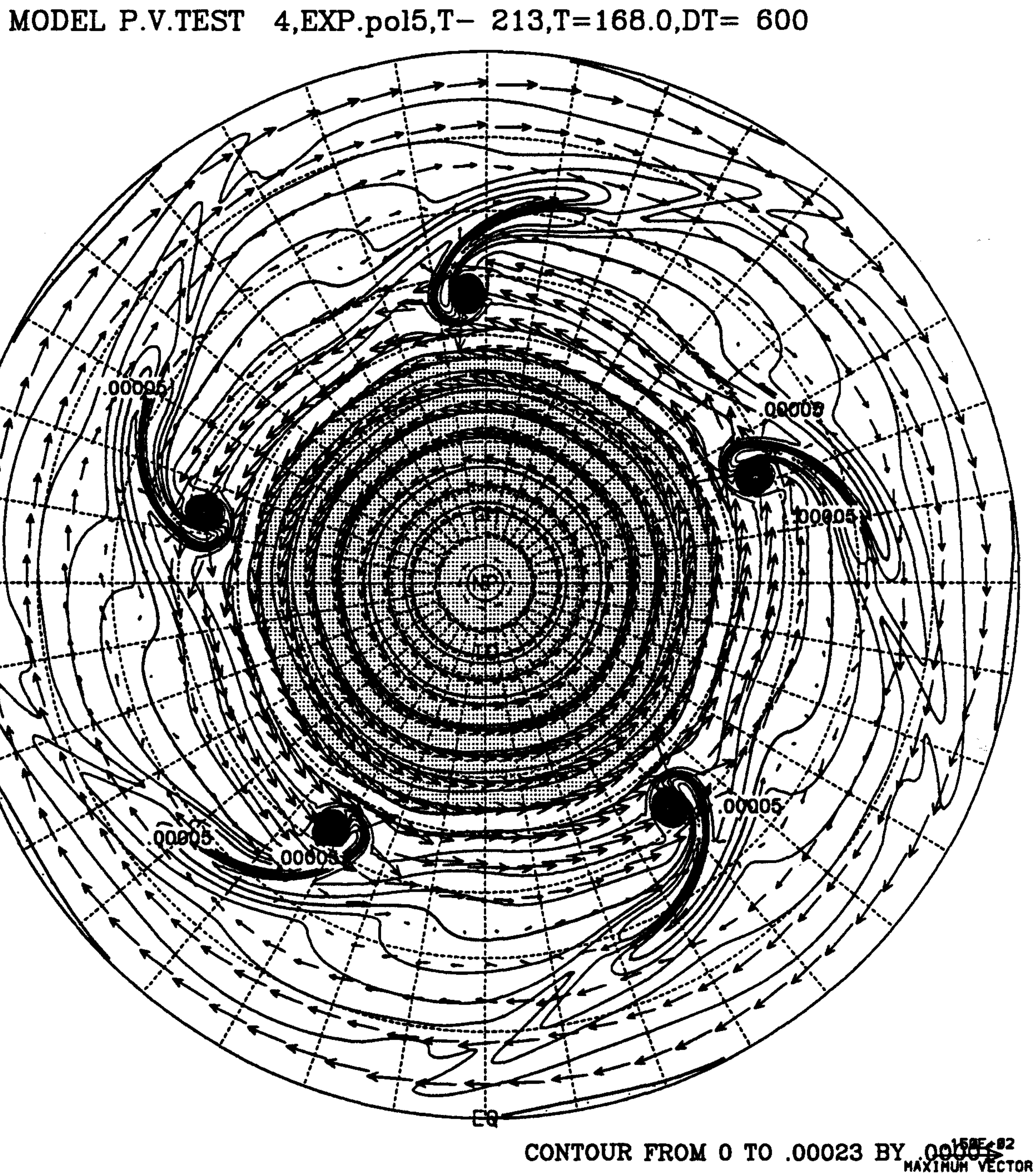

Figure 7.3: (Continued)

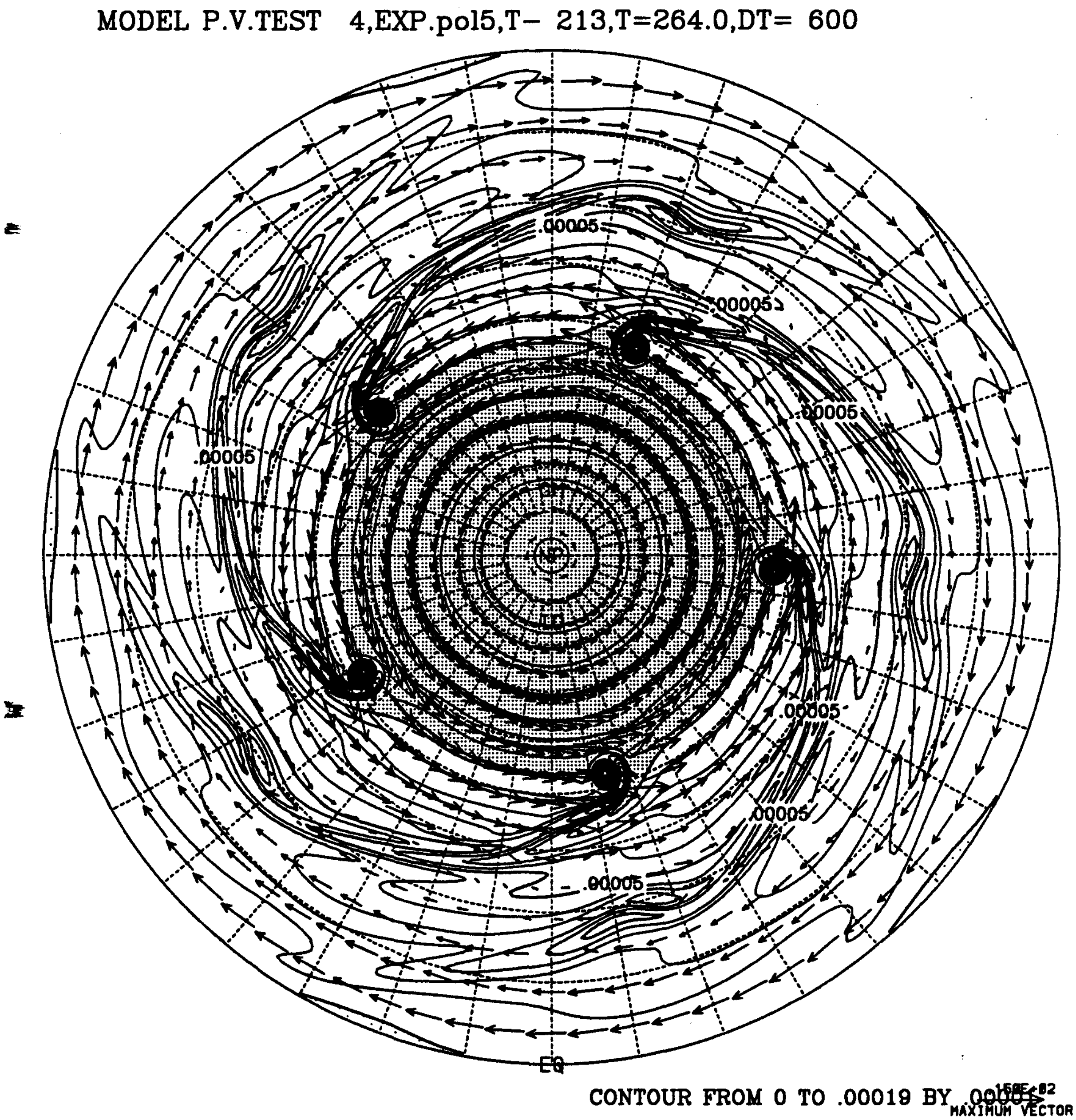

Figure 7.3: (Continued)

Problems

1. Prove that the rotational forms (7.8)–(7.9) are equivalent to the advective forms (7.4)–(7.5). Explain why it is easier to derive the vorticity equation from (7.8)–(7.9) rather than from (7.4)–(7.5).

2. From the shallow water equations (7.4)–(7.6) derive the total energy principle

$$\frac{\partial \left\{ h \left[\frac{1}{2}(u^2+v^2) + \frac{1}{2}gh \right] \right\}}{\partial t} + \frac{\partial \left\{ hu \left[\frac{1}{2}(u^2+v^2) + gh \right] \right\}}{a\cos\phi \partial\lambda} + \frac{\partial \left\{ hv\cos\phi \left[\frac{1}{2}(u^2+v^2) + gh \right] \right\}}{a\cos\phi \partial\phi} = 0.$$

   By integrating this result over the sphere, prove that

$$\frac{d}{dt}\int_{-\pi/2}^{\pi/2}\int_0^{2\pi} h\left[\tfrac{1}{2}(u^2+v^2)+\tfrac{1}{2}gh\right] a\cos\phi \, d\lambda \, d\phi = 0.$$

   This shows that the global integral of the kinetic plus potential energy is invariant with time.

8 Nondivergent Barotropic Equations

8.1 From the divergent barotropic model to the nondivergent barotropic model

The nondivergent barotropic model is a special case of the divergent barotropic model (or shallow water model). In the nondivergent model the continuity equation (7.6) is replaced by

$$\frac{\partial u}{a\cos\phi\partial\lambda}+\frac{\partial(v\cos\phi)}{a\cos\phi\partial\phi}=0, \tag{8.1}$$

which is a statement that the horizontal flow is nondivergent. When the flow is horizontally nondivergent, we can express the horizontal velocity components u and v in terms of a single variable, the streamfunction ψ, i.e.,

$$u=-\frac{\partial\psi}{a\partial\phi},\qquad v=\frac{\partial\psi}{a\cos\phi\partial\lambda}. \tag{8.2}$$

Using (8.2) we see that (8.1) is automatically satisfied and need no longer be considered, i.e., we have reduced the number of unknowns and equations by one. With (8.1) the vorticity equation (7.11) reduces to

$$\frac{D\zeta}{Dt}=0, \tag{8.3}$$

where

$$\begin{aligned}\zeta&=2\Omega\sin\phi+\frac{\partial v}{a\cos\phi\partial\lambda}-\frac{\partial(u\cos\phi)}{a\cos\phi\partial\phi}\\&=2\Omega\sin\phi+\frac{\partial^2\psi}{a^2\cos^2\phi\partial\lambda^2}+\frac{\partial}{a\cos\phi\partial\phi}\left(\cos\phi\frac{\partial\psi}{a\partial\phi}\right)\\&=2\Omega\sin\phi+\nabla^2\psi.\end{aligned} \tag{8.4}$$

Equation (8.3) is a statement of the material conservation of absolute vorticity.

Using (8.2) and (8.4), we can write (8.3) as

$$\frac{\partial\nabla^2\psi}{\partial t}-\frac{\partial\psi}{a\partial\phi}\frac{\partial\nabla^2\psi}{a\cos\phi\partial\lambda}+\frac{\partial\psi}{a\cos\phi\partial\lambda}\frac{\partial\nabla^2\psi}{a\partial\phi}+\frac{2\Omega}{a^2}\frac{\partial\psi}{\partial\lambda}=0, \tag{8.5}$$

so that the nondivergent barotropic model consists of the single equation (8.5) in the single unknown $\psi(\lambda,\phi,t)$. The nondivergent barotropic model is probably the simplest of all atmospheric models. Despite its simplicity, the nondivergent barotropic model is extremely rich in terms of the phenomena it can describe. Note that (8.5) contains two nonlinear terms (the second and third terms) and one linear term (the fourth term). The linear term gives rise to Rossby-Haurwitz waves, which have intricate dispersion properties. The nonlinear terms give rise to two-dimensional turbulence, which has some striking contrasts with three-dimensional turbulence. One of the first to describe the energy cascade that occurs in three-dimensional turbulence was Lewis Fry Richardson (1922), who was inspired by Jonathan Swift's verse:

So, nat'ralists observe, a flea
  Hath smaller fleas that on him prey;
And these have smaller yet to bite 'em,
  And so proceed *ad infinitum*.

Richardson slightly modified this to:

Big whirls have little whirls
  that feed on their velocity,
and little whirls have lesser whirls,
  and so on, to viscosity.

While energy cascades to smaller scales in three-dimensional turbulence, it can cascade the other direction in two-dimensional turbulence. In other words, a stirred vorticity field with fine-scale structure can evolve into large-scale, coherent structures in two-dimensional turbulence, as we shall see next.

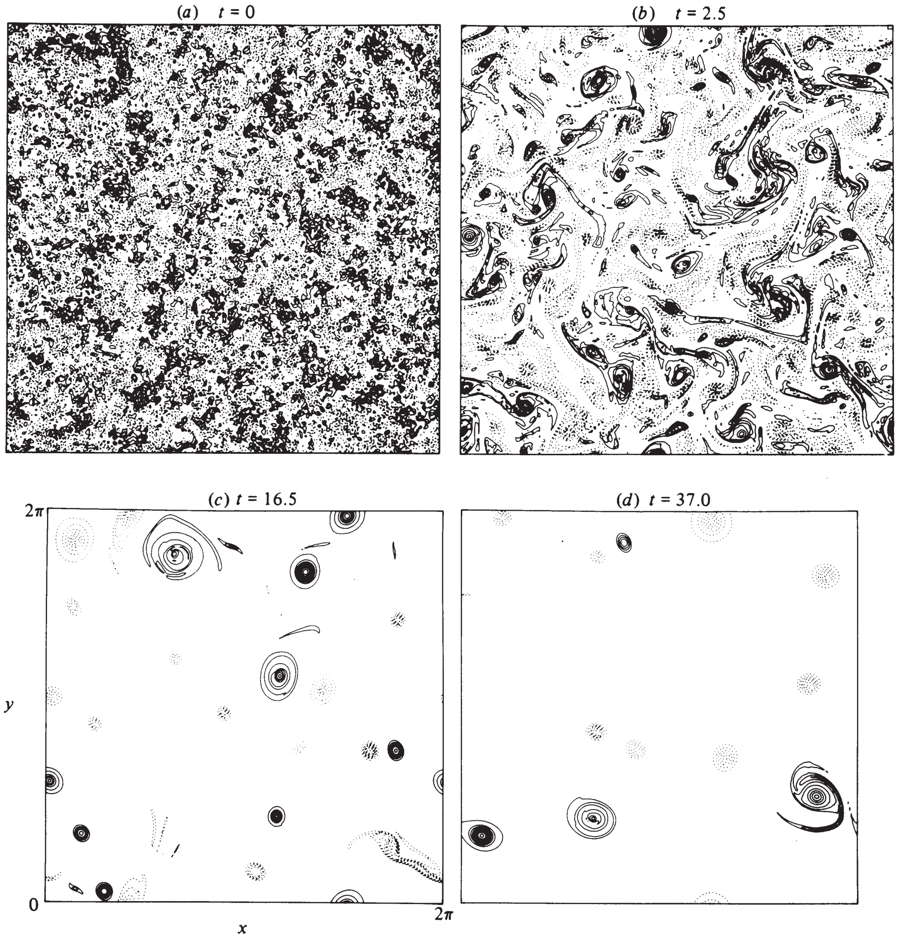

Figure 8.1: Vorticity contours at $t = 0, 2.5, 16.5, 37.0$ dimensionless time units. Time is made dimensionless by $2\pi V^{-1/2}$, the mean eddy turnover time. Positive vorticity contours are solid and negative contours are dashed. From McWilliams 1984.

8.2 Emergence of coherent structures in two-dimensional turbulence

The spherical nondivergent barotropic dynamics governed by (8.5) includes two nonlinear terms that represent horizontal advection of relative vorticity and a linear term that gives rise to Rossby-Haurwitz waves. To isolate the nonlinear advective terms, consider two-dimensional flow on an f-plane rather than on a sphere. Then, the linear Rossby-Haurwitz wave term and all other effects of sphericity disappear, and (8.5) reduces to

$$\frac{\partial \zeta}{\partial t} - \frac{\partial \psi}{\partial y}\frac{\partial \zeta}{\partial x} + \frac{\partial \psi}{\partial x}\frac{\partial \zeta}{\partial y} = \nu \nabla^2 \zeta, \tag{8.6}$$

$$\nabla^2 \psi = \zeta, \tag{8.7}$$

where the Laplacian is now expressed in cartesian coordinates as $\nabla^2 = \partial^2/\partial x^2 + \partial^2/\partial y^2$, and where we have added a diffusion term, with constant diffusion coefficient ν, to the right hand side of (8.6).

We now present a solution of (8.6)–(8.7). The initial condition on the vorticity ζ is shown in Fig. 8.1a, with positive vorticity contours solid and negative vorticity contours dashed. This initial condition looks quite chaotic, with small scale regions of positive and negative vorticity, almost as if the fluid were randomly stirred. As time evolves, small like-signed vorticity regions begin to merge, and a larger scale structure starts to appear (Fig. 8.1b). Later, coherent vortices emerge, and it appears that order has evolved from chaos. This is a remarkable property of two-dimensional turbulence. Figure 8.2 shows the time evolution of the kinetic energy E, the enstrophy V, and the mean wavenumber $\bar{k}$, defined below.

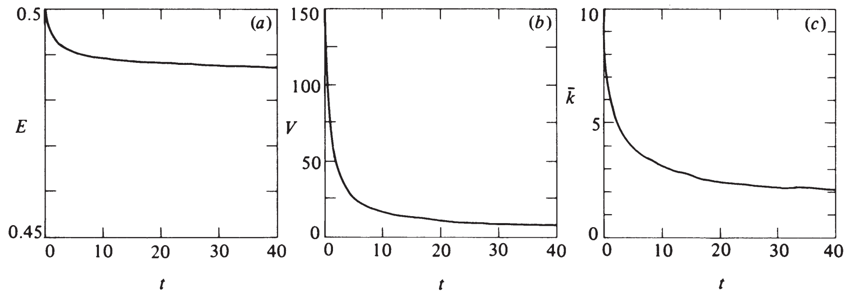

Figure 8.2: Time evolution of kinetic energy E, enstrophy V, and mean wavenumber $\bar{k}$ for the experiment shown in Fig. 8.1. From McWilliams 1984.

To better understand this experiment, we now derive the energy and enstrophy principles from (8.6) and (8.7). Concerning the energy principle, we shall find that all the energy is kinetic, i.e., potential energy and its transformation to kinetic energy are not part of nondivergent barotropic dynamics. To obtain the kinetic energy principle, multiply (8.6) by $-\psi$, which yields

$$\nabla\psi \cdot \nabla\frac{\partial\psi}{\partial t} - \nabla \cdot \left(\psi\nabla\frac{\partial\psi}{\partial t}\right) + \frac{\partial}{\partial x}\left(\psi\frac{\partial\psi}{\partial y}\zeta\right) + \frac{\partial}{\partial y}\left(-\psi\frac{\partial\psi}{\partial x}\zeta\right) = \nu\nabla\cdot(\zeta\nabla\psi - \psi\nabla\zeta) - \nu\zeta^2. \tag{8.8}$$

Now integrate (8.8) over the domain and assume there are no contributions from boundary flux terms. There are many physical arrangements in which the boundary flux terms vanish, e.g., a doubly periodic region, or a closed region in which the velocity component normal to the boundary vanishes, or a zonal channel which is periodic in the east-west direction and has no v component at the north and south boundaries. The integration of (8.8) then yields

$$\frac{dE}{dt} = -2\nu V, \tag{8.9}$$

where

$$E = \iint \tfrac{1}{2}\nabla\psi\cdot\nabla\psi\, dxdy \tag{8.10}$$

is the kinetic energy and

$$V = \iint \tfrac{1}{2}\zeta^2 dxdy \tag{8.11}$$

is the enstrophy. Since $\nu > 0$ and $V > 0$, the diffusion effect always damps the kinetic energy.

To obtain the enstrophy equation, multiply (8.6) by ζ and integrate over the domain. This yields

$$\frac{dV}{dt} = -2\nu P, \tag{8.12}$$

where

$$P = \iint \tfrac{1}{2}\nabla\zeta\cdot\nabla\zeta\, dxdy \tag{8.13}$$

is the palinstrophy. Since $\nu > 0$ and $P > 0$, the diffusion effect always damps the enstrophy.

In the inviscid case ($\nu = 0$), both the kinetic energy E and the enstrophy V are invariant in time. Then, the ratio $(E/V)^{1/2}$, a measure of the mean length scale of the flow, is also invariant, or equivalently, $(V/E)^{1/2}$, a mean wavenumber of the flow, is also invariant. When $\nu \neq 0$, but small in some sense, the situation is very different. To understand this, consider a sequence of model runs (i.e., numerical solutions of (8.6)), all starting with the same initial condition, but with smaller and smaller values of ν. Since the upper bound on V is its initial value, the right hand side of (8.9) goes to zero as $\nu \to 0$, so that E becomes more and more nearly conserved. The behavior of the right hand side of (8.12) is different. As ν becomes smaller, the ζ contours can become closer together before diffusion is effective. When the ζ contours are close together, $\nabla\zeta$ tends to be large, and by (8.13) the palinstrophy is large. Thus, as $\nu \to 0$, the time behavior of the right hand side of (8.12) may not change much, and therefore the time behavior of the enstrophy V may not change much. In this way the enstrophy V may be damped while the kinetic energy E is nearly conserved. This is the phenomenon of *selective decay*, i.e., enstrophy is selectively decayed over kinetic energy. Inspection of Fig. 8.2 reveals that the experiment shown in Fig. 8.1 exhibits strong selective decay.

Now let's prove that, in two-dimensional turbulence, energy and enstrophy move in opposite directions in wavenumber space. Specifically, energy moves to lower wavenumber and enstrophy moves to higher wavenumber. Let k denote the total wavenumber and $E(k)$ the distribution of energy in wavenumber space. Assuming $\nu = 0$ and considering an initial condition in which $E(k)$ is peaked at $k = k_1$, we can say that, if this energy spreads in wavenumber space, then

$$\frac{d}{dt}\int (k-k_1)^2\, E(k)dk > 0. \tag{8.14}$$

Because energy and enstrophy are conserved, we have $d/dt\int E(k)dk = 0$ and $d/dt\int k^2 E(k)dk = 0$. Then, expanding (8.14), and using these last two results, we obtain

$$\frac{d}{dt}\left[\int k^2 E(k)dk - 2k_1\int kE(k)dk + k_1^2\int E(k)dk\right] = -2k_1\frac{d}{dt}\int kE(k)dk > 0 \tag{8.15}$$

Combining (8.15) with energy conservation, we obtain

$$\frac{d}{dt}\left[\frac{\int kE(k)dk}{\int E(k)dk}\right] < 0, \tag{8.16}$$

which states that the wavenumber characterizing the energy-containing scales of motion decreases with time, i.e., energy moves toward large scales.

The argument that enstrophy moves to higher wavenumber proceeds in a similar fashion. If energy spreads, then

$$\frac{d}{dt}\int \left(k^2-k_1^2\right)^2 E(k)dk > 0 \tag{8.17}$$

Again, because energy and enstrophy are conserved

$$\frac{d}{dt}\left[\int k^4 E(k)dk - 2k_1^2\int k^2E(k)dk + k_1^4\int E(k)dk\right] = \frac{d}{dt}\int k^4E(k)dk > 0. \tag{8.18}$$

Thus, defining $Z(k) = k^2E(k)$, and combining (8.18) with enstrophy conservation, we obtain

$$\frac{d}{dt}\left[\frac{\int k^2 Z(k)dk}{\int Z(k)dk}\right] > 0, \tag{8.19}$$

which states that the (squared) wavenumber characterizing the enstrophy-containing scales of motion increases with time, i.e., enstrophy moves toward small scales.

Note that the above arguments contain two ingredients: conservation and irreversibility. Salmon (Lectures on Geophysical Fluid Dynamics) has made the following observation. *The theory of geostrophic turbulence relies almost solely on two components: a conservation principle that energy and potential vorticity are (nearly) conserved and an irreversibility principle in the form of an appealing assumption that breaks the time-reversal symmetry of the exact (inviscid) dynamics. This irreversibility assumption takes a great many superficially dissimilar forms, fostering the misleading impression of a great many competing explanations for the same phenomena. However, broad-minded analysis inevitably reveals that these competing explanations are virtually equivalent.*

These concepts lead to the following idealized picture of forced two-dimensional turbulence on a β-plane (see Fig. 8.3). Energy and enstrophy are input at a certain wavenumber. Energy cascades to lower wavenumbers (larger scales) while enstrophy cascades to higher wavenumbers (smaller scales). The energy cascade to larger scales meets a barrier at the Rhines scale, the scale at which the earth's sphericity becomes important. At this scale Rossby waves are excited. The enstrophy cascade to smaller scales meets a barrier at dissipation scales. A more detailed discussion of the Rhines scale is given in the next section.

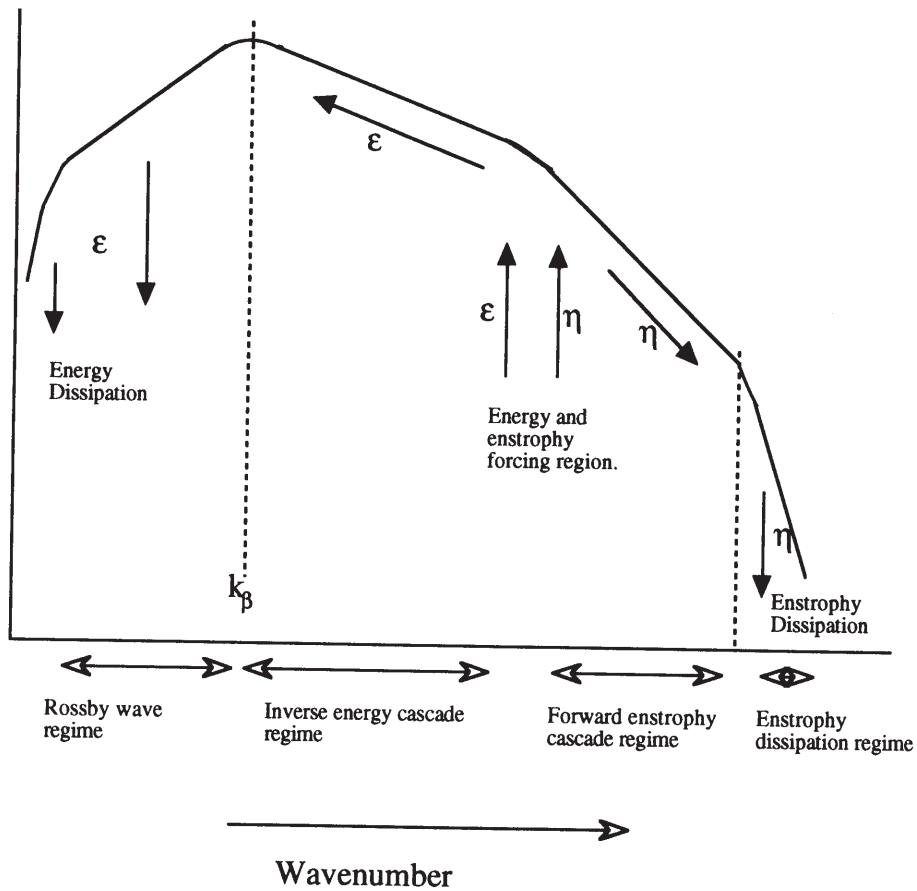

Figure 8.3: Idealized energy spectrum and transfers in two-dimensional turbulence with the β effect. ϵ is the rate of energy input, which equals the transfer rate and dissipation rate. η is the rate of enstrophy input, which equals the transfer rate and dissipation rate. From Vallis and Maltrud 1993.

8.3 Waves and turbulence on the sphere

Equation (8.5) contains nonlinear advection of relative vorticity and a linear term associated with Rossby-Haurwitz waves. Since the Rossby-Haurwitz wave solution of the linearized version of (8.5) is $P_n^m(\mu)e^{i(m\lambda-\omega t)}$ (where m is the zonal wavenumber, n the total wavenumber, ω the wave frequency, and $P_n^m(\mu)$ the associated Legendre function of $\mu = \sin\phi$), the Rossby-Haurwitz wave frequency is given by

$$\frac{2\Omega m}{n(n+1)}. \tag{8.20}$$

The turbulent frequency is given by

$$\frac{[n(n+1)]^{\frac{1}{2}}}{a}V_{\rm rms}, \tag{8.21}$$

where $V_{\rm rms}$ is the root-mean-square velocity. The dynamics is wavelike if

$$\frac{2\Omega m}{n(n+1)} > \frac{[n(n+1)]^{\frac{1}{2}}}{a}V_{\rm rms}, \tag{8.22}$$

while it is dominated by turbulence if

$$\frac{2\Omega m}{n(n+1)} < \frac{[n(n+1)]^{\frac{1}{2}}}{a}V_{\rm rms}. \tag{8.23}$$

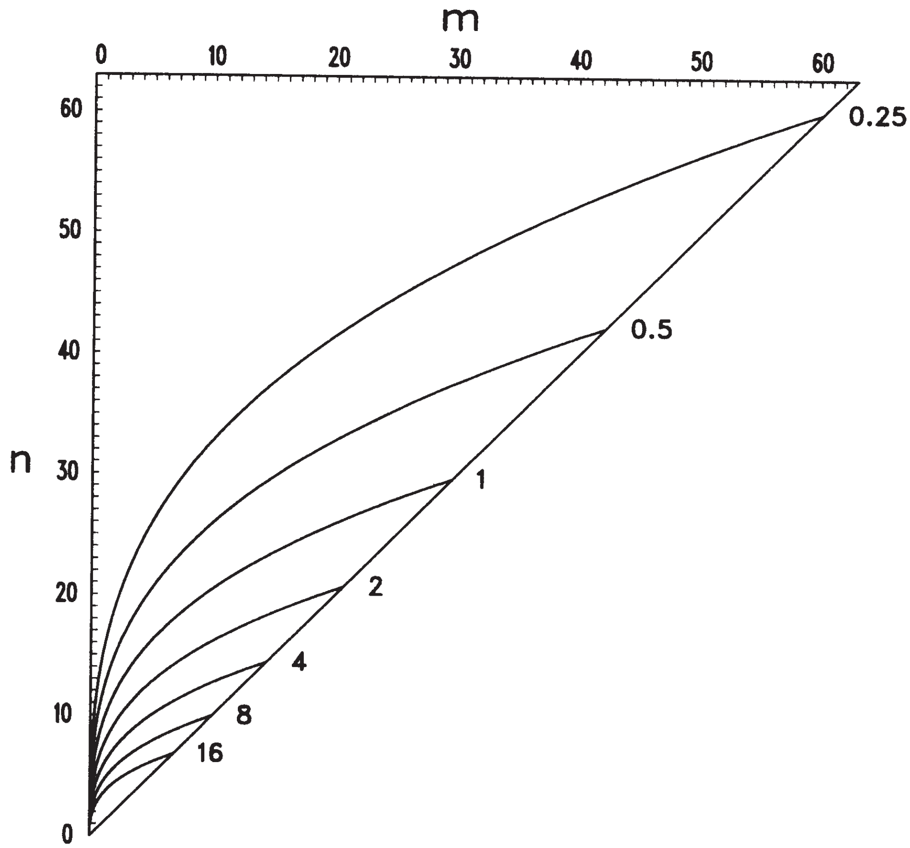

Figure 8.4: Anisotropic Rhines curves in the wavenumber plane of spherical harmonics $Y_n^m(\lambda, \mu) = P_n^m(\mu)e^{im\lambda}$, where m is the zonal wavenumber and n is the total wavenumber. The curves are based on (8.25), with the values of $V_{\rm rms}$ labeled in m s^{-1} on the right. From Huang and Robinson 1998.

The anisotropic Rhines curve, or Rhines barrier, is defined by

$$\frac{2\Omega m}{n(n+1)} = \frac{[n(n+1)]^{\frac{1}{2}}}{a} V_{\rm rms}, \tag{8.24}$$

which, after some rearrangement, can be written as

$$\frac{2\Omega a m}{[n(n+1)]^{\frac{3}{2}}} = V_{\rm rms}. \tag{8.25}$$

For a given $V_{\rm rms}$, (8.25) defines a curve in the spherical harmonic wavenumber plane (m, n). Seven such curves, for different values of $V_{\rm rms}$, are displayed in Fig. 8.4. For a given $V_{\rm rms}$, the region below the appropriate Rhines curve satisfies (8.22) and is hence wavelike, while the region above the curve satisfies (8.23) and is hence dominated by turbulence.

Now consider a set of ten experiments like (8.1), but on the sphere instead of the plane. The initial conditions are all stirred, chaotic ones, with the initial energy centered at $n = 40$ and confined in the range $34 < n < 46$. Figure 8.5 shows the mean energy spectrum (spherical harmonic spectral space m, n), at day 80, for these ten experiments of decaying turbulence. The isolines of energy are normalized to unity, with values greater than 0.1 lightly shaded, and values greater than 0.2 heavily shaded. The energy cascades to lower total wavenumber (i.e., lower n), but is directed to low values of zonal wavenumber m by the Rhines barrier. Since the $m = 0$ spherical harmonics are the zonal harmonics, zonal jets result from the energy cascade, as shown in Fig. 8.6. These alternating easterly and westerly jets are similar to observed patterns on Jupiter and Saturn.

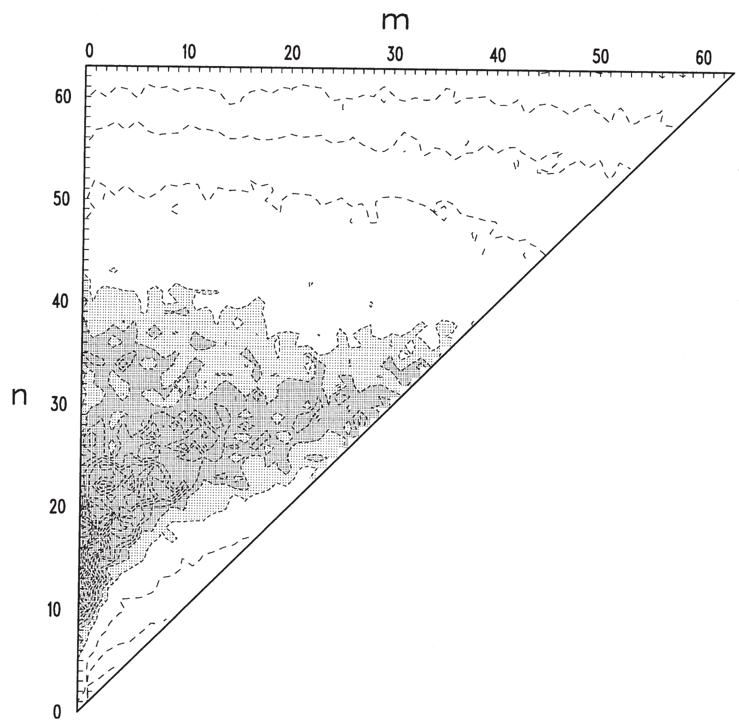

Figure 8.5: Mean energy spectrum (spherical harmonic spectral space m, n), at day 80, for ten experiments of decaying turbulence. The isolines of energy are normalized to unity, with values greater than 0.1 lightly shaded, and values greater than 0.2 heavily shaded. From Huang and Robinson 1998.

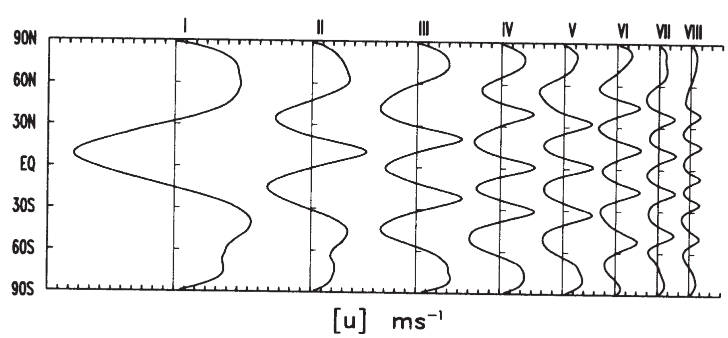

Figure 8.6: Time-mean, zonal mean zonal winds for some two-dimensional turbulence experiments on the sphere. From Huang and Robinson 1998.

Required Reading

- Salmon, sections 4.8–4.10.

A Quote

Concerning turbulence, Horace Lamb is quoted in an address to the British Association for the Advancement of Science as follows:

I am an old man now, and when I die and go to Heaven there are two matters on which I hope for enlightenment. One is quantum electrodynamics, and the other is the turbulent motion of fluids. About the former I am rather optimistic.

Problems

1. Equation (8.9) is the kinetic energy principle for the nondivergent barotropic model on the plane, derived from the nondivergent barotropic vorticity equation (8.6). Derive the kinetic energy principle for the nondivergent barotropic model on the sphere, beginning with (8.5).

9 Vertical Normal Modes of a Continuously Stratified Fluid

9.1 Governing equations and boundary conditions

Consider the motions of a compressible, inviscid, rotating atmosphere in hydrostatic balance. Using $\ln(p_0/p)$ as the vertical coordinate (see Chapter 6, section 3, with the star on z^* dropped for convenience) the linearized horizontal momentum, hydrostatic, continuity and thermodynamic energy equations are

$$\frac{\partial u}{\partial t} - 2\Omega v \sin\phi + \frac{\partial \Phi}{a\cos\phi\partial\lambda} = 0, \tag{9.1}$$

$$\frac{\partial v}{\partial t} + 2\Omega u \sin\phi + \frac{\partial \Phi}{a\partial\phi} = 0, \tag{9.2}$$

$$\frac{\partial \Phi}{\partial z} = RT, \tag{9.3}$$

$$\frac{\partial u}{a\cos\phi\partial\lambda} + \frac{\partial(v\cos\phi)}{a\cos\phi\partial\phi} + e^z\frac{\partial(e^{-z}w)}{\partial z} = 0, \tag{9.4}$$

$$\frac{\partial T}{\partial t} + \Gamma w = \frac{Q}{c_p}, \tag{9.5}$$

where the dependent variables u, v, w, Φ, T represent small-amplitude perturbations about a motionless basic state $\bar\Phi(z), \bar T(z)$ with static stability $\Gamma(z) = \kappa\bar T(z) + d\bar T(z)/dz$. The heat source $Q(\lambda, \phi, z, t)$ represents the effects of radiation and latent heat release on the large-scale flow; we assume this heat source is specified.

The atmosphere is taken to be vertically bounded, with the vertical $\ln p$-velocity required to vanish at the upper boundary, the pressure surface $z = z_T$. At the lower boundary, approximated by the pressure surface $z = 0$, we require that the actual vertical velocity vanish. After linearization these boundary conditions are

$$w = 0 \quad \text{at} \quad z = z_T, \tag{9.6}$$

$$\frac{\partial \Phi}{\partial t} + R\bar T w = 0 \quad \text{at} \quad z = 0. \tag{9.7}$$

It is convenient to eliminate T and w between (9.3)–(9.5) to obtain

$$-e^z\frac{\partial}{\partial z}\left[\frac{e^{-z}}{R\Gamma}\frac{\partial}{\partial z}\left(\frac{\partial(\Phi-\tilde\Phi)}{\partial t}\right)\right] + \frac{\partial u}{a\cos\phi\partial\lambda} + \frac{\partial(v\cos\phi)}{a\cos\phi\partial\phi} = 0. \tag{9.8}$$

where the "forced geopotential" $\tilde\Phi(\lambda, \phi, z, t)$, defined by

$$\frac{\partial}{\partial z}\left(\frac{\partial\tilde\Phi}{\partial t}\right) = \kappa Q, \tag{9.9}$$

is the perturbation geopotential which would result from the heating $Q(\lambda, \phi, z, t)$ if the motion were constrained to be nondivergent. Note that, for a given heating function $Q(\lambda, \phi, z, t)$, the forced geopotential $\tilde\Phi(\lambda, \phi, z, t)$ is not completely determined from (9.9) alone, since there are two constants of integration implicit in this definition. Similarly, eliminating w in the boundary conditions (9.6) and (9.7) using (9.3) and (9.5), we obtain

$$\frac{\partial}{\partial z}\left(\frac{\partial(\Phi-\tilde\Phi)}{\partial t}\right) = 0 \quad \text{at} \quad z = z_T \tag{9.10}$$

$$\frac{\partial}{\partial z}\left(\frac{\partial(\Phi-\tilde\Phi)}{\partial t}\right) - \frac{\Gamma}{\bar T}\left(\frac{\partial(\Phi-\tilde\Phi)}{\partial t}\right) = 0 \quad \text{at} \quad z = 0, \tag{9.11}$$

where we have set $\partial\tilde\Phi/\partial t = 0$ at $z = 0$, thus fixing one of the constants of integration implicit in (9.9).

We have now reduced our problem to the three equations (9.1), (9.2) and (9.8) in the three variables $u(\lambda, \phi, z, t)$, $v(\lambda, \phi, z, t)$ and $\Phi(\lambda, \phi, z, t)$, with the upper and lower boundary conditions (9.10) and (9.11).

9.2 Vertical transform

The only z derivatives in the governing equations (9.1), (9.2) and (9.8) appear in the first term of (9.8). We shall therefore design a vertical transform which eliminates these vertical derivatives. Let us define $\Phi_n(\lambda, \phi, t)$, the vertical integral transform of $\Phi(\lambda, \phi, z, t)$, by

$$\Phi_n(\lambda, \phi, t) = \int_0^{z_T} \Phi(\lambda, \phi, z, t)\Psi_n(z)e^{-z/2}dz, \tag{9.12}$$

where $e^{-z/2}$ is the weight and $\Psi_n(z)$ the kernel of the transform. At this point in our argument the kernel is unspecified. Definitions similar to (9.12) hold for $u_n(\lambda, \phi, t)$ and $v_n(\lambda, \phi, t)$, the vertical integral transforms of $u(\lambda, \phi, z, t)$ and $v(\lambda, \phi, z, t)$.

To vertically transform equation (9.8), we first multiply it by $\Psi_n(z)e^{-z/2}$ and then integrate the resulting equation from $z = 0$ to $z = z_T$. Let's concentrate on what happens to the first term in (9.8) in this process. If we integrate by parts twice, this first term becomes

$$\begin{aligned}
&\int_0^{z_T} \Psi_n e^z \frac{\partial}{\partial z}\left[\frac{e^{-z}}{R\Gamma}\frac{\partial}{\partial z}\left(\frac{\partial(\Phi - \tilde{\Phi})}{\partial t}\right)\right] e^{-z/2}dz \\
&\quad = \int_0^{z_T} \frac{\partial(\Phi - \tilde{\Phi})}{\partial t} e^{z/2}\frac{\partial}{\partial z}\left[\frac{e^{-z}}{R\Gamma}\frac{\partial(e^{z/2}\Psi)}{\partial z}\right] e^{-z/2}dz \\
&\quad - \left[\frac{e^{-z}}{R\Gamma}\left\{\frac{\partial(\Phi - \tilde{\Phi})}{\partial t}\frac{d\left(e^{z/2}\Psi_n\right)}{dz} - e^{z/2}\Psi_n\frac{\partial}{\partial z}\left(\frac{\partial(\Phi - \tilde{\Phi})}{\partial t}\right)\right\}\right]_0^{z_T}.
\end{aligned} \tag{9.13}$$

Suppose we require the so-far-undetermined kernel $\Psi_n(z)$ to satisfy the upper and lower boundary conditions (9.16) and (9.17). Then, also using (9.10) and (9.11), we can easily show that the boundary term in (9.13) vanishes. If we also require that the kernel $\Psi_n(z)$ satisfy the ordinary differential equation (9.15), then (9.13) reduces to

$$\int_0^{z_T} \Psi_n e^z \frac{\partial}{\partial z}\left[\frac{e^{-z}}{R\Gamma}\frac{\partial}{\partial z}\left(\frac{\partial(\Phi - \tilde{\Phi})}{\partial t}\right)\right] e^{-z/2}dz = -\frac{1}{c_n^2}\frac{\partial(\Phi_n - \tilde{\Phi}_n)}{\partial t}, \tag{9.14}$$

which allows (9.8) to be transformed to (9.22).

To summarize, the set of functions $\Psi_n(z)$ are solutions of the Sturm-Liouville eigenproblem

$$e^{z/2}\frac{d}{dz}\left[\frac{e^{-z}}{R\Gamma}\frac{d\left(e^{z/2}\Psi_n\right)}{dz}\right] + \frac{1}{c_n^2}\Psi_n = 0, \tag{9.15}$$

$$\frac{d\left(e^{z/2}\Psi_n\right)}{dz} = 0 \qquad \text{at} \quad z = z_T \tag{9.16}$$

$$\frac{d\left(e^{z/2}\Psi_n\right)}{dz} - \frac{\Gamma}{\overline{T}}e^{z/2}\Psi_n = 0 \quad \text{at} \quad z = 0. \tag{9.17}$$

The inverse transform may be obtained by considering the properties of the solutions of (9.15)–(9.17). It can be shown (e.g., Morse and Feshbach 1953) that if $\Gamma(z)$ is strictly positive and continuously differentiable for $0 \le z \le z_T$ then (9.15)–(9.17) have a countably infinite set of solutions $\{c_n, \Psi_n(z)\}_{n=0}^{\infty}$ with the following properties:

(i) The eigenvalues c_n are real and may be ordered such that $c_0 > c_1 > \ldots > c_n > \ldots > 0$ with $c_n \to 0$ as $n \to \infty$.

(ii) The eigenfunctions $\Psi_n(z)$ are orthogonal and may be chosen to be real.

(iii) The eigenfunctions $\Psi_n(z)$ form a complete set.

We normalize the $\Psi_n(z)$ so that in view of property (ii) we have

$$\int_0^{z_T} \Psi_m(z)\Psi_n(z)dz = \begin{Bmatrix} 1 & m = n \\ 0 & m \neq n \end{Bmatrix}. \tag{9.18}$$

Property (iii) allows us to expand any function, for example $\Phi(\lambda, \phi, z, t)$, as

$$\Phi(\lambda, \phi, z, t) = \sum_{n=0}^{\infty} \Phi_n(\lambda, \phi, t)\Psi_n(z)e^{z/2}, \tag{9.19}$$

and (9.18) implies that the coefficients in this expansion are given by (9.12). Thus, we see that (9.12) and (9.19) form the desired transform pair.

To summarize, applying the transform (9.8) to the governing equations (9.1), (9.2) and (9.8) results in

$$\frac{\partial u_n}{\partial t} - 2\Omega v_n \sin\phi + \frac{\partial \Phi_n}{a\cos\phi\partial\lambda} = 0, \tag{9.20}$$

$$\frac{\partial v_n}{\partial t} + 2\Omega u_n \sin\phi + \frac{\partial \Phi_n}{a\partial\phi} = 0, \tag{9.21}$$

$$\frac{\partial \Phi_n}{\partial t} + c_n^2 \left(\frac{\partial u_n}{a\cos\phi\partial\lambda} + \frac{\partial(v_n\cos\phi)}{a\cos\phi\partial\phi} \right) = \frac{\partial \tilde{\Phi}_n}{\partial t}, \tag{9.22}$$

which is formally equivalent to the linearized divergent barotropic model (i.e., the linearized shallow water equations). The eigenvalue c_n which appears in (9.22) in place of the pure gravity wave phase speed in the divergent barotropic model thus corresponds to the phase speed of a pure gravity wave of a single vertical mode n having vertical structure $\Psi_n(z)e^{z/2}$ in the stratified model. Thus by use of the vertical transform pair (9.12) and (9.19), the solution of the stratified problem has been reduced to a superposition of solutions of the barotropic problems corresponding to the various vertical modes. For this reason we refer to (9.12) and (9.19) as a vertical normal mode transform pair. Solutions of the eigenvalue problem (9.15)–(9.17) for the case of constant static stability are discussed in the next section.

9.3 Solution of the Sturm-Liouville eigenproblem in the constant static stability case

When the static stability Γ is constant, the vertical structure problem (9.15)–(9.17) simplifies to

$$\frac{d^2\Psi_n}{dz^2} + \left(\frac{R\Gamma}{c_n^2} - \frac{1}{4} \right) \Psi_n = 0, \tag{9.23}$$

$$\frac{d\Psi_n}{dz} + \frac{1}{2}\Psi_n = 0 \qquad \text{at} \quad z = z_T, \tag{9.24}$$

$$\frac{d\Psi_n}{dz} + \left(\frac{1}{2} - \frac{\Gamma}{\bar{T}_0} \right) \Psi_n = 0 \quad \text{at} \quad z = 0. \tag{9.25}$$

Note that the character of a solution of (9.23) is evanescent in z if $R\Gamma/c_n^2 < 1/4$ and is oscillatory in z if $R\Gamma/c_n^2 > 1/4$. Since we don't yet know the eigenvalues c_n, we must investigate both possibilities.

Thus, let us consider case 1: $\mu_n^2 > 0$, where

$$\mu_n = \left(\frac{1}{4} - \frac{R\Gamma}{c_n^2} \right)^{\frac{1}{2}}. \tag{9.26}$$

In this case the vertical structure equation (9.23) has the solution

$$\Psi_n(z) = A\cosh(\mu_n z) + B\sinh(\mu_n z). \tag{9.27}$$

When this solution is substituted into the boundary conditions (9.24) and (9.25), we obtain

$$\left[\frac{1}{2} + \mu_n \tanh(\mu_n z_T) \right] A + \left[\frac{1}{2}\tanh(\mu_n z_T) + \mu_n \right] B = 0, \tag{9.28}$$

$$\left[\frac{1}{2} - \frac{\Gamma}{\bar{T}_0}\right] A + \mu_n B = 0, \tag{9.29}$$

which is a homogeneous linear algebraic system in A and B. Requiring the determinant of the coefficients of A and B to vanish, we obtain

$$\left(\frac{R\bar{T}_0}{c_n^2} - \frac{1}{2}\right) \tanh(\mu_n z_T) = \mu_n. \tag{9.30}$$

It can be shown that, if $z_T > 4\Gamma/(\bar{T}_0 - 2\Gamma)$, then (9.30) has precisely one root c_0 with $c_0^2 > 4R\Gamma$, and that if $z_T \leq 4\Gamma/(\bar{T}_0 - 2\Gamma)$, then (9.30) has no roots with $\mu_n^2 > 0$. Thus, (9.30), along with (9.26), defines one phase speed c_0 in the case where $z_T > 4\Gamma/(\bar{T}_0 - 2\Gamma)$. An approximate value for c_0, obtained by assuming $c_0^2 >> 4R\Gamma$ and therefore setting $\mu_0 = 1/2$ in (9.30), is given by

$$c_0 \approx \left[\left(1 - e^{-z_T}\right) R\bar{T}_0\right]^{\frac{1}{2}} \tag{9.31}$$

For $z_T = 2.313$, $\bar{T}_0 = 302.53$K and $\Gamma = 23.79$K, the exact eigenvalue c_0 determined numerically from (9.30) and the approximate eigenvalue determined from (9.31) are given in the row labeled $n = 0$ in Table 9.1. When (9.29) is used to express B in terms of A, the corresponding eigenfunction can be written as

$$\Psi_0(z) = A\left[\cosh(\mu_0 z) - \frac{\gamma}{\mu_0}\sinh(\mu_0 z)\right], \tag{9.32}$$

where $\gamma = 1/2 - \Gamma/\bar{T}_0$. To satisfy the normalization condition given by (9.18), we choose A as

$$A^2 = \frac{2\mu_0^3 c_0^2}{R\Gamma\left[(\mu_0^2 + \gamma^2)\sinh(\mu_0 z_T)\cosh(\mu_0 z_T) - 2\mu_0\gamma\sinh^2(\mu_0 z_T) + (\mu_0^2 - \gamma^2)\mu_0 z_T\right]}. \tag{9.33}$$

The external mode basis function $\Psi_0(z)e^{z/2}$ is plotted in Fig. 9.1.

n	Exact	Approx
0	287.00	279.70
1	56.28	60.84
2	29.79	30.42
3	20.09	20.28
4	15.13	15.21
5	12.13	12.17
6	10.12	10.14
7	8.68	8.69
8	7.59	7.60
9	6.75	6.76
10	6.08	6.08

Table 9.1:

Now consider case 2: $\nu_n^2 > 0$ where

$$\nu_n = \left(\frac{R\Gamma}{c_n^2} - \frac{1}{4}\right)^{\frac{1}{2}}. \tag{9.34}$$

In this case the vertical structure equation (9.23) has the solution

$$\Psi_n(z) = C\cos(\nu_n z) + D\sin(\nu_n z). \tag{9.35}$$

When this solution is substituted into the boundary conditions (9.24) and (9.25), we obtain

$$\left[\frac{1}{2} - \nu_n\tan(\nu_n z_T)\right] C + \left[\frac{1}{2}\tan(\nu_n z_T) + \nu_n\right] D = 0, \tag{9.36}$$

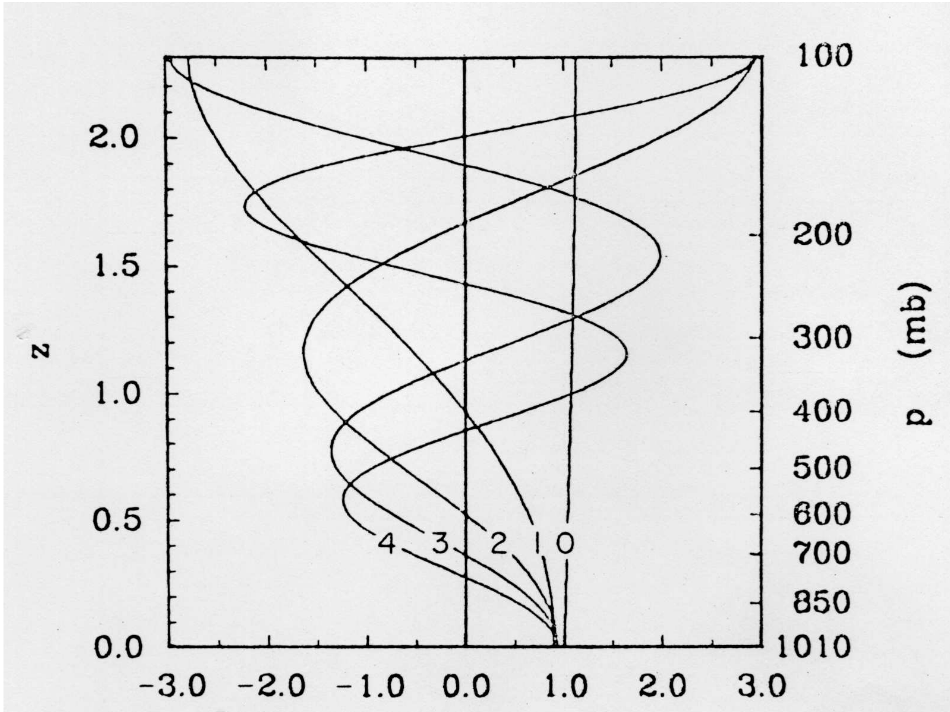

Figure 9.1: Vertical structure functions $\Psi_n(z)e^{z/2}$ for the constant static stability atmosphere for the vertical modes $n = 0, 1, 2, 3, 4$. These five eigenfunctions have the corresponding eigenvalues $c_n = 287.00, 56.28, 29.79, 20.09, 15.13$ ms^{-1}, or in terms of equivalent depth $h_n = c_n^2/g = 8405, 323.2, 90.6, 41.2, 23.4$ m.

$$\left[\frac{1}{2} - \frac{\Gamma}{\bar{T}_0}\right] C + \nu_n D = 0, \tag{9.37}$$

which is a homogeneous linear algebraic system in C and D. Requiring the determinant of the coefficients of C and D to vanish, we obtain

$$\left(\frac{R\bar{T}_0}{c_n^2} - \frac{1}{2}\right) \tan(\nu_n z_T) = \nu_n. \tag{9.38}$$

It can be shown that (9.38) has solutions c_n $(n = 1, 2, \ldots)$ with

$$\frac{4R\Gamma}{[2(n+1)\pi/z_T]^2 + 1} < c_n^2 < \frac{4R\Gamma}{[2n\pi/z_T]^2 + 1},$$

and that if $z_T \leq 4\Gamma/(\bar{T}_0 - 2\Gamma)$, then (9.38) also has one solution c_0 with

$$\frac{4R\Gamma}{[2\pi/z_T]^2 + 1} < c_0^2 < 4R\Gamma.$$

Thus (9.38), along with (9.34), defines a countably set of phase speeds c_n. As c_n becomes smaller, a useful approximation of (9.38) is $\tan(\nu_n z_T) \approx 0$, which has solutions $\nu_n z_T = n\pi$. When this is used in (9.34), we obtain

$$c_n \approx \frac{(R\Gamma)^{\frac{1}{2}} z_T}{n\pi}. \tag{9.39}$$

For $z_T = 2.313$, $\bar{T}_0 = 302.53$K and $\Gamma = 23.79$K, the exact eigenvalues determined numerically from (9.38) and the approximate eigenvalues determined from (9.39) are given in the rows labeled $n = 1, 2, \ldots, 10$ in Table 9.1. The asymptotic behavior $c_n \sim 1/n$ as n becomes large is obvious from the table. When (9.37) is used to express D in terms of C, the corresponding eigenfunctions can be written as

$$\Psi_n(z) = C\left[\cos(\nu_n z) - \frac{\gamma}{\nu_n}\sin(\nu_n z)\right]. \tag{9.40}$$

To satisfy the normalization condition given by (9.18), we choose C as

$$C^2 = \frac{2\nu_n^3 c_n^2}{R\Gamma\left[(\nu_n^2-\gamma^2)\sin(\mu_0 z_T)\cos(\mu_0 z_T) - 2\nu_n\gamma\sin^2(\mu_0 z_T) + (\nu_n^2+\gamma^2)\mu_0 z_T\right]}. \tag{9.41}$$

The internal mode basis functions $\Psi_n(z)e^{z/2}$ are plotted for $n = 1, 2, 3, 4$ in Fig. 9.1.

9.4 Summary

We have now established a procedure for solving the system (9.1)–(9.5) by converting it into an infinite set of shallow water systems. The idea is as follows. Starting from (9.1)–(9.5), eliminate T and w to obtain a system of three equations in three unknowns, the equations being (9.1), (9.2), and (9.8), the unknowns being $u(\lambda,\phi,z,t)$, $v(\lambda,\phi,z,t)$, $\Phi(\lambda,\phi,z,t)$. Defining the vertical transform of these variables as

$$\begin{pmatrix} u_n(\lambda,\phi,t) \\ v_n(\lambda,\phi,t) \\ \Phi_n(\lambda,\phi,t)\end{pmatrix} = \int_0^{z_T}\begin{pmatrix} u(\lambda,\phi,z,t) \\ v(\lambda,\phi,z,t) \\ \Phi(\lambda,\phi,z,t)\end{pmatrix}\Psi_n(z)e^{-z/2}dz, \tag{9.42}$$

derive the shallow water equation set (9.20)–(9.22) for each vertical mode n. Once we have solved each shallow water set, we can perform the inverse vertical transform

$$\begin{pmatrix} u(\lambda,\phi,z,t) \\ v(\lambda,\phi,z,t) \\ \Phi(\lambda,\phi,z,t)\end{pmatrix} = \sum_{n=0}^{\infty}\begin{pmatrix} u_n(\lambda,\phi,t) \\ v_n(\lambda,\phi,t) \\ \Phi_n(\lambda,\phi,t)\end{pmatrix}\Psi_n(z)e^{z/2}, \tag{9.43}$$

to recover the original unknowns $u(\lambda,\phi,z,t)$, $v(\lambda,\phi,z,t)$, $\Phi(\lambda,\phi,z,t)$. The set of constants c_n^2 appearing in the shallow water equations and the set of vertical structure functions $\Psi_n(z)$ $(n = 0, 1, 2, \cdots)$ are determined by solving the eigenvalue-eigenfunction problem (9.15)–(9.17). The eigenvalues c_n^2 and the eigenfunctions $\Psi_n(z)$ depend on our specification of the basic state static stability $\Gamma(z)$, and in section 9.3 we have solved this eigenvalue-eigenfunction problem for the simplest case, i.e., the case when Γ is a constant. When Γ is not a constant, the eigenvalues will differ from those given in Table 9.1 and the eigenfunctions will differ from those plotted in Fig. 9.1. However, for reasonable choices of $\Gamma(z)$, the results will be very similar.

In the following chapters we shall concentrate on solving the shallow water equations, without reference to the vertical structure in which they are embedded. Although we would like to solve the spherical shallow water equations (9.20)–(9.22), this proves somewhat difficult, so we shall concentrate mostly on the f-plane and β-plane approximations of (9.20)–(9.22).

Problems

1. Starting from the complete thermodynamic equation, show that (9.5) is the form resulting from linearization about a resting basic state.
2. Starting from (9.3)–(9.5) eliminate T and w to obtain (9.8).
3. Derive the boundary conditions (9.10) and (9.11) from (9.6) and (9.7).
4. For Γ =constant, prove that (9.15) reduces to (9.23).

10 The Shallow Water Equations on an f-plane

10.1 Linearization and nondimensionalization

In this chapter we shall study the process by which an initially unbalanced flow adjusts to geostrophic balance. The initially unbalanced state could be a flow without a corresponding pressure gradient, or a pressure gradient without a corresponding flow. In either case there will be a transient adjustment process which leads to a final geostrophic balance. We are ultimately interested in how this process occurs in the stratified atmosphere on the spherical earth. Unfortunately, this is mathematically complicated, and it is best to start with f-plane, shallow water arguments. With the f-plane approximation, the shallow water equations (7.4)–(7.6) become

$$\frac{Du}{Dt} - fv + g\frac{\partial h}{\partial x} = 0, \tag{10.1}$$

$$\frac{Dv}{Dt} + fu + g\frac{\partial h}{\partial y} = 0, \tag{10.2}$$

$$\frac{Dh}{Dt} + h\left(\frac{\partial u}{\partial x} + \frac{\partial v}{\partial y}\right) = Q(x,y)\alpha^2 t e^{-\alpha t}, \tag{10.3}$$

where u and v are velocity components in the x- and y-directions, respectively, f is the constant Coriolis parameter,

$$\frac{D}{Dt} = \frac{\partial}{\partial t} + u\frac{\partial}{\partial x} + v\frac{\partial}{\partial y} \tag{10.4}$$

is the material derivative, and $Q(x,y)\alpha^2 t e^{-\alpha t}$ is the mass source or sink. We have assumed that the mass source or sink can be factored into space-dependent and time-dependent parts, with the time-dependent part given by $\alpha^2 t e^{-\alpha t}$. Small α corresponds to slow forcing and large α to rapid forcing, but the total forcing is independent of α, since $\int_0^\infty \alpha^2 t e^{-\alpha t} dt = 1$.

Although the f-plane equations (10.1)–(10.3) are simpler than the spherical equations (7.4)–(7.6), they are still very complicated because of nonlinearity. Thus, we shall consider small amplitude motions about a basic state of rest. The linearized shallow water equations governing such motions are

$$\frac{\partial u}{\partial t} - fv + g\frac{\partial h}{\partial x} = 0, \tag{10.5}$$

$$\frac{\partial v}{\partial t} + fu + g\frac{\partial h}{\partial y} = 0, \tag{10.6}$$

$$\frac{\partial h}{\partial t} + \bar{h}\left(\frac{\partial u}{\partial x} + \frac{\partial v}{\partial y}\right) = Q(x,y)\alpha^2 t e^{-\alpha t}, \tag{10.7}$$

where $\bar{h}$ is the constant mean depth of the layer and h should now be interpreted as the deviation of the actual depth from the mean depth.

Before solving (10.5)–(10.7) it is convenient to put the problem in nondimensional form by defining $c = (g\bar{h})^{1/2}$ and choosing $1/f$, c/f, $\bar{h}$ and c as units of time, horizontal distance, vertical distance, and speed, respectively. The resulting equations may be written as

$$\frac{\partial u}{\partial t} - v + \frac{\partial h}{\partial x} = 0, \tag{10.8}$$

$$\frac{\partial v}{\partial t} + u + \frac{\partial h}{\partial y} = 0, \tag{10.9}$$

$$\frac{\partial h}{\partial t} + \frac{\partial u}{\partial x} + \frac{\partial v}{\partial y} = Q(x,y)\alpha^2 t e^{-\alpha t}, \tag{10.10}$$

where all quantities are now nondimensional.

At large times the right hand side of (10.10) is very small and, if the solution has settled into a steady state (i.e., if $\partial u/\partial t = 0$, $\partial v/\partial t = 0$, and $\partial h/\partial t = 0$), we see that $u = -\partial h/\partial y$, $v = \partial h/\partial x$ and $\partial u/\partial x + \partial v/\partial y = 0$, i.e., the flow is geostrophic and horizontally nondivergent. Our goal in this chapter is to show how the atmosphere naturally evolves into such steady geostrophic states, no matter what the initial condition or the forcing.

10.2 Geostrophic adjustment: One-dimensional case

Let us first consider the y-independent case, so that (10.8)–(10.10) reduce to

$$\frac{\partial u}{\partial t} - v + \frac{\partial h}{\partial x} = 0, \tag{10.11}$$

$$\frac{\partial v}{\partial t} + u = 0, \tag{10.12}$$

$$\frac{\partial h}{\partial t} + \frac{\partial u}{\partial x} = Q(x)\alpha^2 t e^{-\alpha t}. \tag{10.13}$$

The linearized potential vorticity principle derived from (10.12) and (10.13) is simply

$$\frac{\partial}{\partial t}\left(\frac{\partial v}{\partial x} - h\right) = -Q(x)\alpha^2 t e^{-\alpha t}, \tag{10.14}$$

so that the potential vorticity $\partial v/\partial x - h$ locally increases if there is a mass sink ($Q < 0$), but is locally conserved during the geostrophic adjustment process if $Q = 0$.

In the y-independent case, u does not contribute to the vorticity and v does not contribute to the divergence. Thus, it is appropriate to refer to u as the divergent part of the flow and v as the rotational part of the flow. Equations (10.11)–(10.13) constitute a set of constant coefficient, linear partial differential equations in the dependent variables $u(x,t)$, $v(x,t)$, $h(x,t)$. We shall treat the x-domain as infinite. Note that the solution depends on specification of the initial conditions $u(x,0)$, $v(x,0)$, $h(x,0)$ and the mass source/sink $Q(x)$. If $v(x,0)$ and $h(x,0)$ are specified in such a way that $v(x,0) \neq \partial h(x,0)/\partial x$, the initial fields are out of geostrophic balance, and a transient adjustment will occur.

We can construct the solution of (10.11)–(10.13) by using Fourier transform methods. First, we introduce the Fourier transform pair

$$u(x,t) = (2\pi)^{-1/2} \int_{-\infty}^{\infty} \hat{u}(k,t) e^{ikx} dk, \tag{10.15a}$$

$$\hat{u}(k,t) = (2\pi)^{-1/2} \int_{-\infty}^{\infty} u(x,t) e^{-ikx} dx, \tag{10.15b}$$

where k is the horizontal wavenumber. Similar transform pairs exist for $v(x,t)$, $\hat{v}(k,t)$, for $h(x,t)$, $\hat{h}(k,t)$, and for $Q(x)$, $\hat{Q}(k)$. We refer to $u(x,t)$ as the physical space representation of the divergent flow and $\hat{u}(k,t)$ as the spectral space representation of the divergent flow. Transforming (10.11)–(10.13) via (10.15), assuming that the solution is localized in space, we obtain

$$\frac{d\hat{u}}{dt} - \hat{v} + ik\hat{h} = 0, \tag{10.16}$$

$$\frac{d\hat{v}}{dt} + \hat{u} = 0, \tag{10.17}$$

$$\frac{d\hat{h}}{dt} + ik\hat{u} = \hat{Q}\alpha^2 t e^{-\alpha t}, \tag{10.18}$$

with k now regarded as a parameter. Equations (10.16)–(10.18) form a coupled set of three ordinary differential equations in the unknowns $\hat{u}(k,t)$, $\hat{v}(k,t)$ and $\hat{h}(k,t)$. We can form three decoupled equations by combining them in the following three ways: $(1+k^2)^{1/2}\cdot(10.16)+i\cdot(10.17)+k\cdot(10.18)$, $-(1+k^2)^{1/2}\cdot(10.16)+i\cdot(10.17)+k\cdot(10.18)$, and $ik\cdot(10.17)-(10.18)$. These operations result in

$$\frac{d}{dt}\left[\ \ (1+k^2)^{1/2}\hat{u}+i\hat{v}+k\hat{h}\right]+i(1+k^2)^{1/2}\left[\ \ (1+k^2)^{1/2}\hat{u}+i\hat{v}+k\hat{h}\right]=k\hat{Q}\alpha^2te^{-\alpha t}, \tag{10.19}$$

$$\frac{d}{dt}\left[-(1+k^2)^{1/2}\hat{u}+i\hat{v}+k\hat{h}\right]-i(1+k^2)^{1/2}\left[-(1+k^2)^{1/2}\hat{u}+i\hat{v}+k\hat{h}\right]=k\hat{Q}\alpha^2te^{-\alpha t}, \tag{10.20}$$

$$\frac{d}{dt}\left[ik\hat{v}-\hat{h}\right]=-\hat{Q}\alpha^2te^{-\alpha t}. \tag{10.21}$$

Note that (10.21) is the transformed version of the potential vorticity equation (10.14). Equations (10.19)–(10.21) are decoupled if we think of $(1+k^2)^{1/2}\hat{u}+i\hat{v}+k\hat{h}$, $-(1+k^2)^{1/2}\hat{u}+i\hat{v}+k\hat{h}$, and $ik\hat{v}-\hat{h}$ as the unknowns. Equation (10.21) can easily be solved by integration to yield (10.24) below. Equations (10.19) and (10.20) can also easily be solved by integration if we first multiply them by $e^{i(1+k^2)^{1/2}t}$ and $e^{-i(1+k^2)^{1/2}t}$ respectively; this allows the two terms on the left hand sides of (10.19) and (10.20) to be collapsed into single terms, after which integration can be performed. In this way we obtain the solutions

$$\begin{aligned}(1+k^2)^{1/2}\hat{u}(k,t)+i\hat{v}(k,t)+k\hat{h}(k,t)=&\left[\ \ (1+k^2)^{1/2}\hat{u}(k,0)+i\hat{v}(k,0)+k\hat{h}(k,0)\right]e^{-i(1+k^2)^{1/2}t}\\&+\frac{k\alpha^2\hat{Q}}{\left[\alpha-i(1+k^2)^{1/2}\right]^2}\left\{e^{-i(1+k^2)^{1/2}t}-\left[1+\left(\alpha-i(1+k^2)^{1/2}\right)t\right]e^{-\alpha t}\right\},\end{aligned} \tag{10.22}$$

$$\begin{aligned}-(1+k^2)^{1/2}\hat{u}(k,t)+i\hat{v}(k,t)+k\hat{h}(k,t)=&\left[-(1+k^2)^{1/2}\hat{u}(k,0)+i\hat{v}(k,0)+k\hat{h}(k,0)\right]e^{i(1+k^2)^{1/2}t}\\&+\frac{k\alpha^2\hat{Q}}{\left[\alpha+i(1+k^2)^{1/2}\right]^2}\left\{e^{i(1+k^2)^{1/2}t}-\left[1+\left(\alpha+i(1+k^2)^{1/2}\right)t\right]e^{-\alpha t}\right\},\end{aligned} \tag{10.23}$$

$$ik\hat{v}(k,t)-\hat{h}(k,t)=ik\hat{v}(k,0)-\hat{h}(k,0)+\hat{Q}\left[(1+\alpha t)e^{-\alpha t}-1\right]. \tag{10.24}$$

We shall now consider separately the evolution of a flow in the unforced, initial value case and the evoluion of a forced flow developed from a state of rest. First consider the unforced case, which allows neglect of the $\hat{Q}$ terms in (10.22)–(10.24). When the initial condition is in v and h only (i.e., $u(x,0)=0$), the solutions (10.22)–(10.24) can be combined to obtain

$$\hat{u}(k,t)=\left[\hat{v}(k,0)-ik\hat{h}(k,0)\right]\frac{\sin[(1+k^2)^{1/2}t]}{(1+k^2)^{1/2}}, \tag{10.25}$$

$$\hat{v}(k,t)=\left[\hat{v}(k,0)-ik\hat{h}(k,0)\right]\frac{\cos[(1+k^2)^{1/2}t]}{1+k^2}-\left[ik\hat{v}(k,0)-\hat{h}(k,0)\right]\frac{ik}{1+k^2}, \tag{10.26}$$

$$\hat{h}(k,t)=\left[\hat{v}(k,0)-ik\hat{h}(k,0)\right]\frac{ik\cos[(1+k^2)^{1/2}t]}{1+k^2}-\left[ik\hat{v}(k,0)-\hat{h}(k,0)\right]\frac{1}{1+k^2}. \tag{10.27}$$

Formulas (10.25)–(10.27) constitute the spectral space solutions of the unforced geostrophic adjustment problem. To obtain the physical space solutions we simply use (10.25)–(10.27) in the Fourier transform relations (e.g., (10.15a)) to obtain

$$u(x,t) = (2\pi)^{-1/2} \int_{-\infty}^{\infty} \left[\hat{v}(k,0) - ik\hat{h}(k,0)\right] \frac{\sin[(1+k^2)^{1/2}t]}{(1+k^2)^{1/2}} e^{ikx} dk, \tag{10.28}$$

$$\begin{aligned} v(x,t) = (2\pi)^{-1/2} \int_{-\infty}^{\infty} \left[\hat{v}(k,0) - ik\hat{h}(k,0)\right] \frac{\cos[(1+k^2)^{1/2}t]}{1+k^2} e^{ikx} dk \\ -(2\pi)^{-1/2} \int_{-\infty}^{\infty} \left[ik\hat{v}(k,0) - \hat{h}(k,0)\right] \frac{ik}{1+k^2} e^{ikx} dk, \end{aligned} \tag{10.29}$$

$$\begin{aligned} h(x,t) = (2\pi)^{-1/2} \int_{-\infty}^{\infty} \left[\hat{v}(k,0) - ik\hat{h}(k,0)\right] \frac{ik\cos[(1+k^2)^{1/2}t]}{1+k^2} e^{ikx} dk \\ -(2\pi)^{-1/2} \int_{-\infty}^{\infty} \left[ik\hat{v}(k,0) - \hat{h}(k,0)\right] \frac{1}{1+k^2} e^{ikx} dk. \end{aligned} \tag{10.30}$$

Note that the $\hat{v}(k,0)$ and $\hat{h}(k,0)$ functions appearing in (10.28)–(10.30) are given in terms of the initial $v(x,0)$ and $h(x,0)$ by

$$\hat{v}(k,0) = (2\pi)^{-1/2} \int_{-\infty}^{\infty} v(x,0) e^{-ikx} dx, \tag{10.31}$$

$$\hat{h}(k,0) = (2\pi)^{-1/2} \int_{-\infty}^{\infty} h(x,0) e^{-ikx} dx. \tag{10.32}$$

Equations (10.28)–(10.30) constitute the analytic solution of the unforced initial value problem (10.11)–(10.13). The construction of plots of the physical space solutions can be summarized as follows: (1) From the specified initial conditions $v(x,0)$ and $h(x,0)$, calculate $\hat{v}(k,0)$ and $\hat{h}(k,0)$ from (10.31) and (10.32); (2) Use these results in (10.28)–(10.30) to obtain $u(x,t)$, $v(x,t)$ and $h(x,t)$. Note that this procedure allows us to compute the solution at time t without computing the solution at all intermediate times, as would be required by a time-stepping procedure applied to the original partial differential equations (10.11)–(10.13). It is also interesting to note that, while the solution for $u(x,t)$ consists of a time dependent part only, the solutions for $v(x,t)$ and $h(x,t)$ consist of two parts—a time dependent part (the gravity-inertia waves) and a time independent part (the final geostrophic flow). When we make diagrams of the solutions for $v(x,t)$ and $h(x,t)$ we can plot these two parts separately. Such a partition into gravity-inertia waves and geostrophic flow is not possible if we use a brute force time-stepping procedure applied to the original partial differential equations (10.11)–(10.13).

Although the Fourier integrals in (10.31)–(10.32) can usually be done analytically (if $v(x,0)$ and $h(x,0)$ are not too complicated functions of x), the Fourier integrals involved in (10.28)–(10.30) must usually be evaluated numerically because the integrands are such complicated functions of k.

There are interesting alternative ways of expressing (10.28)–(10.30). For example, noting that

$$\hat{v}(k,0) - ik\hat{h}(k,0) = (2\pi)^{-1/2} \int_{-\infty}^{\infty} \left[v(x',0) - h_{x'}(x',0)\right] e^{-ikx'} dx',$$

we can rewrite (10.28) as

$$u(x,t) = \int_{-\infty}^{\infty} \left[v(x',0) - h_{x'}(x',0)\right] \left[\frac{1}{2\pi} \int_{-\infty}^{\infty} \frac{\sin[(1+k^2)^{1/2}t]}{(1+k^2)^{1/2}} e^{ik(x-x')} dk\right] dx'.$$

Since (see the Fourier transform tables of Erdelyi et al. 1954, page 26),

$$\frac{1}{2\pi} \int_{-\infty}^{\infty} \frac{\sin[(1+k^2)^{1/2}t]}{(1+k^2)^{1/2}} e^{ik(x-x')} dk = \begin{cases} \frac{1}{2} J_0\left(\left[t^2 - (x-x')^2\right]^{1/2}\right) & \text{if } x-t < x' < x+t \\ 0 & \text{otherwise} \end{cases} \tag{10.33}$$

we can write the solution $u(x,t)$ as

$$u(x,t) = \tfrac{1}{2} \int_{x-t}^{x+t} \left[v(x',0) - h_{x'}(x',0)\right] J_0\left(\left[t^2 - (x-x')^2\right]^{1/2}\right) dx', \tag{10.34}$$

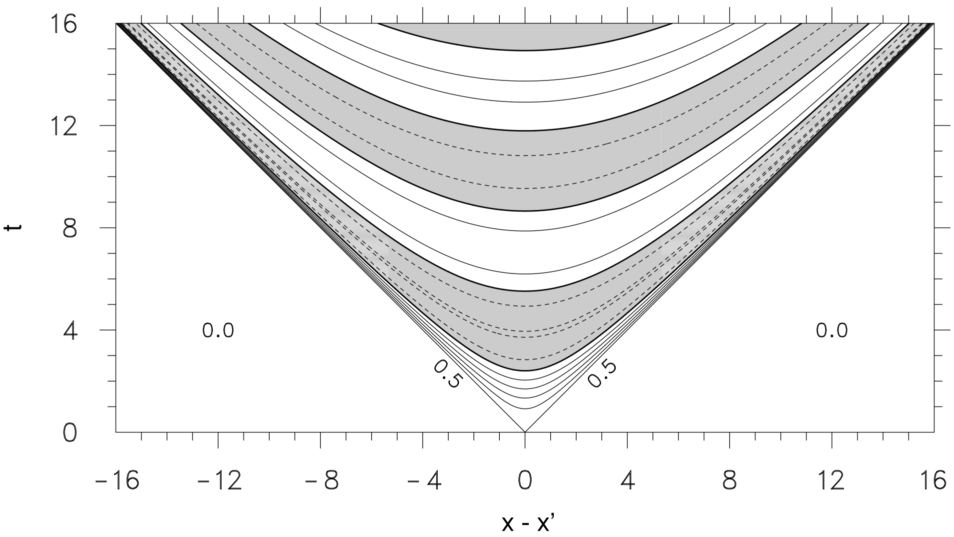

Figure 10.1: Isolines of the right hand side of (10.33), with $x - x'$ on the abscissa and t on the ordinate. Below the two diagonal lines $|x - x'| = t$ the right hand side of (10.33) is zero. Across these diagonals there is a jump from zero to 0.5. Above the diagonals, isolines are drawn every 0.1 with negative values shaded. Note the damping at large times, i.e., the divergent part of the wind decays with time so that the rotational part of the wind comes into geostrophic balance.

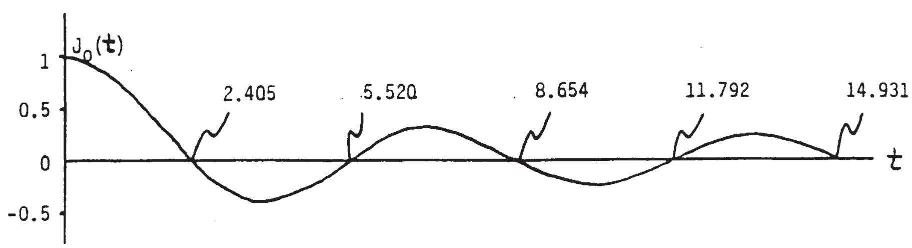

Figure 10.2: The zero order Bessel function $J_0(t)$. The asymptotic form is $J_0(t) \sim [2/(\pi t)]^{1/2} \cos(t - \frac{1}{4}\pi)$ as $t \to \infty$, so that $J_0(t)$ decays as $t^{-1/2}$ and the interval between the nodes approaches π as $t \to \infty$.

where J_0 is the zero order Bessel function. Isolines of the right hand side of (10.33) in the $(x - x', t)$-plane are shown in Fig. 10.1.

If $v(x, 0) - h_x(x, 0) = \delta(x)$, the Dirac delta function, (10.34) simplifies to

$$u(x,t) = \begin{cases} \frac{1}{2} J_0 \left[(t^2 - x^2)^{1/2} \right] & t > |x|, \\ 0 & t < |x|. \end{cases} \tag{10.35}$$

Figure 10.2 displays $J_0(t)$, which is the solution for u at $x = 0$. Figure 10.3 shows curved lines in the (x, t) plane along which $J_0[(t^2 - x^2)^{1/2}] = 0$ and straight lines along which $J_0[(t^2 - x^2)^{1/2}] = 1$. We can understand the solution both by examining the oscillation in time at a fixed x point and by examining the oscillation in space at a fixed t. The oscillation of $u(x, t)$ with time at $x = 5$ is shown in Fig. 10.4. Note that u remains zero until $t = 5$, then increases instantaneously and begins a damped oscillation. The solution at $t = 10$ as a function of x is shown in Fig. 10.5. Some important aspects of Fig. 10.5 are as follows: (1) The initial point disturbance causes oscillation in the domain $|x| < t$ and the domain expands in space as time increases. (2) For $t >> |x|$, the solution oscillates with an approximate frequency f in dimensional terms, but the oscillation gradually damps. (3) Across the lines $t = |x|$, $J_0[(t^2 - x^2)^{1/2}]$ jumps and divergence is momentarily infinite, causing a sudden change in the free surface height.

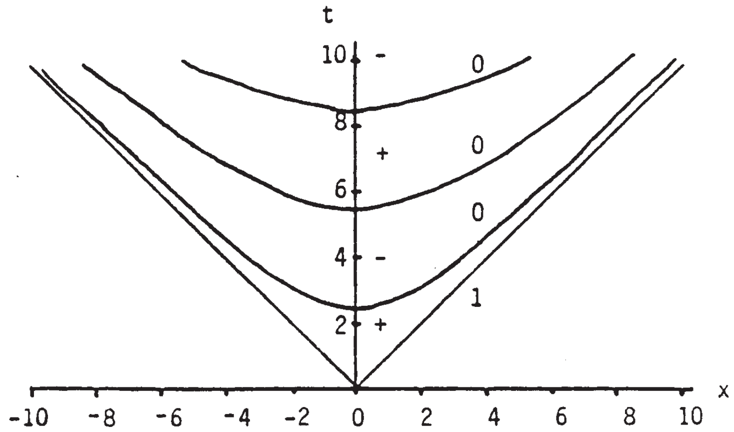

Figure 10.3: Nodal lines of the solution (10.35) in the (x,t)-plane.

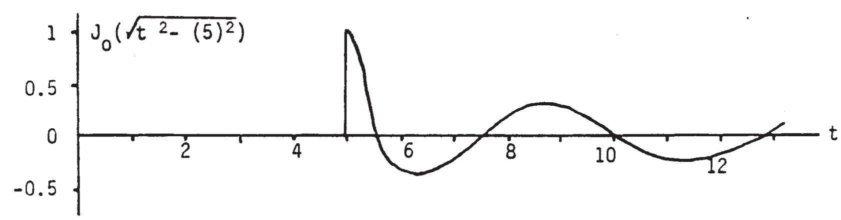

Figure 10.4: The oscillation of $u(x,t)$ in time at $x=5$, according to (10.35).

Let us now return to the discussion of the general solutions (10.28)–(10.30). What we have just observed is the tendency for the gravity-inertia wave part of the initial disturbance to disperse over a wide area. This is a robust feature of the solutions (10.28)–(10.30), i.e., it is true for any initial condition, not just the particular one illustrated in Fig. 10.2–10.4. The only term on the right hand side of (10.28), the first term on the right hand side of (10.29), and the first term on the right hand side of (10.30) are all oscillatory in time in spectral space. In physical space they represent propagating gravity-inertia waves. If one waits long enough for the gravity-inertia waves to disperse to infinity, only the final balanced flow remains. Then (10.29) and (10.30) yield

$$v(x,\infty) = -(2\pi)^{-1/2}\int_{-\infty}^{\infty}\left[ik\hat{v}(k,0)-\hat{h}(k,0)\right]\frac{ik}{1+k^2}e^{ikx}dk, \tag{10.36}$$

$$h(x,\infty) = -(2\pi)^{-1/2}\int_{-\infty}^{\infty}\left[ik\hat{v}(k,0)-\hat{h}(k,0)\right]\frac{1}{1+k^2}e^{ikx}dk. \tag{10.37}$$

Note that to have any final rotational wind or pressure disturbance, we must have some initial potential vorticity disturbance (i.e., nonzero $ik\hat{v}(k,0)-\hat{h}(k,0)$). Now define $\hat{v}_g(k,0)$ and $\hat{h}_g(k,0)$ by $\hat{v}_g(k,0)=ik\hat{h}(k,0)$ and $\hat{v}(k,0)=ik\hat{h}_g(k,0)$ respectively. Then, (10.36) and (10.37) can be written as

$$v(x,\infty) = (2\pi)^{-1/2}\int_{-\infty}^{\infty}\left[\left(\frac{k^2}{1+k^2}\right)\hat{v}(k,0)+\left(\frac{1}{1+k^2}\right)\hat{v}_g(k,0)\right]e^{ikx}dk, \tag{10.38}$$

$$h(x,\infty) = (2\pi)^{-1/2}\int_{-\infty}^{\infty}\left[\left(\frac{k^2}{1+k^2}\right)\hat{h}_g(k,0)+\left(\frac{1}{1+k^2}\right)\hat{h}(k,0)\right]e^{ikx}dk. \tag{10.39}$$

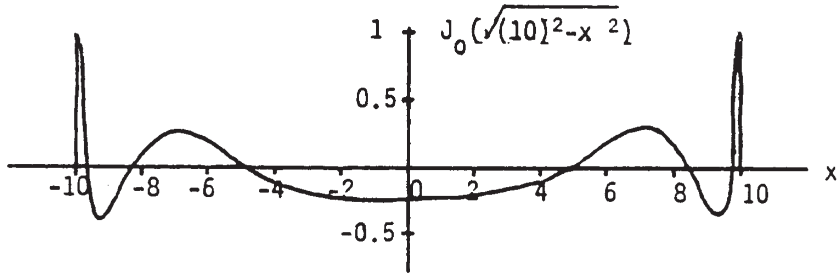

Figure 10.5: The oscillation of $u(x,t)$ in space at $t=10$, according to (10.35).

Equation (10.38) states that the final wind $v(x,\infty)$ is a spectral space weighted average of the initial wind $\hat{v}(k,0)$ [weight $k^2/(1+k^2)$] and the initial geostrophic wind $\hat{v}_g(k,0)$ [weight $1/(1+k^2)$]. Equation (10.39) states that the final pressure field $h(x,\infty)$ is a spectral space weighted average of the initial geostrophic height $\hat{h}_g(k,0)$ [weight $k^2/(1+k^2)$] and the initial pressure field $\hat{h}(k,0)$ [weight $1/(1+k^2)$]. The two important weighting functions are shown in Fig. 10.6. We may interpret $k^2/(1+k^2)$ as the spectral modification of an initial rotational wind disturbance and note that low wavenumbers are eliminated. Likewise, $1/(1+k^2)$ is the spectral modification of an initial pressure disturbance, with high wavenumbers being eliminated.

10.3 Case 1: An initial unbalanced wind disturbance

Now consider the case $v(x,0)=v_0 e^{-\frac{1}{2}(x/b)^2}$ and $h(x,0)=0$, where the constants v_0 and b denote the magnitude and horizontal size of the initial wind disturbance. From (10.31) and (10.32) we obtain $\hat{h}(k,0)=0$ and

$$\hat{v}(k,0)=\left(\frac{2}{\pi}\right)^{1/2} v_0\int_0^\infty e^{-\frac{1}{2}(x/b)^2}\cos(kx)dx = v_0 b e^{-\frac{1}{2}k^2b^2}. \tag{10.40}$$

Using these results in (10.28)–(10.30) we obtain

$$u(x,t)= \left(\frac{2}{\pi}\right)^{1/2} v_0 b\int_0^\infty \frac{1}{(1+k^2)^{1/2}} e^{-\frac{1}{2}k^2b^2}\sin[(1+k^2)^{1/2}t]\cos(kx)dk, \tag{10.41}$$

$$\begin{aligned} v(x,t)= &\left(\frac{2}{\pi}\right)^{1/2} v_0 b\int_0^\infty \left(\frac{1}{1+k^2}\right) e^{-\frac{1}{2}k^2b^2}\cos[(1+k^2)^{1/2}t]\cos(kx)dk \\ &+\left(\frac{2}{\pi}\right)^{1/2} v_0 b\int_0^\infty \left(\frac{k^2}{1+k^2}\right) e^{-\frac{1}{2}k^2b^2}\cos(kx)dk, \end{aligned} \tag{10.42}$$

$$\begin{aligned} h(x,t)= &-\left(\frac{2}{\pi}\right)^{1/2} v_0 b\int_0^\infty \left(\frac{k}{1+k^2}\right) e^{-\frac{1}{2}k^2b^2}\cos[(1+k^2)^{1/2}t]\sin(kx)dk \\ &+\left(\frac{2}{\pi}\right)^{1/2} v_0 b\int_0^\infty \left(\frac{k}{1+k^2}\right) e^{-\frac{1}{2}k^2b^2}\sin(kx)dk. \end{aligned} \tag{10.43}$$

From the inverse transform of (10.40) we have

$$v(x,0)=\left(\frac{2}{\pi}\right)^{1/2} v_0 b\int_0^\infty e^{-\frac{1}{2}k^2b^2}\cos(kx)dk, \tag{10.44}$$

while from (10.42) we deduce that

$$v(x,\infty)=\left(\frac{2}{\pi}\right)^{1/2} v_0 b\int_0^\infty \left(\frac{k^2}{1+k^2}\right) e^{-\frac{1}{2}k^2b^2}\cos(kx)dk \approx \begin{cases} v(x,0) & \text{if } b<<1, \\ 0 & \text{if } b>>1. \end{cases} \tag{10.45}$$

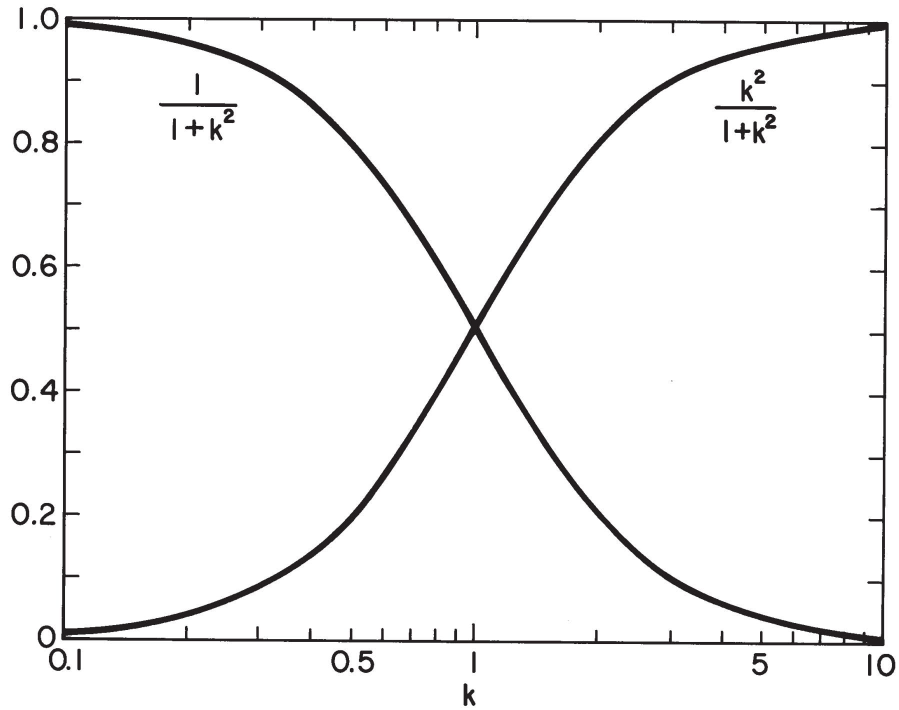

Figure 10.6: Weighting functions $1/(1+k^2)$ and $k^2/(1+k^2)$.

Note that the only difference in the integrals of (10.44) and (10.45) is the weighting function $k^2/(1+k^2)$. Thus, by comparing (10.44) and (10.45), we deduce that, if $b << 1$, the pressure adjusts to the wind, while if $b >> 1$, the wind adjusts to the pressure.

10.4 Case 2: An initial unbalanced pressure disturbance

Now consider the case $v(x,0) = 0$ and $h(x,0) = h_0 e^{-\frac{1}{2}(x/b)^2}$, where the constants h_0 and b denote the magnitude and horizontal size of the initial pressure disturbance. From (10.31) and (10.32) we obtain $\hat{v}(k,0) = 0$ and

$$\hat{h}(k,0) = \left(\frac{2}{\pi}\right)^{1/2} h_0 \int_0^\infty e^{-\frac{1}{2}(x/b)^2} \cos(kx)dx = h_0 b e^{-\frac{1}{2}k^2 b^2}. \tag{10.46}$$

Using these results in (10.28)–(10.30) we obtain

$$u(x,t) = \left(\frac{2}{\pi}\right)^{1/2} h_0 b \int_0^\infty \frac{k}{(1+k^2)^{1/2}} e^{-\frac{1}{2}k^2b^2} \sin[(1+k^2)^{1/2}t] \sin(kx) dk, \tag{10.47}$$

$$\begin{aligned} v(x,t) = {} & \left(\frac{2}{\pi}\right)^{1/2} h_0 b \int_0^\infty \left(\frac{k}{1+k^2}\right) e^{-\frac{1}{2}k^2b^2} \cos[(1+k^2)^{1/2}t] \sin(kx) dk \\ & - \left(\frac{2}{\pi}\right)^{1/2} h_0 b \int_0^\infty \left(\frac{k}{1+k^2}\right) e^{-\frac{1}{2}k^2b^2} \sin(kx) dk, \end{aligned} \tag{10.48}$$

$$\begin{aligned} h(x,t) = {} & \left(\frac{2}{\pi}\right)^{1/2} h_0 b \int_0^\infty \left(\frac{k^2}{1+k^2}\right) e^{-\frac{1}{2}k^2b^2} \cos[(1+k^2)^{1/2}t] \cos(kx) dk \\ & + \left(\frac{2}{\pi}\right)^{1/2} h_0 b \int_0^\infty \left(\frac{1}{1+k^2}\right) e^{-\frac{1}{2}k^2b^2} \cos(kx) dk. \end{aligned} \tag{10.49}$$

From the inverse transform of (10.46) we have

$$h(x,0) = \left(\frac{2}{\pi}\right)^{1/2} h_0 b \int_0^\infty e^{-\frac{1}{2}k^2b^2} \cos(kx) dk, \tag{10.50}$$

while from (10.49) we deduce that

$$h(x,\infty) = \left(\frac{2}{\pi}\right)^{1/2} h_0 b \int_0^\infty \left(\frac{1}{1+k^2}\right) e^{-\frac{1}{2}k^2b^2} \cos(kx) dk \approx \begin{cases} 0 & \text{if } b << 1, \\ h(x,0) & \text{if } b >> 1. \end{cases} \tag{10.51}$$

Thus, by comparing (10.50) and (10.51), if $b << 1$, the pressure adjusts to the wind, while if $b >> 1$, the wind adjusts to the pressure.

10.5 Invertibility principle

Now let us see if we can bypass the solution of the transient problem altogether and go directly to the final adjusted state in physical space. This is the simplest possible example of the *invertibility principle*. As an example let us now find the final geostrophically adjusted state when the initial state is

$$u(x,0) = v(x,0) = 0, \qquad h(x,0) = \begin{cases} -1 & |x| < b \\ 0 & |x| > b. \end{cases} \tag{10.52}$$

According to the linearized potential vorticity principle (10.14),

$$\frac{dv(x,\infty)}{dx} - h(x,\infty) = \frac{dv(x,0)}{dx} - h(x,0). \tag{10.53}$$

Regardless of the initial conditions, we know that the time evolution of the divergent part of the flow is such that u approaches zero in an oscillatory decay. Then, if we wait long enough, (10.11) implies that

$$v(x,\infty) = \frac{dh(x,\infty)}{dx}. \tag{10.54}$$

When (10.52) and (10.54) are substituted into (10.53), we obtain

$$\frac{d^2h(x,\infty)}{dx^2} - h(x,\infty) = \begin{cases} 1 & |x| < b \\ 0 & |x| > b. \end{cases} \tag{10.55}$$

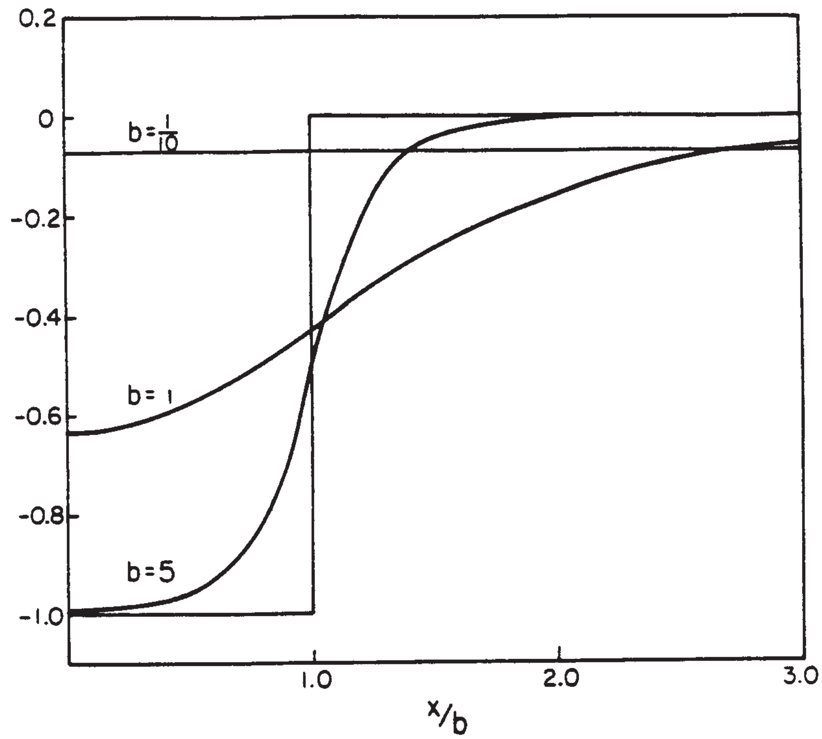

Figure 10.7: Plot of the final adjusted state (10.56).

The solution of (10.55) with $h(x,\infty)$ and $dh(x,\infty)/dx$ continuous is

$$h(x,\infty) = \begin{cases} -e^{x}\sinh(b) & -\infty < x \le -b \\ e^{-b}\cosh(x) - 1 & -b \le x \le +b \\ -e^{-x}\sinh(b) & +b \le x < +\infty \end{cases} \tag{10.56}$$

$$v(x,\infty) = \begin{cases} -e^{x}\sinh(b) & -\infty < x \le -b \\ e^{-b}\sinh(x) & -b \le x \le +b \\ e^{-x}\sinh(b) & +b \le x < +\infty \end{cases} \tag{10.57}$$

Figure 10.7 displays $h(x,\infty)$ as a function of x/b for three different values of b. Since the unit for measuring b is the Rossby length c/f, we obtain the following "dimensional form" of geostrophic adjustment rules.

- $\star$ For $b >> c/f$ (horizontal scale of initial disturbance is much larger than the Rossby length) or $b/c >> 1/f$ (propagation time of gravity wave out of disturbed region is much longer than Foucault pendulum period), the pressure hardly changes and *the wind adjusts to the pressure*.
- $\star$ For $b << c/f$ (horizontal scale of initial disturbance is much smaller than the Rossby length) or $b/c << 1/f$ (propagation time of gravity wave out of disturbed region is much shorter than Foucault pendulum period), the wind hardly changes and *the pressure adjusts to the wind*.

The total energy principle associated with (10.11)–(10.13) can be found by adding u times (10.11), v times (10.12), and h times (10.13). This results in

$$\frac{\partial}{\partial t}\left[\tfrac{1}{2}(u^2 + v^2 + h^2)\right] + \frac{\partial(uh)}{\partial x} = 0. \tag{10.58}$$

Integrating (10.58) over the domain we obtain

$$\frac{d}{dt}\int_{-\infty}^{\infty} \tfrac{1}{2}(u^2+v^2+h^2)dx = 0. \tag{10.59}$$

Let us now define

$$P_0 = \int_{-\infty}^{\infty} \tfrac{1}{2}h^2(x,0)dx \tag{10.60}$$

to be the initial potential energy. Since there is no initial kinetic energy, P_0 can also be interpreted as the initial total energy. Let us also define

$$K_\infty + P_\infty = \int_{-\infty}^{\infty} \tfrac{1}{2}\left[v^2(x,\infty)+h^2(x,\infty)\right]dx \tag{10.61}$$

as the final total energy associated with the geostrophic flow. Using the initial condition (10.52) in (10.60) we can evaluate the integral and obtain the initial potential energy P_0. Similarly, using the solution (10.56)–(10.57) we can evaluate the integral in (10.61) to obtain $K_\infty + P_\infty$. The ratio of the final energy in the geostrophic flow to the initial energy is

$$\frac{K_\infty + P_\infty}{P_0} = 1 + \frac{1}{2b}\left(e^{-2b}-1\right). \tag{10.62}$$

This relationship is plotted in Fig. 10.8, from which we obtain the following "dimensional" rules.

- ⋆ For $b >> c/f$ (horizontal scale of initial disturbance is much larger than the Rossby length) or $b/c >> 1/f$ (propagation time of gravity wave out of disturbed region is much longer than Foucault pendulum period), only a small percentage of the initial energy escapes with the gravity-inertia waves.
- ⋆ For $b << c/f$ (horizontal scale of initial disturbance is much smaller than the Rossby length) or $b/c << 1/f$ (propagation time of gravity wave out of disturbed region is much shorter than Foucault pendulum period), a large percentage of the initial energy escapes with the gravity-inertia waves.

10.6 The concept of a balanced model

Suppose the mass source/sink term in (10.13) varies slowly enough in time that the magnitude of $\partial u/\partial t$ remains small compared to the magnitude of the Coriolis and pressure gradient terms in (10.11). In other words, the rotational flow v is always close to geostrophic balance. However, the fluid is evolving from one geostrophic state to another since both v and h are changing as mass is added or removed from the fluid layer. Then we might approximate the primitive equation system (10.11)–(10.13) by the balanced system

$$v = \frac{\partial h}{\partial x}, \tag{10.63}$$

$$\frac{\partial v}{\partial t} + u = 0, \tag{10.64}$$

$$\frac{\partial h}{\partial t} + \frac{\partial u}{\partial x} = Q(x)\alpha^2 t e^{-\alpha t}. \tag{10.65}$$

This does not mean we are assuming $\partial u/\partial t$ is zero, but rather that its magnitude is small compared to v and $\partial h/\partial x$. In fact, we shall see that the balanced system produces solutions with nonzero $\partial u/\partial t$. However, if the nonzero $\partial u/\partial t$ is small, the solutions of the balanced system (10.63)–(10.65) will be very close to the solutions of the primitive system (10.11)–(10.13).

It can be argued that the form of (10.63)–(10.65), while correct for our balanced model, is inconvenient because v and h are independently predicted by (10.64) and (10.65), but according to (10.63) these two fields are diagnostically coupled and do not independently evolve. According to this argument, a convenient form of the balanced system is one

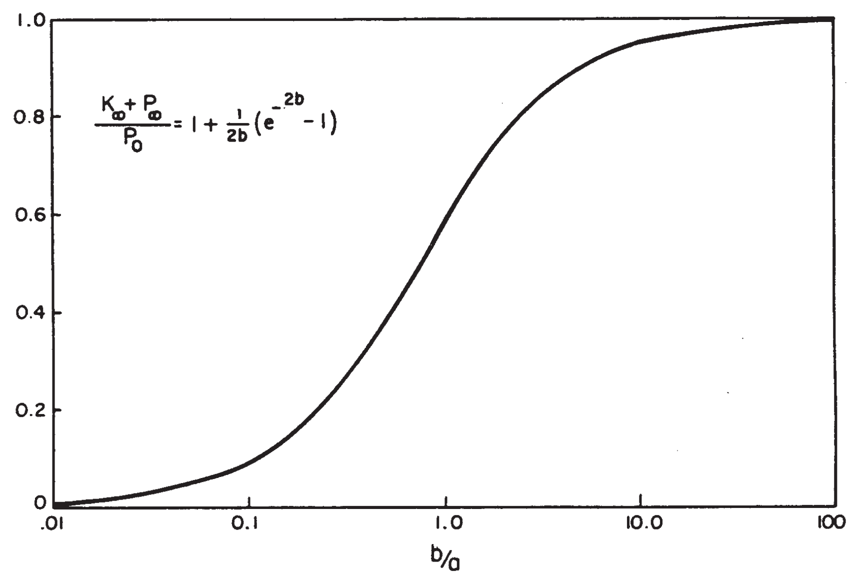

Figure 10.8: Plot of the energy partition according to (10.62).

that consists of a single prognostic equation. If we take $\partial/\partial x$ of (10.65), and then subtract (10.64) from the resulting equation, we obtain (10.67) below. Since (10.67) is derived from (10.64) and (10.65), if we are going to use (10.67) as one of our equations, we must discard either (10.64) or (10.65). Let us discard (10.64). Then our balanced system can be written as

$$\frac{\partial h}{\partial t} + \frac{\partial u}{\partial x} = Q\alpha^2 te^{-\alpha t}, \tag{10.66}$$

$$\frac{\partial^2 u}{\partial x^2} - u = \frac{\partial Q}{\partial x}\alpha^2 te^{-\alpha t}, \tag{10.67}$$

$$v = \frac{\partial h}{\partial x}, \tag{10.68}$$

which consists of one prognostic equation for h and two diagnostic equations to determine u and v from h.

Another convenient form of the balanced system can be obtained as follows. If we take $\partial/\partial x$ of (10.64), and then subtract (10.65) from the resulting equation, we obtain (10.69) below, where P is defined by the invertibility relation (10.70). Then our balanced system can be written as

$$\frac{\partial P}{\partial t} = -Q\alpha^2 te^{-\alpha t}, \tag{10.69}$$

$$\frac{\partial^2 h}{\partial x^2} - h = P, \tag{10.70}$$

$$v = \frac{\partial h}{\partial x}, \tag{10.71}$$

which consists of one prognostic equation for the potential vorticity P and two diagnostic equations to determine h and v. Note that the divergent wind component u does not need to be determined in this form of balanced theory. Note also that the invertibility problem (10.70) is the same problem discussed in section 10.5 for the final geostrophically balanced state in our geostrophic adjustment theory. An important difference is that in section 10.5 the invertibility problem was solved only once for the final balanced state; in contrast, (10.70) is solved at every time as P and the associated wind and mass fields continuously evolve from one balanced state to another.

The concept of a balanced model fits well with our experience looking at daily weather maps. For example, consider a time sequence of 500 mb charts. What we see is a flow which is always close to geostrophic balance, but which changes from day to day. The PV field is evolving in time as troughs and ridges shift their positions and change their shapes. It seems that PV is the one field that should be predicted and that the balanced wind and mass fields should be obtained by inverting the PV, just as in (10.70). Of course, in a practical sense, (10.69)–(10.71) do not constitute a useful numerical weather prediction model because they omit vertical structure and all the nonlinear terms. However, they are a conceptually useful guide in formulating quasi-geostrophic and semi-geostrophic theories, topics which will be explored in later chapters.

10.7 The two-dimensional case

To generalize the one-dimensional results of the previous sections let us now return to the two-dimensional equations (10.8)–(10.10). These equations were first solved by Obukhov (1949) using a Green's function approach. Here we take a different approach, solving (10.8)–(10.10) via a horizontal normal mode transform.

We construct the horizontal normal mode transform in two steps as follows. First, we introduce the double Fourier transform pair

$$u(x, y, t) = \frac{1}{2\pi} \iint_{-\infty}^{\infty} \hat{u}(k, l, t) e^{i(kx+ly)} dk dl, \tag{10.72a}$$

$$\hat{u}(k, l, t) = \frac{1}{2\pi} \iint_{-\infty}^{\infty} u(x, y, t) e^{-i(kx+ly)} dx dy, \tag{10.72b}$$

where k and l are horizontal wavenumbers. Similar transform pairs exist for v and h. Transforming (10.8)–(10.10) and assuming that the solution is localized in space we obtain

$$\frac{d\hat{u}}{dt} - \hat{v} + ik\hat{h} = 0, \tag{10.73}$$

$$\frac{d\hat{v}}{dt} + \hat{u} + il\hat{h} = 0, \tag{10.74}$$

$$\frac{d\hat{h}}{dt} + ik\hat{u} + il\hat{v} = 0, \tag{10.75}$$

with k and l now regarded as parameters. We can write (10.73)–(10.75) in matrix form as

$$\frac{d\hat{\mathbf{w}}}{dt} + A\hat{\mathbf{w}} = 0, \tag{10.76}$$

where

$$\hat{\mathbf{w}} = \begin{bmatrix} \hat{u} \\ \hat{v} \\ \hat{h} \end{bmatrix}, \qquad A = \begin{bmatrix} 0 & -1 & ik \\ 1 & 0 & il \\ ik & il & 0 \end{bmatrix}. \tag{10.77}$$

Note that the vector components here refer to the three dependent variables $\hat{u}, \hat{v}, \hat{h}$ rather than to three space coordinates.

Second, we reduce (10.76) to three decoupled scalar equations by diagonalizing A. Since A is skew-Hermitian (i.e., $A^* = -A$, where the asterisk denotes the conjugate transpose), its eigenvalues are pure imaginary; therefore, we write the eigenvalue problem as

$$A\hat{\mathbf{\Psi}}^{(r)} + i\nu_r \hat{\mathbf{\Psi}}^{(r)} = 0 \qquad (r = 0, 1, 2). \tag{10.78}$$

The eigenvalues are given by $\nu_0 = 0, \nu_1 = -\nu$ and $\nu_2 = +\nu$, where $\nu = (1 + k^2 + l^2)^{1/2}$, with the corresponding eigenvectors

$$\hat{\mathbf{\Psi}}^{(0)} = \frac{1}{\nu} \begin{bmatrix} il \\ -ik \\ -1 \end{bmatrix}, \quad \hat{\mathbf{\Psi}}^{(1)} = \frac{1}{\mu\nu\sqrt{2}} \begin{bmatrix} \nu k + il \\ \nu l - ik \\ \mu^2 \end{bmatrix}, \quad \hat{\mathbf{\Psi}}^{(2)} = \frac{1}{\mu\nu\sqrt{2}} \begin{bmatrix} -\nu k + il \\ -\nu l - ik \\ \mu^2 \end{bmatrix}, \tag{10.79}$$

where $\mu = (k^2+l^2)^{1/2}$. Since A is skew-Hermitian these eigenvectors are orthogonal; they have also been normalized so that

$$\left[\hat{\mathbf{\Psi}}^{(r)}\right]^* \hat{\mathbf{\Psi}}^{(s)} = \begin{cases} 1 & r = s \\ 0 & r \neq s. \end{cases} \tag{10.80}$$

Using this orthonormality we can complete the horizontal normal mode transform by defining

$$\hat{w}_r(k,l,t) = \left[\hat{\mathbf{\Psi}}^{(r)}\right]^* \hat{\mathbf{w}}(k,l,t) \quad (r = 0,1,2), \tag{10.81a}$$

or in expanded form

$$\begin{bmatrix} \hat{w}_0(k,l,t) \\ \hat{w}_1(k,l,t) \\ \hat{w}_2(k,l,t) \end{bmatrix} = \begin{bmatrix} -\frac{il}{\nu} & \frac{ik}{\nu} & -\frac{1}{\nu} \\ \frac{\nu k - il}{\mu\nu\sqrt{2}} & \frac{\nu l + ik}{\mu\nu\sqrt{2}} & \frac{\mu^2}{\mu\nu\sqrt{2}} \\ \frac{-\nu k - il}{\mu\nu\sqrt{2}} & \frac{-\nu l + ik}{\mu\nu\sqrt{2}} & \frac{\mu^2}{\mu\nu\sqrt{2}} \end{bmatrix} \begin{bmatrix} \hat{u}(k,l,t) \\ \hat{v}(k,l,t) \\ \hat{h}(k,l,t) \end{bmatrix}. \tag{10.81b}$$

The inverse of (10.81) is

$$\hat{\mathbf{w}}(k,l,t) = \sum_{r=0}^{2} \hat{w}_r(k,l,t)\hat{\mathbf{\Psi}}^{(r)}(k,l), \tag{10.82a}$$

or in expanded form

$$\begin{bmatrix} \hat{u}(k,l,t) \\ \hat{v}(k,l,t) \\ \hat{h}(k,l,t) \end{bmatrix} = \hat{w}_0(k,l,t)\frac{1}{\nu}\begin{bmatrix} il \\ -ik \\ -1 \end{bmatrix} + \hat{w}_1(k,l,t)\frac{1}{\mu\nu\sqrt{2}}\begin{bmatrix} \nu k + il \\ \nu l - ik \\ \mu^2 \end{bmatrix} + \hat{w}_2(k,l,t)\frac{1}{\mu\nu\sqrt{2}}\begin{bmatrix} -\nu k + il \\ -\nu l - ik \\ \mu^2 \end{bmatrix}. \tag{10.82b}$$

Substituting (10.82) into (10.76) we obtain the oscillation equation

$$\frac{d\hat{w}_r}{dt} - i\nu_r\hat{w}_r = 0 \quad (r = 0,1,2), \tag{10.83}$$

which can be solved directly to yield

$$\hat{w}_r(k,l,t) = \hat{w}_r(k,l,0)e^{i\nu_r t} \quad (r = 0,1,2). \tag{10.84}$$

To see the solution in more detail we can use (10.84) in (10.82b) to obtain

$$\hat{u}(k,l,t) = \frac{il}{\nu}\hat{w}_0(k,l,0) + \frac{\nu k + il}{\mu\nu\sqrt{2}}\hat{w}_1(k,l,0)e^{-i\nu t} + \frac{-\nu k + il}{\mu\nu\sqrt{2}}\hat{w}_2(k,l,0)e^{i\nu t}, \tag{10.85a}$$

$$\hat{v}(k,l,t) = -\frac{ik}{\nu}\hat{w}_0(k,l,0) + \frac{\nu l - ik}{\mu\nu\sqrt{2}}\hat{w}_1(k,l,0)e^{-i\nu t} + \frac{-\nu l - ik}{\mu\nu\sqrt{2}}\hat{w}_2(k,l,0)e^{i\nu t}, \tag{10.85b}$$

$$\hat{h}(k,l,t) = -\frac{1}{\nu}\hat{w}_0(k,l,0) + \frac{\mu}{\nu\sqrt{2}}\hat{w}_1(k,l,0)e^{-i\nu t} + \frac{\mu}{\nu\sqrt{2}}\hat{w}_2(k,l,0)e^{i\nu t}, \tag{10.85c}$$

where

$$\hat{w}_0(k,l,0) = \frac{1}{\nu}\left[\hat{\zeta}(k,l,0) - \hat{h}(k,l,0)\right],$$

$$\hat{w}_1(k,l,0) = \frac{1}{\mu\nu\sqrt{2}}\left[-i\nu\hat{\delta}(k,l,0) + \hat{\zeta}(k,l,0) + \mu^2\hat{h}(k,l,0)\right],$$

$$\hat{w}_2(k,l,0) = \frac{1}{\mu\nu\sqrt{2}}\left[\ \ i\nu\hat{\delta}(k,l,0) + \hat{\zeta}(k,l,0) + \mu^2\hat{h}(k,l,0)\right],$$

$$\hat{\zeta} = ik\hat{v} - il\hat{u},$$

$$\hat{\delta} = ik\hat{u} + il\hat{v}.$$

Equations (10.85a–c) constitute the solution in spectral space. The first term in each equation is the geostrophic mode while the remaining two terms are the gravity-inertia modes. To get $u(x,y,t)$, $v(x,y,t)$ and $h(x,y,t)$ we substitute (10.85a–c) into (10.72a) and its companions. For the special case where the initial divergence is zero (i.e., $\hat{\delta}(k,l,0) = 0$), this results in

$$\begin{aligned} u(x,y,t) = \; & \frac{1}{2\pi}\iint_{-\infty}^{\infty} \frac{i}{\mu^2\nu^2}\left[\hat{\zeta}(k,l,0) + \mu^2\hat{h}(k,l,0)\right]\left[l\cos(\nu t) - \nu k \sin(\nu t)\right] e^{i(kx+ly)} dkdl \\ & + \frac{1}{2\pi}\iint_{-\infty}^{\infty} \frac{il}{\nu^2}\left[\hat{\zeta}(k,l,0) - \hat{h}(k,l,0)\right] e^{i(kx+ly)} dkdl, \end{aligned} \tag{10.86}$$

$$\begin{aligned} v(x,y,t) = & -\frac{1}{2\pi}\iint_{-\infty}^{\infty} \frac{i}{\mu^2\nu^2}\left[\hat{\zeta}(k,l,0) + \mu^2\hat{h}(k,l,0)\right]\left[k\cos(\nu t) + \nu l \sin(\nu t)\right] e^{i(kx+ly)} dkdl \\ & - \frac{1}{2\pi}\iint_{-\infty}^{\infty} \frac{ik}{\nu^2}\left[\hat{\zeta}(k,l,0) - \hat{h}(k,l,0)\right] e^{i(kx+ly)} dkdl, \end{aligned} \tag{10.87}$$

$$\begin{aligned} h(x,y,t) = \; & \frac{1}{2\pi}\iint_{-\infty}^{\infty} \frac{1}{\nu^2}\left[\hat{\zeta}(k,l,0) + \mu^2\hat{h}(k,l,0)\right]\cos(\nu t) e^{i(kx+ly)} dkdl \\ & - \frac{1}{2\pi}\iint_{-\infty}^{\infty} \frac{1}{\nu^2}\left[\hat{\zeta}(k,l,0) - \hat{h}(k,l,0)\right] e^{i(kx+ly)} dkdl. \end{aligned} \tag{10.88}$$

In summary, for the unforced case, the solution of (10.8)–(10.10) is obtained as follows. First, the initial conditions are transformed to spectral space using (10.72b) and its companions. The solution at time t can then be computed from (10.86)–(10.88). In this way the solution may be obtained at any finite time t without having to integrate the system (10.8)–(10.10) in time from 0 to t. In general the integrals over k and l must be evaluated by numerical quadrature.

An interesting way to look at the solution (10.86)–(10.88) is in terms of the two parts of the potential vorticity $\zeta(x,y,t) - h(x,y,t)$. Taking $\partial(10.87)/\partial x - \partial(10.86)/\partial y$, we can show that the solution for the vorticity field can be written as

$$\begin{aligned} \zeta(x,y,t) = & \frac{1}{2\pi}\iint_{-\infty}^{\infty} \left(\frac{1}{1+k^2+l^2}\right)\left[\hat{\zeta}(k,l,0) + (k^2+l^2)\hat{h}(k,l,0)\right]\cos[(1+k^2+l^2)^{1/2}t] e^{i(kx+ly)} dkdl \\ & + \frac{1}{2\pi}\iint_{-\infty}^{\infty} \left(\frac{k^2+l^2}{1+k^2+l^2}\right)\left[\hat{\zeta}(k,l,0) - \hat{h}(k,l,0)\right] e^{i(kx+ly)} dkdl, \end{aligned} \tag{10.89}$$

while (10.88) can be written in the somewhat expanded form

$$\begin{aligned} h(x,y,t) = & \frac{1}{2\pi}\iint_{-\infty}^{\infty} \left(\frac{1}{1+k^2+l^2}\right)\left[\hat{\zeta}(k,l,0) + (k^2+l^2)\hat{h}(k,l,0)\right]\cos[(1+k^2+l^2)^{1/2}t] e^{i(kx+ly)} dkdl \\ & - \frac{1}{2\pi}\iint_{-\infty}^{\infty} \left(\frac{1}{1+k^2+l^2}\right)\left[\hat{\zeta}(k,l,0) - \hat{h}(k,l,0)\right] e^{i(kx+ly)} dkdl. \end{aligned} \tag{10.90}$$

The first terms on the right of (10.89) and (10.90) are identical and represent the gravity-inertia wave part of the solution. When (10.90) is subtracted from (10.89) to form the potential vorticity $\zeta(x,y,t) - h(x,y,t)$, the gravity-inertia wave contributions cancel. This cancellation of terms is equivalent to the statements that *the gravity-inertia waves have zero potential vorticity* and *gravity-inertia waves are invisible on potential vorticity maps*. If we wait long enough the gravity-inertia waves will propagate away from a region which is initially out of geostrophic balance, and local geostrophic balance will be reestablished. Then, only the last terms of (10.89) and (10.90) will be locally relevant. Now define $\hat{\zeta}_g(k,l,0)$ and $\hat{h}_g(k,l,0)$ by $\hat{\zeta}_g(k,l,0) = -(k^2+l^2)\hat{h}(k,l,0)$ and $\hat{\zeta}(k,l,0) = -(k^2+l^2)\hat{h}_g(k,l,0)$ respectively. Then, (10.89) and (10.90) can be written as

$$\zeta(x,y,\infty) = \frac{1}{2\pi}\iint\limits_{-\infty}^{\infty} \left\{ \left(\frac{k^2+l^2}{1+k^2+l^2}\right)\hat{\zeta}(k,l,0) + \left(\frac{1}{1+k^2+l^2}\right)\hat{\zeta}_g(k,l,0)\right\} e^{i(kx+ly)}dkdl, \tag{10.91a}$$

$$h(x,y,\infty) = \frac{1}{2\pi}\iint\limits_{-\infty}^{\infty} \left\{ \left(\frac{k^2+l^2}{1+k^2+l^2}\right)\hat{h}_g(k,l,0) + \left(\frac{1}{1+k^2+l^2}\right)\hat{h}(k,l,0)\right\} e^{i(kx+ly)}dkdl. \tag{10.91b}$$

We may interpret $(k^2+l^2)/(1+k^2+l^2)$ as the spectral modification of an initial vorticity disturbance and note that low wavenumbers are eliminated. Likewise, $1/(1+k^2+l^2)$ is the spectral moditication of an initial geopotential disturbance, with high wavenumbers being eliminated.

Problems

1. Derive the nondimensional equations (10.8)–(10.10) from the dimensional equations (10.5)–(10.7).
2. Prove that (10.56) is the solution of (10.55) with the required continuity properties.
3. Derive (10.62). Hint: To save work, evaluate the energy integrals only over half the domain ($0 \le x < \infty$), then multiply this result by two in order to obtain the energy over the whole domain.
4. Derive the spectral space equations (10.73)–(10.75) from the physical space equations (10.8)–(10.10).
5. Prove the $\hat{\Psi}^{(1)}$ is orthogonal to $\hat{\Psi}^{(2)}$.
6. Derive (10.83) from (10.76).

Appendix 10A: The Laplace Transform Method

We now wish to solve the one-dimensional, f-plane, geostrophic adjustment problem

$$u_t - v + h_x = 0, \tag{10A.1}$$

$$v_t + u = 0, \tag{10A.2}$$

$$h_t + u_x = 0, \tag{10A.3}$$

by Laplace transforms. It's easy to eliminate v and h from the system (10A.1)–(10A.3). The procedure is to take the time derivative of (10A.1), use (10A.2) to eliminate v_t, and then use the x-derivative of (10A.3) to eliminate h_{tx}. We then obtain

$$u_{tt} + u - u_{xx} = 0, \tag{10A.4}$$

a second order partial differential equation for $u(x,t)$. It's harder, but still possible, to eliminate u and h from (10A.1)–(10A.3) to obtain a single second order partial differential equation for v, or to eliminate u and v to obtain a single second order partial differential equation for h. Both of these derivations require use of the potential vorticity conservation principle. The potential vorticity conservation principle is obtained by subtracting (10A.3) from the x-derivative of (10A.2), which results in

$$(v_x - h)_t = 0. \tag{10A.5}$$

The local conservation principle (10A.5) can be integrated to yield

$$v_x(x,t) - h(x,t) = v_x(x,0) - h(x,0). \tag{10A.6}$$

To obtain the single equation for v, take the time derivative of (10A.2), use (10A.1) to eliminate u_t, and then use the x-derivative of (10A.6) to eliminate h_x. We then obtain

$$v_{tt} + v - v_{xx} = -[v_x(x,0) - h(x,0)]_x. \tag{10A.7}$$

To obtain the single equation for h, take the time derivative of (10A.3), use the x-derivative of (10A.1) to eliminate u_{xt}, and then use (10A.6) to eliminate v_x. We then obtain

$$h_{tt} + h - h_{xx} = -[v_x(x,0) - h(x,0)]. \tag{10A.8}$$

Thus, we could solve the coupled, first order system (10A.1)–(10A.3) for $u(x,t)$, $v(x,t)$, and $h(x,t)$, or we could solve each of the single equations (10A.4), (10A.7), and (10A.8).

The one sided Laplace transforms of $u(x,t)$, $v(x,t)$, and $h(x,t)$ are defined by

$$\hat{u}(x,s) = \int_0^\infty u(x,t)e^{-st}dt, \tag{10A.9}$$

$$\hat{v}(x,s) = \int_0^\infty v(x,t)e^{-st}dt, \tag{10A.10}$$

$$\hat{h}(x,s) = \int_0^\infty h(x,t)e^{-st}dt. \tag{10A.11}$$

The Laplace transforms $\hat{u}(x,s)$, $\hat{v}(x,s)$, and $\hat{h}(x,s)$ are functions of the complex variable s. If the integrals (10A.9)–(10A.11) converge at a point $s = s_0$, then they converge for every s such that $\text{Re } s > \text{Re } s_0$. The inverse transforms of (10A.9)–(10A.11) are the Bromwich integrals

$$u(x,t) = \frac{1}{2\pi i}\int_{c-i\infty}^{c+i\infty} \hat{u}(x,s)e^{st}ds, \tag{10A.12}$$

$$v(x,t) = \frac{1}{2\pi i}\int_{c-i\infty}^{c+i\infty} \hat{v}(x,s)e^{st}ds, \tag{10A.13}$$

$$h(x,t) = \frac{1}{2\pi i}\int_{c-i\infty}^{c+i\infty} \hat{h}(x,s)e^{st}ds, \tag{10A.14}$$

where c is chosen so that the contour of integration lies to the right of all poles.

The Laplace transforms of the partial differential equations (10A.1)–(10A.3) are the ordinary differential equations

$$s\hat{u}(x,s) - \hat{v}(x,s) + \hat{h}_x(x,s) = u(x,0), \tag{10A.15}$$

$$s\hat{v}(x,s) + \hat{u}(x,s) = v(x,0), \tag{10A.16}$$

$$s\hat{h}(x,s) + \hat{u}_x(x,s) = h(x,0). \tag{10A.17}$$

Again, it's easy to eliminate $\hat{v}$ and $\hat{h}$ from the system (10A.15)–(10A.17). The procedure is to multiply (10A.15) by s, use (10A.16) to eliminate $s\hat{v}$, and then use the x-derivative of (10A.17) to eliminate $\hat{h}_x$. We then obtain

$$\hat{u}_{xx} - (1+s^2)\hat{u} = -su(x,0) + h_x(x,0) - v(x,0), \tag{10A.18}$$

a second order ordinary differential equation for $\hat{u}(x,s)$. Equation (10A.18) can also be obtained by Laplace transforming (10A.4). To obtain the single ordinary differential equation for $\hat{v}$, or the one for $\hat{h}$, we again need the potential vorticity principle. This is obtained by substracting (10A.17) from the x-derivative of (10A.16), which yields

$$\hat{v}_x - \hat{h} = \frac{1}{s}\left[v_x(x,0) - h(x,0)\right]. \tag{10A.19}$$

To obtain the single equation for $\hat{v}$, multiply (10A.16) by s, use (10A.15) to eliminate $s\hat{u}$, and then use the x-derivative of (10A.19) to eliminate $\hat{h}_x$. We then obtain

$$\hat{v}_{xx} - (1+s^2)\hat{v} = u_x(x,0) - sh(x,0) + \frac{1}{s}[v_x(x,0) - h(x,0)]. \tag{10A.20}$$

To obtain the single equation for $\hat{h}$, multiply (10A.17) by s, use (10A.15) to eliminate $s\hat{u}$, and then use the x-derivative of (10A.18) to eliminate $\hat{h}_x$. We then obtain

$$\hat{h}_{xx} - (1+s^2)\hat{h} = -h_t(x,0) - sh(x,0) + \frac{1}{s}[v_x(x,0) - h(x,0)]. \tag{10A.21}$$

Note that (10A.20) and (10A.21) can also be obtained by Laplace transforming (10A.7) and (10A.8) respectively.

Let's first solve (10A.18) for the case $u(x,0) = 0$ and $v(x,0) - h_x(x,0) = \delta(x-x')$. The solution is

$$\hat{u}(x,s) = \tfrac{1}{2}\left(1+s^2\right)^{-1/2} e^{-(1+s^2)^{1/2}|x-x'|}, \tag{10A.22}$$

so that, by (10A.12),

$$u(x,t) = \frac{1}{2\pi i}\int_{c-i\infty}^{c+i\infty} \tfrac{1}{2}\left(1+s^2\right)^{-1/2} e^{-(1+s^2)^{1/2}|x-x'|} e^{st} ds. \tag{10A.23}$$

This integral can be evaluated (Oberhettinger and Badii, page 261) to give

$$u(x,t) = \begin{cases} \tfrac{1}{2}J_0\left(\left[t^2 - (x-x')^2\right]^{1/2}\right) & \text{if } x'-t < x < x'+t \\ 0 & \text{otherwise} \end{cases} \tag{10A.24}$$

which is the same solution we obtained using Fourier transforms.

Appendix 10B: Riemann's Method

We want to solve the initial value problem

$$u_{tt} + u - u_{xx} = 0, \tag{10B.1}$$

with $u(x,0)$ and $u_t(x,0)$ given. Let $U(x,t)$ be a solution of the equation

$$U_{tt} + U - U_{xx} = 0, \tag{10B.2}$$

with different initial conditions. Multiplying (10B.1) by U and (10B.2) by u, and then taking the difference of these two results, we obtain

$$(Uu_x - uU_x)_x + (uU_t - Uu_t)_t = u\,(U_{tt} + U - U_{xx}) - U\,(u_{tt} + u - u_{xx}) = 0, \tag{10B.3}$$

where the first equality is easily confirmed by expanding the derivatives of the products on the left hand side, and where the second equality follows because $u(x,t)$ and $U(x,t)$ are solutions of (10B.1) and (10B.2) respectively. We now integrate (10B.3) over the domain D, a region of the (x,t)-plane bounded by the closed curve C. Since the left hand side of (10B.3) is a divergence in the (x,t)-plane, we obtain

$$\begin{aligned} 0 &= \iint_D \left[(Uu_x - uU_x)_x + (uU_t - Uu_t)_t\right] dx\,dt \\ &= \int_C \left\{(Uu_t - uU_t)dx + (Uu_x - uU_x)dt\right\} \\ &= \int_C \left\{U(u_t dx + u_x dt) - u(U_t dx + U_x dt)\right\}. \end{aligned} \tag{10B.4}$$

Now consider D to be the triangular domain defined by PQR in Fig. 10B.1. Then, since $dt = 0$ on QR, $dx = -dt$ on RP, and $dx = dt$ on PQ, (10B.4) becomes

$$0 = \int_{QR} (Uu_t - uU_t)dx - \int_{RP} \left\{U(u_t dt + u_x dx) - u(U_t dt + U_x dx)\right\} \tag{10B.5}$$

$$+ \int_{PQ} \left\{U(u_t dt + u_x dx) - u(U_t dt + U_x dx)\right\} \tag{10B.6}$$

$$= \int_{QR} (Uu_t - uU_t)dx - \int_{RP} (Udu - udU) + \int_{PQ} (Udu - udU) \tag{10B.7}$$

We have the freedom to choose the values of $U(x,t)$ along the lines RP and PQ. If $U = 1$ on both RP and PQ, then $dU = 0$ on both RP and PQ and (10B.5) can be simplified and rearranged to yield

$$u_P = \tfrac{1}{2}u_Q + \tfrac{1}{2}u_R + \tfrac{1}{2}\int_{QR} (Uu_t - uU_t)dx. \tag{10B.8}$$

U is often referred to as the Riemann-Green[1] function. The Riemann-Green function is obviously a function of (x,t), but it also depends on (x',t') since, as we move the point P, we also move the lines along which $U = 1$. To remind ourselves of this dependence we shall use the notation $U(x,t;x',t')$ for the Riemann-Green function and $U_t(x,t;x',t')$ for its partial derivative with respect to t. Identifying the point P as $(x,t) = (x',t')$, the point Q as $(x,t) = (x'-t',0)$, and the point R as $(x,t) = (x'+t',0)$, we can write (10B.6) in the alternative form

$$u(x',t') = \tfrac{1}{2}u(x'-t',0) + \tfrac{1}{2}u(x'+t',0) + \tfrac{1}{2}\int_{x'-t'}^{x'+t'} \left[U(x,0;x',t')u_t(x,0) - u(x,0)U_t(x,0;x',t')\right] dx. \tag{10B.9}$$

[1] In honor of Bernhard Riemann (1826–1866), Professor of Mathematics at the University of Göttingen, Germany, and George Green (1793–1841), the self-taught son of a miller from Nottingham, England; it was Green who made the first attempt at a mathematical theory of electromagnetism, later beautifully formulated by James Clerk Maxwell in *the* triumph of 19th century physics.

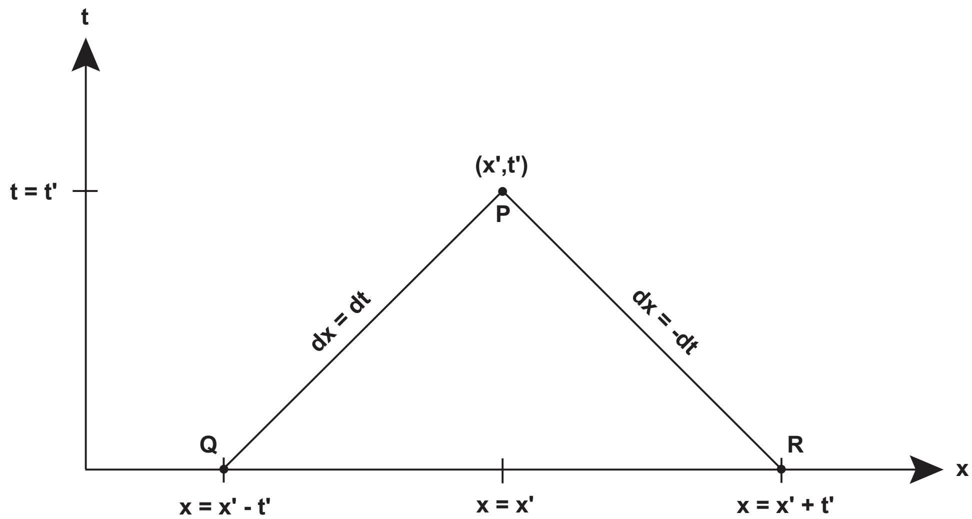

Figure 10B.1: Triangular domain D of the (x, t)-plane, with the domain D defined by PQR. Note that $dt = 0$ along the line QR, while $dx = -dt$ along the line RP, and $dx = dt$ along the line PQ.

Equation (10B.7) expresses the solution of the initial value problem (10B.1) in terms of the initial conditions $u(x, 0)$ and $u_t(x, 0)$, and in terms of the solution $U(x, t; x', t')$ of (10B.2).

To find the Riemann-Green function, consider the infinite series

$$U(x, t; x', t') = 1 + \sum_{k=1}^{\infty} \frac{a_k}{(k!)^2} \left[(t - t')^2 - (x - x')^2\right]^k, \tag{10B.10}$$

where the coefficients a_k are yet-to-be-determined. Since $t = t' + (x - x')$ along the line PQ and $t = t' - (x - x')$ along the line RP, then along these lines $(t - t')^2 - (x - x')^2 = 0$, and, according to (10B.8), $U = 1$. Substituting (10B.8) into (10B.2), we obtain

$$1 + 4a_1 + \sum_{k=1}^{\infty} \frac{a_k + 4a_{k+1}}{(k!)^2} \left[(t - t')^2 - (x - x')^2\right]^k = 0, \tag{10B.11}$$

so that $a_1 = -1/4$ and $a_{k+1} = -(1/4)a_k$ for $k = 1, 2, \ldots$, or equivalently $a_k = (-1/4)^k$. Using this last result in (10B.8), we obtain

$$U(x, t; x', t') = \sum_{k=0}^{\infty} \frac{(-1)^k}{2^{2k}(k!)^2} \left[(t - t')^2 - (x - x')^2\right]^k. \tag{10B.12}$$

Since the zero order Bessel function is given by (see Abramowitz and Stegun, 1964, page 360)

$$J_0(z) = \sum_{k=0}^{\infty} \frac{(-1)^k}{2^{2k}(k!)^2} z^{2k} = 1 - \frac{1}{2^2} z^2 + \frac{1}{2^2 4^2} z^4 - \frac{1}{2^2 4^2 6^2} z^6 + \cdots \tag{10B.13}$$

we conclude that

$$U(x, t; x', t') = J_0\left(\left[(t - t')^2 - (x - x')^2\right]^{1/2}\right). \tag{10B.14}$$

Assuming $u(x, 0) = 0$, using (10B.12) in (10B.7), and switching the roles of the dummy variables (x, t) and (x', t'), we obtain

$$u(x, t) = \tfrac{1}{2} \int_{x-t}^{x+t} u_t(x', 0) J_0\left(\left[t^2 - (x' - x)^2\right]^{1/2}\right) dx', \tag{10B.15}$$

which is identical to the solution we derived by Fourier transforms.